



Radiocommunications Agency  
Ministry of Economic Affairs

# Comparison

of UHF measurements with  
the propagation model  
of Recommendation  
ITU-R P.1546



# Authors

B.A.Witvliet

P.W.Wijninga

E.van Maanen

B.Smith

# Team Members

W.R.van Hoek

F.Holl

W.Koers

G.Lanphen

R.P.Oskam

T.Scheepmaker

J.Schot

## **Colophon**

© 2010 Radiocommunications Agency Netherlands

ISBN 978 90 815732 3 8

*Commissioned by*  
Ministry of Economic Affairs

*Conducted by*  
Radiocommunications Agency Netherlands

*Contact details*  
Radiocommunications Agency Netherlands  
PO Box 450  
9700 AL Groningen  
+31 (0)50 58 77 444  
[www.agentschap-telecom.nl](http://www.agentschap-telecom.nl)  
[agentschaptelecom@at-ez.nl](mailto:agentschaptelecom@at-ez.nl)



Radiocommunications Agency  
Ministry of Economic Affairs

# Comparison

of UHF measurements with  
the propagation model  
of Recommendation  
ITU-R P.1546



# Summary

This report describes a radio propagation measurement campaign that has been performed along paths between the Netherlands and the United Kingdom.

The campaign focused on UHF propagation on mixed land/sea paths. Special attention was given to calibration accuracy and validation of the measurement data. The result is a highly accurate and very extensive set of measurement data, that can be used for validation of existing propagation models and models being (re)developed.

Inaccuracies in the model have been indicated by several parties since the introduction in 2001 of the propagation model of Rec. ITU-R P. 1546, specifically on paths where radio waves travel partly over land and partly over sea. This research seeks to check the existence of these inaccuracies and assess their impact. Furthermore an analysis is made of possible causes in order to initiate discussion on how to correct them.

The measurement results have been compared with calculations using the propagation model of Recommendation ITU-R P.1546-4. The differences between the model and measurements have been analyzed to obtain conclusions on the existence and the magnitude of the error.

# Conclusions

Comparison of the results of the propagation measurement campaign with the P.1546 predictions strongly suggest that this ITU-R propagation model requires improvement for mixed paths, but also for paths over very flat terrain. Also some flaws in commercially available propagation prediction (planning) software have been found. The development of a quality assurance procedure for implementations of propagation models seems advisable. Specific test cases with known results would be helpful for verification, and peer review of software tools used by negotiating administrations should be promoted.

Some initial analysis has been performed to track any obvious errors in the P.1546 model. Although some indications for possible improvements could be given, no all inclusive solution has been found. This may indicate that the model has more than one flaw, making error tracking difficult.

A correction on the implementation of the Terrain Clearance Angle (TCA) at the receive side is solicited. A modified version of P.1546-4 with added improved TCA correction shows promising results, at least for very flat terrain (typical of the Netherlands) and distances up to 100 kilometres.

As doubts have risen on the correctness of the 100% cold sea curves, further efforts should be focused on those issues. Detailed measurements to confirm the 100% sea (and 100% land) curves are needed. The interpolation method for mixed path should be verified.

# Acknowledgement

## **Tony O'Neill**

We would like to thank Tony for his great hospitality and all support given to us. Tony is the director of the National Vintage Wireless & TV Museum, situated in the historical High Lighthouse in Harwich. He made the lantern room of the lighthouse available to us and even allowed us to modify his computer network for our data transmission.

## **Ron Stanley and John Sullivan**

We would like to thank Ron and John for their hospitality at the Ofcom RF monitoring station at Baldock, for hosting our receiver set-up, for using their frequency standard and telephone line, and for the installation of the measurement antenna.

## **Bob Brouwer and the crew of HSS 'Discovery'**

We would like to thank them for their excellent hospitality, flexibility and practical assistance. We would like to thank Stena Line for allowing us to use their ship as a platform for our path profile measurements.

All these persons supported this research in a very practical, yet essential way. Without their support, these results would not have been possible.



# Table of contents

Summary	5
Conclusions	6
Acknowledgements	7
<b>1 Introduction</b>	<b>12</b>
1.1 Radio propagation	13
1.2 Radio propagation models	14
1.3 ITU propagation model of Recommendation ITU-R P.1546	14
1.4 Regional Radio Conference 2006	14
1.5 Suspected model inaccuracies	14
1.6 Model verification	15
<b>2 The measurement campaign</b>	<b>16</b>
2.1 The radio propagation measurement campaign	17
2.1.1 Objectives	17
2.1.2 Original plan not feasible	17
2.1.3 A better approach	17
2.1.4 The propagation paths	18
2.2 The signal sources	20
2.3 The measurement sites	21
2.3.1 Hoek van Holland	21
2.3.2 Stena HSS 'Discovery'	24
2.3.3 Harwich	26
2.3.4 Baldock	28
2.4 The measurement method	30
2.4.1 Measuring weak signals	30
2.4.2 Automation	30
2.4.3 Following slow frequency drift	31
2.4.5 Doppler shift	32
2.4.6 Remote control	32
2.4.7 Data collection	33
2.5 Data processing	34
2.5.1 A faster data format	34
2.5.2 Application of calibration factors	34
2.5.3 Filtering of events	35
2.5.4 Statistical processing	35
<b>3 Calibration and validation</b>	<b>36</b>
3.1 Calibration	37
3.1.1 Antenna gain measurement	37
3.1.2 Antenna misalignment	37
3.1.3 Dynamic antenna misalignment correction	37
3.1.4 Antenna factor calculation	38
3.1.5 Cable loss	38
3.1.6 Combiner network	38
3.1.7 Narrow filter impulse response	39
3.1.8 Total calibration factor per site	39

3.2	Validation	40
3.2.1	Overview of the collected measurements	40
3.2.2	Verification process	40
3.2.3	Transmitter outages	41
3.2.4	Frequency jumps	41
3.2.5	Field strength changes (not suitable)	42
3.2.6	Pre-filtering	43
3.2.7	Signal to noise ratio	43
3.2.8	Correlation between fixed and maritime measurements	43
3.2.9	Number of measurements left after validation	45
4	The measurement results	46
4.1	The measurement results: general observations	47
4.1.1	Frequency dependency of the propagation	47
4.1.2	Probability density function is not Gaussian	48
4.1.3	Composition of the probability density function	49
4.1.4	Seasonal influences	51
4.2	The measurement results for each path	52
4.2.1	Path 1: fixed locations	52
4.2.2	Path 1: maritime mobile measurements	53
4.2.3	Paths 2, 3 and 4	54
4.2.4	Paths 5, 6 and 7	56
4.2.5	An overview of all paths (measurements)	57
4.3	Measurement uncertainty	58
5	Predictions using itu-r p.1546	60
5.1	Model used and input parameters	61
5.1.1	Version of the model	61
5.1.2	Propagation prediction software verification	61
5.1.3	Model input parameters	61
5.1.4	Transmitter input parameters	62
5.1.5	Receiver input parameters	63
5.1.6	Path specific input parameters	65
5.2	Field strength predictions using ITU-R P.1546-4	66
5.2.1	Path 1: fixed locations	66
5.2.2	Path 1: maritime mobile measurements	66
5.2.3	Paths 2, 3 and 4	67
5.2.4	Paths 5, 6 and 7	68
5.2.5	An overview of all paths (predictions)	68
5.3	Prediction uncertainty	69

## 6 Comparison of measurements and predictions 70

### 6.1 Comparison: a non-Gaussian distribution? 71

### 6.2 Comparison of the measurements with the P.1546 predictions 73

#### 6.2.1 Wasserstein Metric 74

#### 6.2.2 Match between measurement and prediction 75

#### 6.2.3 Fixed paths: a poor match 75

#### 6.2.4 Maritime measurement: a poor match 76

#### 6.2.5 Comparison with P370-7 77

### 6.3 Suggestions for improvement of P.1546 78

#### 6.3.1 $\Delta h$ correction 78

#### 6.3.2 TCA correction at the receive side 78

#### 6.3.3 Effect of the modifications 79

### 6.4 Conclusions 81

## References 82

## Annexes 84

### A Overview of path details 85

### B Measurement results and predictions 86

#### B 1 Measured values 86

#### B 2 Predicted values 86

### C Calibration figures 87

#### C 1 Antenna gain 87

#### C 2 Antenna misalignment corrections 87

#### C 3 Cable losses 87

#### C 4 Combiner network losses 87

#### C 5 Narrow filter correction 88

#### C 6 Overview of all calibration factors per site 89

### D Measurement uncertainty calculation 90

#### D 1 Description of measurement 90

#### D 2 Mathematical model 90

#### D 3 Description of individual sources of uncertainty 90

#### D 4 Combined measurement uncertainty 93

#### D 5 Overview of all measurement uncertainty values 94

### E Prediction uncertainty calculation 95

#### E 1 Description of prediction 95

#### E 2 Mathematical model 95

#### E 3 Description of input parameters 95

#### E 4 Combined prediction uncertainty calculation 96

#### E 5 Overview of all prediction uncertainty values 97

# 1

# Introduction

This chapter introduces the concept of radio propagation and the purpose of radio propagation models. It explains the need for propagation model verification.

Radio propagation plays an important role in everyday life. Television images, radio programs, computer data and telephone signals are carried by electromagnetic waves to wherever we are. We do not pay much attention to this normally. The mechanisms involved are of no concern to us when we switch on the car radio and listen to a radio program, or when we use our mobile phone to call somebody. It just works, and that is all we care about. Only when things do not work is a little interest in the subject sparked: we step towards the window to see if it improves the reception of the mobile phone, or we move our wireless internet modem somewhere else to see if coverage becomes better. If well planned, those radio, television and data networks “just work”. This planning is done by engineers, and the normal user is not bothered by propagation mechanisms, antenna systems, modulation techniques and the like. The radio engineer understands the mechanisms involved and chooses the best parameters to create the coverage the consumer needs. In the beginning of radio, these planning processes involved a lot of trial-and-error. Today the calculation tools that are used are very sophisticated, and include complicated calculation models of different aspects of nature. One of those aspects is what we call “radio propagation”.

## 1.1 Radio propagation

Radio propagation is the process of a radio wave travelling from a transmitter to a receiver over some distance and undergoing all kinds of changes. The signal becomes weaker, the signal strength becomes less stable, the signal shape may be smeared out in time and even its frequency may change. We'll concentrate on the signal strength for a moment. The signal weakens when the radio wave is transmitted over a great distance. This can be understood when one remembers that the total amount of energy contained in the radio wave remains the same, while the radio wave fans out over an ever increasing surface. The power density therefore decreases with increasing distance and with it the field strength. Radio waves in free space travel in straight lines. A radio wave that travels a great distance through the earth's atmosphere can travel much farther than the optical horizon though. Differences in moisture and temperature in the troposphere, the lower part of the atmosphere, can enhance the propagation of radio waves by bending their path over the horizon. This effect is not stable; it changes with local temperature, air pressure and moisture levels. It may cause a sudden very spectacular rise in signal strength levels at great distances of the transmitter. So radio propagation is very much “alive” and to some extent unpredictable. It resembles the weather in that aspect, and radio propagation could without offence be called “radio weather”.

## 1.2 Radio propagation models

Radio propagation is also just as hard to predict as weather. Too many parameters have to be measured real-time, and too many details of terrain and obstacles have to be modelled to get accurate results. The average values of radio propagation are much easier to predict, as short term effects and anomalies have little effect on the average values. In addition to this, we can describe the deviations from the average value in statistical terms: what percentage of the time they occur and what their magnitude is. So although we cannot achieve accurate short-term predictions, we can obtain statistical information on the propagation over a longer period of time, and put this information in a calculation model. When the signal travels in free space, calculating field strength at a certain distance is not too difficult. But when the signal travels over sea or land and beyond the optical horizon, it becomes a challenge. Terrain properties may cause shielding, scattering, reflection or refraction of the signal. Horizontal air layers of different temperature and moisture may cause bending of the line of travel over the horizon. A sophisticated computer model is needed to simulate the effect of all these conditions, and even then only statistical approximations can be given. Creating a radio propagation model that takes all these processes into account is not easy. Generally a model starts with a detailed physical model of the environment in which the radio wave travels. That model generates an approximation of reality. That model is then compared with measurements and correction factors are applied to compensate for imperfections of the model. Then still more measurements are performed to verify if the model is applicable in all circumstances, and the model accuracy is evaluated. Such models are of great value to radio engineers. They can be used to plan the location, antenna height and power of a new broadcast transmitter when a certain coverage area is wanted. They also can be used to calculate possible interference on the coverage area of another transmitter that is already on air. As an example, when a country is planning to put a new television broadcasting station on the air, it needs to follow certain rules and procedures to ensure that no interference is caused to existing broadcasting stations in adjacent countries. Those rules and procedures generally prescribe the use of a specific propagation model.

### 1.3 ITU propagation model of Recommendation ITU-R P.1546

The ITU-R (International Telecommunication Union, Radio Sector) has developed a propagation model for frequencies between 30 MHz and 3 GHz. This model is known as P.1546 and is named after the ITU-R Recommendation describing it in detail [1]. P.1546 was created in 2001 by combining several propagation models: P.370 [2] for VHF/UHF broadcasting, P.529 for land mobile communication, P.616 for maritime communication and P.1146 for land mobile and broadcasting from 1 to 3 GHz. The new model was also updated and improved for other radio systems to become the point-to-area model for all terrestrial services. In 2009 the latest version P.1546-4 was approved.

### 1.4 Regional Radio Conference 2006

One of the first major events where P.1546 was used extensively was the Regional Radio Conference 2006 (RRC-06). With the introduction of digital terrestrial television (DVB-T) in Europe, the analogue television channels had to be switched off, and the frequencies becoming available had to be redistributed among the countries involved. This is a highly complicated administrative and technical process, and the economical consequences of obtaining more or less frequency space are large. So in May and June 2006, the ITU-R organized the Regional Radio Conference in Geneva. Over 1000 delegates from 104 countries from Europe, Africa and the Middle East were present. They had to find optimum solutions for the needs of each individual country, and use the available frequency space as efficiently as possible. Preparing this conference alone took most participants several years of negotiating with their neighbours and developing plans, all based on the propagation model P.1546. At the conference, a special version of P.1546 was adopted as a mandatory part of the agreement. During the conference, an enormous amount of calculations had to be performed to find the best scenarios and to avoid mutual interference problems. This was realized by using a computer grid of several hundreds of computers, forming some sort of a super-computer [3].

### 1.5 Suspected model inaccuracies

As with every model, P.1546 is a huge simplification of reality. It is impossible to include all small environmental influences for all specific situations. During preparations of the RRC-06, there were great concerns in the Netherlands on the accuracy of P.1546 when calculating mixed land/sea paths. The Netherlands has wide areas with dominant land/sea paths to its neighbouring countries. A flaw in the calculation of mixed land/sea path has a significant impact on the Dutch frequency-plan. Since the introduction of this new radio propagation model in 2001, effort has been taken to verify its accuracy with empirical data. An excellent example is the document “UHF long distance propagation over land and sea paths from 1999 to 2001” of BBC Research [4]. This earlier research was very valuable and useful. However, it was not suited for our own verification as it lacked sufficient detail for the situations specific to our case, and measured path profiles were missing. Also, before a discussion on the accuracy of the model can be started, the measurement accuracy also has to be treated.

### 1.6 Model verification

Because of these reasons, the Radio Communications Agency Netherlands decided to perform propagation measurements on mixed land/sea paths to get experimental data to evaluate the P.1546 propagation model. The main purpose of this research was to confirm model errors indicated by others, find other flaws if present and to find out the magnitude of the differences between model and measurements, and the specific situations in which they occur. The first results, documented in a preliminary report, were delivered in 2006 to be used in negotiations during the Regional Radio Conference. The present report seeks to document all our findings in a more thorough and complete fashion. It can be used as input for P.1546 model improvement and other studies.





# 2

## The measurement campaign

The practical realisation of the propagation measurement campaign is described here. Television towers, lighthouses and high speed ferry boats, they all play a role in this project.

## 2.1 The radio propagation measurement campaign

### 2.1.1 Objectives

The aim was to perform radio propagation measurements on mixed land/sea paths, and to compare the results with calculations using the P.1546 propagation model.

One end of the propagation path had to be in the Netherlands. Measurements had to be performed around the clock and on a daily basis, to get reliable year averages and median values, and to include the effect of the seasons. As many paths as possible with different percentages of distance-over-land versus distance-over-sea were to be measured. Also path profile measurements had to be performed.

The frequency range of interest was 174 - 230 MHz and 470 - 862 MHz, the television broadcasting bands III, IV and V.

### 2.1.2 Original plan not feasible

The initial idea was to use the fixed monitoring network of the Radio Communications Agency Netherlands to measure and log the signal strength of some strong television transmitters from the United Kingdom. In addition to this path profile measurements could be performed with a hired ship, and with measurement vehicles on land.

This idea was not feasible for several reasons:

- the signals arriving in the Netherlands were very weak, so mobile measurements were not feasible.
- the fixed monitoring network was neither conceived for, nor easily adapted to do calibrated field strength measurements.
- the signals of the stations to be measured were too weak for the installed receivers.
- because of the low signal strength it was very difficult to assure that the measured field strength was indeed from the wanted signal.

### 2.1.3 A better approach

These problems could be solved by employing customized antennas and narrowband measurement receivers, and by reversing the propagation path direction. By putting up measurement stations in the United Kingdom to measure Dutch television transmissions, we had more means of verifying the reception of the proper station. We could monitor the transmit frequencies and compare them with the signals received abroad. The signal strength issue could be handled with high gain antennas and by measuring the vision carrier power using narrow filters.

As absolute field strength had to be measured, accurate and calibrated measurement equipment was used. Special attention was given to antenna gain calibration, cable losses and other calibration involved. More details concerning the measurement method and calibration can be found in chapters 2.4, 2.5 and 3.1.

Measurements could be automated by modifying an existing LabView™ program developed by the Radio Communications Agency Netherlands. For the verification of proper day-to-day functioning of the measurement equipment and for data collection, some sort of remote control needed to be devised using a telephone connection or another means of communication.

As a signal source, three high power analogue TV broadcast stations were selected. These stations were ideal for our purpose, as they are on air 24 hours a day and 365 days per year. With their high power and high antenna structures, they provided a strong and stable signal source. This is very important: in order to do an objective assessment of the average propagation and the variance of this value, the signal has to be received during poor propagation as well.

Being closest to the Dutch North Sea coast, the television towers of Goes, Lopik and Wieringen seemed to be our best options.

### 2.1.4 The propagation paths

With the signal sources selected, reception sites had to be found that would result in paths with different percentages of sea. After several surveys along the North Sea coast and further inland in the United Kingdom, seven radio paths were selected:

- 1 from Lopik to Baldock;
- 2 from Goes to Hoek van Holland;
- 3 from Goes to Harwich;
- 4 from Goes to Baldock;
- 5 from Wieringen to Hoek van Holland;
- 6 from Wieringen to Harwich;
- 7 from Wieringen to Baldock.

They are shown on the map below. The above path numbers will be used throughout this document. All these paths are mixed land-sea paths.

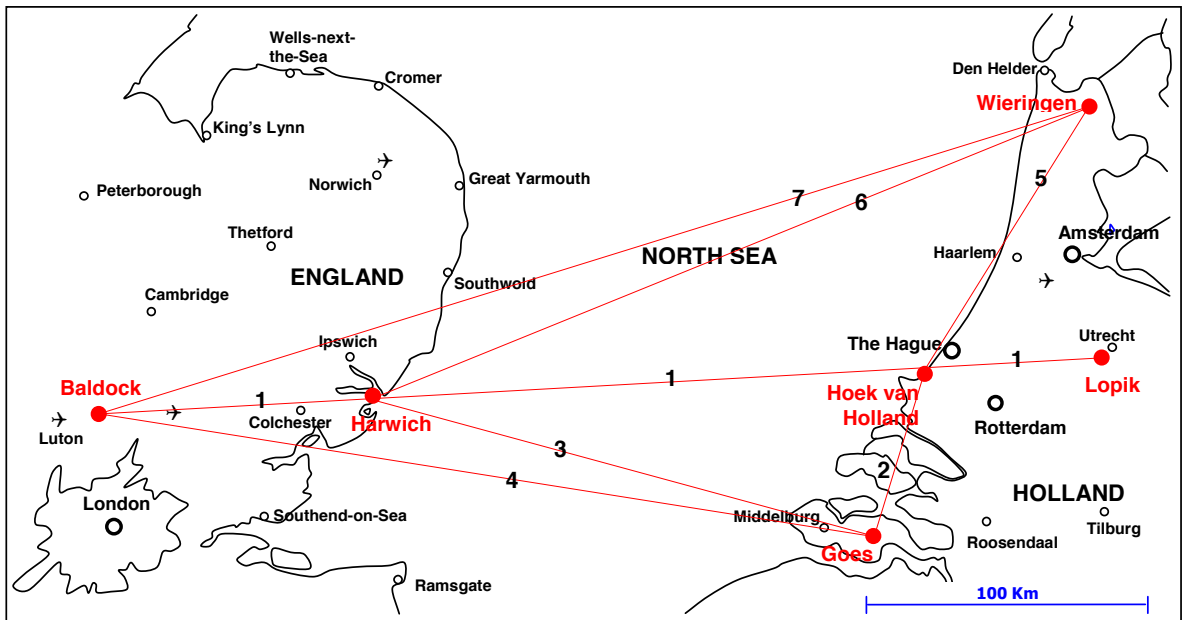


Figure 2-1: Map of measured propagation paths

The percentage of the distance the signal travels over sea versus the total path length is important in our propagation study. It is an important parameter in the propagation model. The measured paths represent a wide range of percentages sea-over-land, see table 2-2 below.

	<b>Goes</b>	<b>Lopik</b>	<b>Wieringen</b>
Hoek v Holland	17% sea – 55 km	0% sea – 64 km	45% sea – 121 km
Harwich	85% sea – 186 km	75% sea – 258 km	88% sea – 277 km
Baldock	56% sea – 282 km	53% sea – 356 km	58% sea – 367 km

Table 2-2: Percentage sea and length of the transmission paths

The best documented path runs from Lopik, in the very heart of the Netherlands, to Baldock, near Cambridge in the United Kingdom. On this path we installed three measurement stations for round-the-clock measurements and did sea path profile measurements on a monthly basis.

Also we wanted to do path profile measurements at sea, using a ship. Hiring a small vessel and mounting antennas on it would have been possible, but expensive. If the ship were too small, the movements of the ship would make aiming the antenna very difficult, resulting in large measurement errors. Hiring a more stable ship would be out of our budget, especially if we wanted to repeat the profile measurements several times. For that reason, we started to look at regular cargo and passenger ferries.

Studying the map, we realized that the fast ferry from Stena Line, running from Hoek van Holland to Harwich, ran very close to a straight line from Lopik to the United Kingdom. See figure 2-3. As seen from the transmitter, the deviation in azimuth angle from the radio path is less than  $8^\circ$  on most instances along the path.

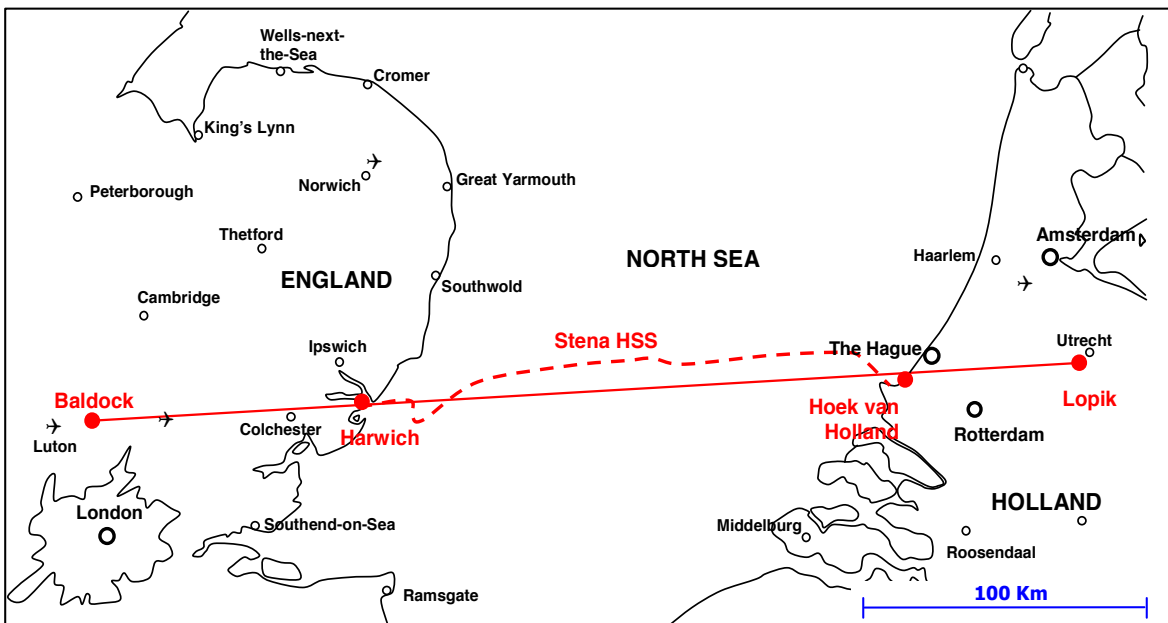


Figure 2-3: The radio path from Lopik to Baldock and the path of the ferry

When we approached Stena Line with our request, they were very cooperative. We could board as normal passengers, but we were given the opportunity to mount our antennas, do our measurements and ask the crew for assistance when needed. With the sea path profile measurement fixed, we had to fill in the other measurement sites. To support the sea path profile measurements, we required fixed measurement locations near the points where the radio path from Lopik to Harwich crosses the coastal line. We also decided that a third measurement site would best be located farther inland on the same line.

After a short survey, three excellent measurement locations were found. The measurement site near the point where the signal starts its journey over water was easy. The Radio Communications Agency Netherlands has a radio monitoring post on top of the dunes near Hoek van Holland, overlooking the North Sea. It is also close to the Stena Line terminal, from where our sea path profile measurements would start, so ideal for this purpose.

On the other side of the North Sea, we searched for high buildings at the sea front, with a clear view towards the Netherlands. We found our ideal spot in the 'High Lighthouse' in Old Harwich. Being a monument now, it once served as a beacon for sailors returning to safe harbour. It presently contains the 'National Vintage Television and Wireless Museum'. The director of the museum gave us a warm welcome and offered us the lantern room to set up our equipment. The third and most remote location was found at the Baldock Radio Monitoring Station of Ofcom, about 20 kilometres from Cambridge. They have a high tower on a hill that we could use and offered us all the assistance and facilities we needed.

## 2.2 The signal sources

Our aim was to measure the signals during poor as well as during normal propagation conditions, even farther inland. So we had to select the strongest transmitters available as our signal sources. Based on their location, the television towers of Goes, Lopik and Wieringen were chosen. Their eight, high power broadcasting transmitters provided a strong and stable signal source. They transmit around the clock, 365 days per year and have automatic backup transmitters.



Figure 2-4: Goes antenna tower



Figure 2-5: Lopik antenna tower



Figure 2-6: Wieringen antenna tower

Figures 2-4, 2-5 and 2-6 show the three antenna towers. The antenna of Lopik tower is higher than the Eiffel tower in Paris. Technical information can be found in table 2-7.

Site name	<b>Goes</b>	<b>Lopik</b>	<b>Wieringen</b>
Coordinates	51° 30' 39" North 003° 53' 04" East	52° 00' 36" North 005° 03' 13" East	52° 54' 31" North 005° 03' 30" East
Power	250 kW	1000 kW	300 kW ERP*
Antenna height	137 m	363 m	196 m AGL*
Ground level	+ 0 m	2 m	- 3 m ASL*
Vision frequency (channel)	535 MHz (ch.29) 559 MHz (ch.32) 583 MHz (ch.35)	519 MHz (ch.27) 543 MHz (ch.30)	615 MHz (ch.39) 639 MHz (ch.42) 663 MHz (ch.45)

\* ERP= Effective Radiated Power, AGL = (height) Above Ground Level, ASL = (height) Above Sea Level.

Table 2-7: Parameters of the three transmitting sites

The main parameters of these sites can be found in the table above. The Netherlands has no high power VHF band III transmissions on air near the coast, and signals of French or Belgian VHF band III transmission were too weak to be useable, so no band III transmissions were measured.

## 2.3 The measurement sites

### 2.3.1 Hoek van Holland

The Radio Communications Agency Netherlands has a radio monitoring post on top of the dunes near Hoek van Holland, overlooking the North Sea. It is also close to the Stena Line terminal, from where our sea path profile measurements started. The site has a clear view all around and is ideal for this purpose. See figures 2-8 and 2-9.



Figure 2-8: Hoek van Holland measurement site



Figure 2-9: Map showing the measurement site and the Stena Line terminal

The monitoring post is located at:

51° 59' 03" North  
004° 06' 58" East

The antenna is mounted just above the roof of the building, at 5 metres above ground. This is 23 metres above sea level.

We did not mount them in the lattice mast, as this would create too much height difference with the sea path profile measurements.

At this site, the direction of all three transmitters is different. Therefore we mounted three receive antennas, each aimed at one transmitter. We calculated the antenna directions using the 'CoordinateCalculator' software [5]. The roof of the building is oriented 23°–203°, and we used that to aim the antennas roughly for the first test. Later the antennas were adjusted exactly, and we also verified that the chosen directions corresponded with maximum signal strength.





Figure 2-10: Measurement antennas

Because of the high wind speeds present at this site and the proximity to the sea, Wipac 12 element Yagi antennas, type 'FWS 412 03' were selected. These are heavy duty antennas designed for central antenna systems. The antennas are manufactured for a specified channel group and have high gain. The antenna gain calibration is described in chapter 3.1. The fed element is encapsulated in a radome to avoid deterioration due to corrosion or salt residues. See figure 2-10.

The three measurement antennas were connected to the receiver through a passive combiner. The unwanted pickup through the other two antennas was measured on each frequency. The spatial isolation between the three antennas was not sufficient due to their diagrams alone, and frequency filtering was added to solve this.



Figure 2-11: Measurement equipment

We used a digital spectrum analyzer as a receiver, as it offered us very narrow filters and high long term stability. As the IF part of the analyzer is completely digital, the filter pass band is well defined and very stable. In Hoek van Holland we used IF filters with 100 Hz bandwidth. Narrower filters would have given us an even better signal-to-noise ratio and rejection of unwanted signals, but receiver frequency drift would have required an external high precision frequency reference. Regarding the high signal levels of the Dutch transmitters in Hoek van Holland, we decided there was no need for that.

A LabView™ program made by the Radio Communications Agency was used to control the spectrum analyzer via the GPIB interface [6]. The program ran on a standard laptop and made the receiver scan a predefined set of frequencies with settings chosen by the user. See figure 2-11.

A planning could be made to start and stop measurements, and measurement data was written to a binary file. We programmed it so that all eight transmit frequencies were measured subsequently and all data was stored at midnight. The LabView™ software could even make periodic spectrum analyzer self-calibration possible on command.

The laptop in turn could be remote controlled using modems and a telephone line, and Symantec 'PCAnywhere™' software. See figure 2-12. Measurement files could be downloaded and new frequency sets uploaded at wish. Even resetting the laptop was possible that way.

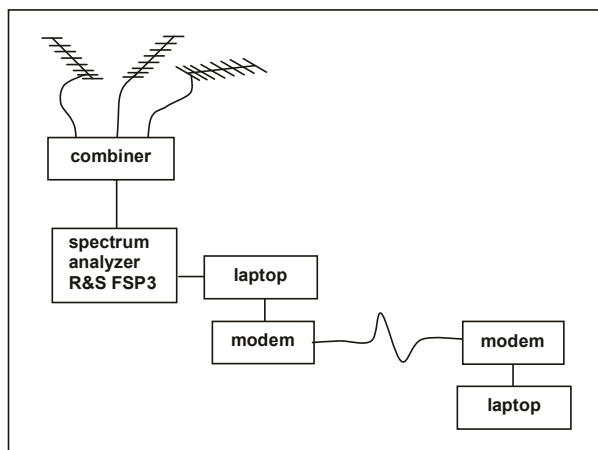


Figure 2-12: Block diagram Hoek van Holland



### 2.3.2 Stena HSS 'Discovery'

For path profile measurements between Hoek van Holland and Harwich, we used the regular Stena Line fast ferry for our measurements. The Stena HSS 1500 high-speed catamaran weighs 19,638 GRT and is 127 metres long. This provided us with a very stable ship, making accurate measurements much easier. Also the fares for ferry passengers are substantially lower than hiring even a small boat, making a larger number of measurements possible. See figure 2-13.



Figure 2-13: Stena HSS 'Discovery'

The ferry is built in Finland and is named HSS 'Discovery'. HSS stands for 'High Speed Service'. With its two 78 MW power turbines, it cruises at 40 knots, which is almost 70 km/h. The ferry crosses the Channel in 3:45 hours.



Figure 2-14: Antenna in radome and DGPS

The high stability of the ship eliminated the problem of a moving and tilting antenna, and allowed us to use an antenna with higher vertical gain. This made it possible to measure the signal up to Harwich harbour. The height of the ship eliminated the need for an antenna mast. We chose not to realize a permanent automated measurement set-up on board, as this would complicate mechanical constructions and introduce safety issues. So we boarded as normal passengers, and limited the measurements to approximately once a month.

Measurements were performed on the journey from Hoek van Holland to Harwich only, but not on the return trip. We mounted the antenna on the rear balcony at 15 metres above sea level. The presence of the ship's hull as a reflector was no serious problem. By using a screen reflector antenna with a high front-to-back discrimination and by mounting the antenna on the absolute tail end of the ship, no reflections from the ship could reach the main lobe of the antenna.

A Hirschmann type 'FESA 805' was modified for our purpose. The grid reflector was replaced with a solid screen, and the impedance matching was adapted. The antenna was mounted in a radome for seawater protection and combined with the DGPS antenna on one frame. The lightweight frame could be easily hung over, and clamped to the railing. A double cable for the television signal and the DGPS signal and cable was attached to the railing and led to the passenger's cabin where the measurement equipment was set-up. This antenna set-up was custom built by the Technical Department of the Radio Communications Agency Netherlands.

The measurement set-up consisted of a Rohde & Schwarz FSP3 spectrum analyzer used as a fixed frequency receiver, and a LabView program installed on a laptop computer. During the sailing measurements, only the two transmitters on Lopik tower were measured. Both frequencies were measured in turns, using a laptop and a measurement program controlling the receiver.

As the crossing time is relatively short, no external frequency standard was used. The receiver was warmed up, calibrated and manually tuned to the television transmitters just before the ferry sailed, after which the frequencies were entered in the measurement table of the laptop.

### 2.3.3 Harwich



Figure 2-15: The High Lighthouse

We were very lucky in acquiring a measurement location at the point where the radio path crosses the Essex coast. Searching for a high location with sea view, we found the historical High Lighthouse in Harwich.

It is the higher of two lighthouses that were built in 1818 to guide ships towards the harbour of Harwich. When both lights could be seen aligned one above the other, the sailor was on the right course towards the harbour and around the sand banks. By using a double light, tricking the sailors with fake fires was also prevented. The lantern room of the high Lighthouse has a beautiful view over the harbour, looking towards the Netherlands.



Figure 2-16: The location of the High Lighthouse

These days, the lighthouse accommodates the National Vintage Wireless & TV Museum, consisting of a large collection of historic radio and television receivers and attributes as well as a section dedicated to the era of offshore pirate stations. The director of the museum, Mr. Tony O'Neill, was very interested in our project and helped us in all possible ways to make our measurement project possible.

The High Lighthouse can be found in Old Harwich.

The exact position is:

51° 56' 40" North

001° 17' 19" East

The antenna was installed in the lantern room at 18 metres above ground. This is 20 metres above sea level.

The difference in direction of the three television transmitters is around 30°. Therefore we installed a Hirschmann type 'FESA 805' screen reflector antenna that has a relatively broad horizontal lobe. We aimed it at Lopik, and corrected for the misalignment loss on the two other sites.



Figure 2-17: The antenna in the lantern room

The antenna was installed inside the lantern room, so the grid of the windows caused some distortion of the antenna pattern. We compensated for this and for any misalignment loss by comparing the antenna gain with a reference antenna outside the tower at the same height. For antenna gain calibration, see chapter 3.1.



Figure 2-18: The equipment rack

An equipment rack was installed in the lantern room, directly underneath the antenna. It contained the Rohde & Schwarz FSP3 spectrum analyzer that was used as a narrow-band measurement receiver. A Rubidium high precision frequency standard was built in the measurement equipment rack, to serve as a reference for the measurement receiver. That way the receiver could be kept on exactly the same frequency as was measured in the Netherlands. That in turn enabled the use of very narrow IF filters. We used a 30 Hz filter in Harwich during the entire measurement campaign.

As the lighthouse was unattended for long intervals, we installed a UPS to take over the power supply should the mains supply fail. It is not shown on the photograph that was taken just after first installation. The measurement set-up was controlled by measurement software on a laptop.

We needed a remote contact with our measurement set-up for the verification of proper operation, remote control and data for collection. This proved to be difficult, as there was no telephone connection or other network access available from the lighthouse. Installing a telephone line was not possible either because of the historic value of the site. We solved this problem by routing a Virtual Private Network (VPN) through the computer system of the director of the museum, living nearby. A small SHF wireless LAN was set-up behind one of the lighthouse windows to link the lighthouse with his apartment building. National regulations were observed when building this set-up.

### 2.3.4 Baldock

Farther inland we put up a measurement station in Baldock, near Cambridge. We were given hospitality at the Baldock Monitoring Station of Ofcom. The location of their monitoring station is excellent.



Figure 2-19: Some of the HF antennas at the Baldock Monitoring station



Figure 2-20: Map showing the location of the Baldock Monitoring station

The antenna position is:  
 $52^{\circ} 00' 00''$  North  
 $000^{\circ} 07' 45''$  West

The antenna was mounted in a free standing tower at 29 metres above the ground, with clear view all around.

The tower is standing on a hill. This resulted in an antenna height of 136 metres above sea level.

Large size RF cables were run down from the antenna mast to a brick building nearby.





Figure 2-21: The antenna tower



Figure 2-22: The measurement antenna

As Baldock is 367 km away from Wieringen, we expected very weak signals. We therefore installed a high gain long Yagi antenna near the top of the mast to improve signal strength as much as possible. The antenna used was a 21 elements Yagi antenna used in central television-antenna installations, a Wipic type 'FWS 429 02'. For antenna gain calibration, see chapter 3.1.

The horizontal -3 dB beam width of the antenna is specified as  $23^\circ$ . Because of its clean diagram with a narrow main lobe, it also decreased the risk of interference from other stations and improved signal-to-noise in general. The angular difference between the different Dutch television transmitters as seen from Baldock is small. We aligned the antenna on Lopik, and compensated the misalignment loss for the other two sites.



Figure 2-23: Rack mounted receiver and laptop

As in Hoek van Holland and Harwich, a Rohde & Schwarz FSP3 spectrum analyzer was used as a very selective receiver. The spectrum analyzer, an un-interruptible power supply (UPS) and a laptop running the measurement automation software were mounted in an existing equipment rack in the building. The high precision frequency standard of the Ofcom Monitoring Station was used as a reference for our receiver.

Remote control was realized via an analogue telephone line, as in Hoek van Holland.

## 2.4 The measurement method

### 2.4.1 Measuring weak signals

The signals we wanted to measure in this measurement campaign were weak and had a large amplitude variation. This required special attention if we wanted to have meaningful measurement results. As these were no laboratory measurements, but field measurements in real life circumstances, interference from other signals, transmitter outage, transmit frequency drift etcetera had to be expected and taken into account.

The channel bandwidth for an analogue PAL-B television signal is 8 MHz, but the transmitter power is not evenly spread over this bandwidth. The luminance carrier is the strongest frequency component within this 8 MHz wide signal. All other frequency components are at least 20 dB weaker. We could take advantage of this fact to improve our measurement capabilities.

If we measure the power in the full channel bandwidth, we also collect background noise power in 8 MHz bandwidth. Yet the total signal power will be delivered mainly by the luminance carrier.

Reducing the receiver bandwidth to 30 Hz lowers the background noise power by 54 dB. If we tune the receiver to the frequency of the strongest component of the vision carrier and measure only this power, the amount of signal power we measure will only be slightly lower than in the case of a measurement in the 8 MHz wide bandwidth. So this way we could improve the signal-to-noise ratio with over 50 dB, which is substantial.

Using a small IF filter also counteracts interference from other television transmitters because of the low probability of interferers being present within 30 Hz of the wanted transmitter.

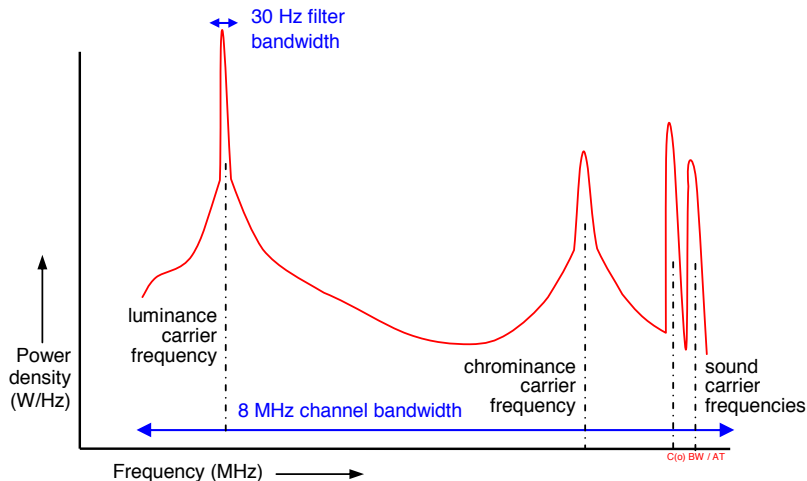


Figure 2-24: Power spectrum of an analogue television signal

This approach however caused two important issues that required special attention:

- 1 Even a slight frequency drift in the television transmitter would cause the signal to drift out of the very narrow receive filters.
- 2 Within the narrow filter bandwidth, the power of the synchronization pulse of the television signal could not be measured. The measured field strength was therefore slightly lower than the real value, and needed to be corrected. This is described in the paragraph on calibration.

### 2.4.2 Automation

As the field strength measurements were performed around the clock, the measurements were automated. Using previous experience with automation of measurement receivers and spectrum analyzers using LabView™ software, two previously conceived programs were combined to realize the wanted functionality. LabView™ software is independent of the automation platform used (hardware as well as operating system) and has an extensive set of drivers for equipment of many manufacturers.

The program controlled the Rohde & Schwarz spectrum analyzer via its GPIB interface and scanned frequencies that were previously stored in a frequency list. The measurement values were stored together with a time stamp in a binary file. That file was terminated at the end of each day and downloaded later for further processing. Special provisions were made to ensure that a power failure could be survived, taking into account the booting time delay for the external spectrum analyzer etc.

The maritime measurements were conducted using the same program, which now also stored the GPS-coordinates with each time stamp.

### 2.4.3 Following slow frequency drift

The TV transmitters have good frequency stability. If observed with a very stable receiver using a 30 Hz filter, however, even the daily slow frequency drift of the transmitter becomes a concern. The transmitters in Goes uses precision offset, and therefore has a frequency stability of a fraction of a Hertz. The other transmitters have no such stability, and tend to slowly drift out of the pass band of the receiver.

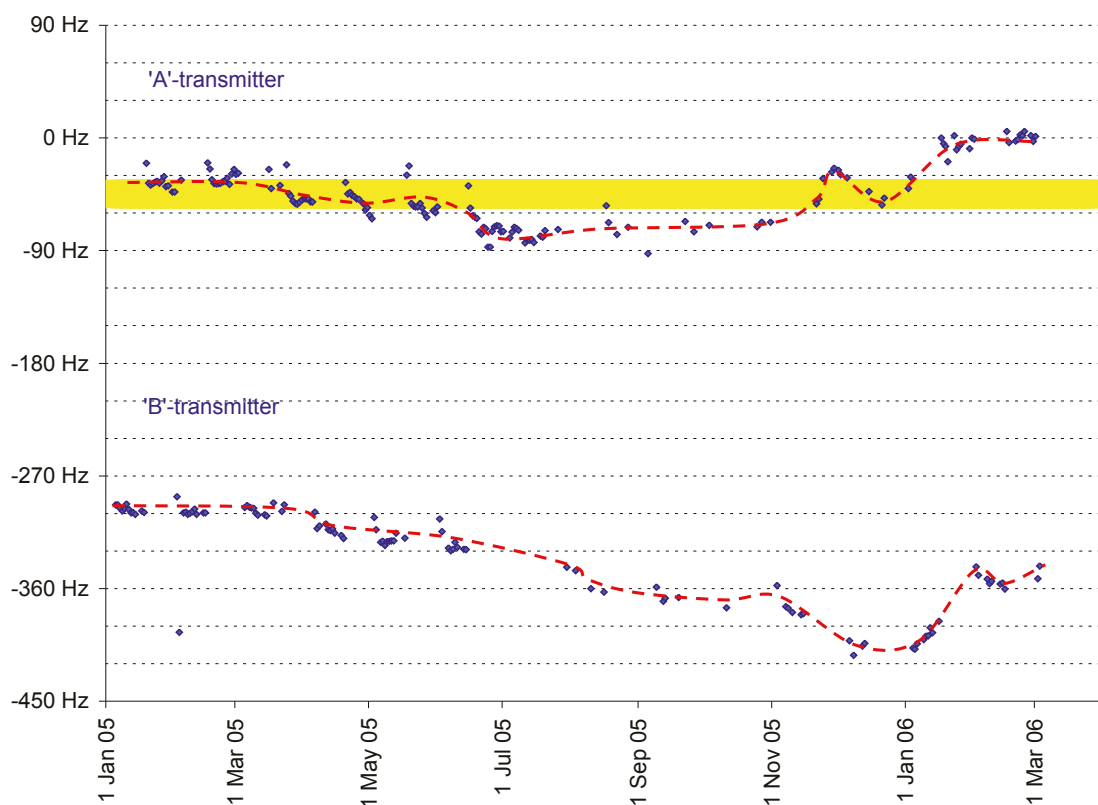


Figure 2-25: Frequency drift versus receiver bandwidth

Figure 2-25 shows the frequency drift of the Wieringen TV1 transmitter. The vertical axis shows the frequency relative to the intended 615.250000 MHz. Dashed lines are shown at 30 Hz distance. One receiver bandwidth of 30 Hz is shown as a yellow bar. It is clear that using one single receiver with a 30 Hz bandwidth would not be sufficient to capture the signal at all times.

This problem was solved by measuring a sufficient number of adjacent frequency bins simultaneously. If the signal drifts slowly out of the pass band of the receiver on the first frequency, it is still captured on the adjacent frequency. We used Gaussian shaped filters, overlapping at the -3 dB points. So even if the signal fell exactly on the border between two adjacent frequency filters, the total power could easily be calculated out of the signal values in both frequency bins.

To avoid the risk that finally the TV transmitter would even drift out of this pre-programmed capture range, the exact frequency of the TV transmitters was measured daily at the Monitoring Station of the Radio Communications Agency with a very high accuracy. With that information the frequencies used in the automation software could be set and adapted afterwards.



The receive sites at Harwich and Baldock had an absolute frequency accuracy of a couple of Hertz due to the Rubidium atomic frequency reference used. So setting their frequency with the information of the Monitoring Station assured correct measurements. The receive site of Hoek van Holland did not have such an external reference. The measurements at Hoek van Holland were done using 100 Hz filters, allowing for much more drift. The signal levels at Hoek van Holland were such that narrower filters were not needed.

As also can be seen in figure 2-25, there was a notable frequency difference between the ‘normal’ transmitter and the ‘backup’ transmitter. The second transmitter had identical circuitry as the first one and could take over in case of a failure or in case of planned maintenance. To assure equal wear on both transmitters, switching over between them was done on a regular basis. Both frequencies had to be programmed in the receiver software to assure the signal is captured at all times.

#### 2.4.4 Doppler shift

As the sailing speed of the Stena HSS was high, sometimes over 70 km/h, Doppler shift during the sea path measurements was not negligible. This can be seen in figure 2-26. This spectrogram was made just after leaving the harbour of Hoek van Holland, when the ship picked up speed.

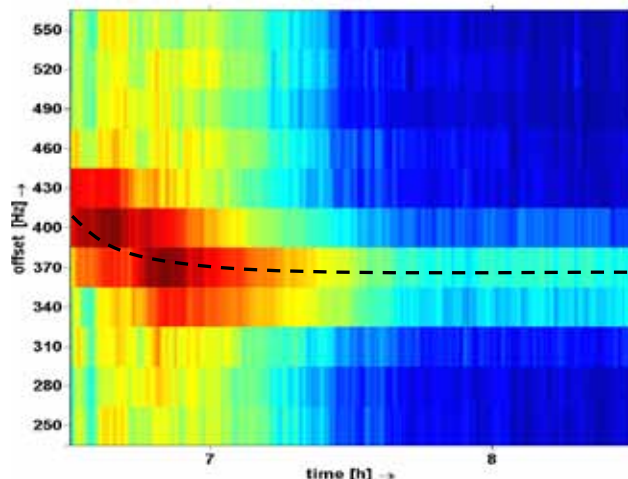


Figure 2-26. Doppler shift caused by increasing high sailing speed

The expected Doppler shift at a speed of 70 km/h on a nominal frequency of 543 MHz, is:

$$f_{OBSERVED} = f_{TX} \cdot \left( \frac{c}{c + v_{BOAT}} \right) \approx 35 Hz$$

To counter this Doppler shift, and possible transmitter frequency drift, a number of additional frequencies just next to the initial frequencies were measured as well. This was done by adding them to the frequency list of the measurement program.

#### 2.4.5 Remote control

At the fixed measurement locations, the equipment was left unattended for a long period of time. So a way had to be found to check if the set-up was still operating, to readjust the frequencies in the frequency list, and to download the measurement data.

For the fixed receive stations in Baldock and Hoek van Holland, this was realized using a telephone connection and Symantec PCAnywhere™ software. This software allowed the user to view the screen of the remote computer and to control its keyboard. With it, the measurement program was controlled completely from a distance.

In Harwich, a Virtual Private Network (VPN) was set up through a private ADSL connection and a wireless LAN link to the lighthouse. Now we could browse through, download and upload files on the measurement laptop. This was not as comfortable as using PCAnywhere™, but it met our minimum requirements.

The maritime measurements were not remote controlled. This receiver set-up was not a permanent installation and was installed and supervised each time by two technicians. They programmed the frequencies and stored the measurement data after the boat trip from Holland to the United Kingdom.

#### **2.4.6 Data collection**

The data of all measurement sites was collected at regular intervals, often daily. This was done to avoid data loss when the laptop of a measurement station would crash. The measurement data was downloaded, and the contents of the file were checked with a simple viewer. If everything looked well, the file was then stored on a data server. The name of the file reflected the date of the measurement and the name of the measurement site.

## 2.5 Data processing

The data files were stored in a fail safe binary format by the measurement software to guarantee data integrity even in the case of a possible crash or power outage. To achieve archival quality storage of data, the files were converted to ASCII using the format described in Recommendation ITU-R SM.1809. These data files were later processed using software written in MatLab. The post-processing was done in four steps:

- 1 conversion to a faster data format;
- 2 application of calibration factors;
- 3 filtering;
- 4 statistical processing.

All four steps are explained below.

### 2.5.1 A faster data format

Processing the SM.1809 format ASCII-files turned out to be slow. Batch processing of a large number of files was needed, e.g. to check the files on integrity, to filter measurement data collected during transmitter outages and to apply a number of calibration factors. Also the statistical processing and other analysis steps required the reading of a large amount of data, so fast access to the measurement data was a necessity.

Therefore the ASCII-files were batch converted to the MatLab workspace format that MatLab internally uses and subsequently stored in a so called workspace file. This type of file could be recalled much faster, and a speed improvement of about 1000 times was realized. At the same time, the original file, containing the measurements for all eight transmitters, was split-up in eight separate files. This step greatly simplified further statistical processing when a huge amount of data had to be read and processed. Reading and parsing all 1390 ASCII-files took more than 3 hours. After converting the files, the processing of all measurements took only 30 seconds.

To avoid unnecessary manual labour (and mistakes), the MatLab program was designed to synchronize its intermediate MatLab data files with the available crude ASCII-files. When new ASCII-files were added, the corresponding MatLab-files were created automatically.

### 2.5.2 Application of calibration factors

A second intermediate step was taken to add all calibration factors and other corrections to the files. The application of the calibration factors could be automated in a fairly easy way, using the same synchronization technique as was described in the previous paragraph. The calibration factors that had to be applied were:

- Free space antenna gain;
- Antenna misalignment loss;
- Cable loss;
- Combiner/filter loss;
- Narrow Filter (peak-RMS) correction;

The antenna misalignment loss for the maritime measurements was dynamic, as the direction of the ship changed during the crossing. The position information of the ship was differentiated to calculate the ship's momentary direction of travel, and a small routine in the same MatLab program applied the correct misalignment loss for every individual measurement point of the crossing.

The combiner/filter loss applied only to the Hoek van Holland receive site. Its value changed with time, as the original antenna combiner was replaced by a better one during the measurement campaign.

The correct attenuation values were applied for each period.

Determining the exact figures for all calibration factors is not described here. This alone is a time consuming and precise work. The factors themselves can be found in annex C.

### 2.5.3 Filtering of events

The files containing calibrated measurement values also contained measurements during intervals that the transmitter was off air, and periods where the transmitter had drifted out of the capture range of the frequency bins that were scanned. Also the antennas had been disconnected for short maintenance tests. Those events were rare, but the measurements concerned had to be rejected when further analysis was done. All the measurements corresponding to these events had to be marked as not good for further use. These discarded measurement samples would have added to the lower side of the amplitude distribution of the combined measurements, and the resulting median values would have become slightly lower.

For each individual measurement and for each transmitter, several frequency bins were available, but only one of these bins contains the actual value. The others bins contained noise. A dynamic filter was applied to select the bins containing the actual transmitter signal. The resulting values were used for the final step: the statistical processing.

### 2.5.4 Statistical processing

Using MatLab workspace-files, reading all data files of one transmitter is a matter of minutes. To make a field strength distribution diagram of all measurements of one path, or of one frequency on one path, all files were read, and the measurement values were sorted according to their amplitude. The resulting distribution gave a good indication of the average and median value of the field strength and also of the spread of the values. It was easier to express the properties of varying field strength in statistical figures. Therefore the field strength distribution was integrated, producing a graph showing minimum field strength against probability. The 50%, 10% and 1% median values that are often used can be read directly from this graph. This process was also automated, and the analysis program determined the values and plotted the points in the graph.

The statistical processing of the maritime measurements was done in a slightly different way. A graph had to be produced showing the 50%, 10% and 1% median values as a path profile. As these measurements were performed only once a month, less data is available. This resulted in less accurate values, especially for the 1% median line. The number of available measurement samples for the statistical routines was slightly improved by using a sliding window. The windowing process clusters measurement samples that are taken at positions close to each other and used to generate a median value for that particular part of the profile.

# 3 Calibration and validation

All measurements had to be calibrated to obtain accurate values, and they had to be screened to avoid contamination of the results by interference.

## 3.1 Calibration

This chapter describes the effort that was made to calibrate the measurements so as to express the measured values in absolute field strength. All individual calibration values used can be found in annex C.

### 3.1.1 Antenna gain measurement

#### Hoek van Holland

In Hoek van Holland, three antennas were used, each pointing in the direction of one of the transmitter sites. We used three Wipic FWS 412 03, professional 12 element Yagi antennas intended for Central Antenna Installations. Their antenna gain claimed by the manufacturer is 12 dBd, and the -3 dB beam width is 35°.

The actual gain depends on the working frequency and was somewhat lower than specified. We measured the real antenna gain on our working frequencies using distance scanning and the 'three antenna method' [7]. This method yields absolute free space antenna gain for each antenna used. The results can be found in annex C. The two reference antennas used were stable versions of the Emco 3146 Log Periodic Dipole Arrays that were free space calibrated at the National Physical Laboratories (NPL) in London. The three antenna method also yielded antenna gain values for these reference antennas. These values fell very close to the antenna gain values delivered by the NPL.

#### Stena HSS

The antenna for the maritime mobile measurements was a Hirschmann FESA 805 commercial multiple dipole screen reflector antenna, but mounted on a solid metal reflector, fitted with new impedance matching and protected with a radome. We measured the antenna gain ourselves using distance scanning and the three antenna method.

#### Harwich

The Harwich antenna was also a Hirschmann FESA 805 multiple dipole screen reflector antenna, but with the original grid reflector and a modified antenna matching network. The antenna gain claimed by the manufacturer is 10-13 dBd, but this seems high. The antenna was calibrated after installation. This was necessary because the antenna was placed behind the lighthouse lantern window that contained metal and may have affected the antenna diagram. Calibration figures were obtained by making a simultaneous registration of the wanted television signals on this antenna and on a calibrated reference antenna outside the lighthouse. The reference antenna was pointed towards each individual transmitter in turn. That way, the actual gain of the antenna in the direction of each transmitter was measured. The results were statistically processed and compared. The reference antenna used was an Emco 3146 Log Period Dipole Antenna that was calibrated at the National Physical Laboratory (NPL) in London for free space gain.

#### Baldock

The antenna at Baldock was a Wipic FWS 429 031, a 21 elements long Yagi. The antenna gain of this antenna was given as 15 dBd. We measured this antenna ourselves also. The actual gain depends on the working frequency and was somewhat lower than specified. We measured the actual antenna gain on the frequencies using distance scan and the three antenna method. Two Log Period Dipole Arrays that were calibrated at the National Physical Laboratory (NPL) in London served as reference antennas.

### 3.1.2 Antenna misalignment

The only static misalignment correction was needed at Baldock, where a single antenna was used for the measurement of all transmitters. The antenna at Baldock was aimed at the transmitter Lopik, this resulted in a misalignment error for Wieringen and Goes that could be determined using the antenna pattern of the antenna. This pattern was measured by the antenna manufacturer and checked by us using simulations.

### 3.1.3 Dynamic antenna misalignment correction

For the measurements performed at sea, the misalignment errors were not constant but dependent on the small variations of the ship's course. A NEC simulation of the antenna was used to derive the antenna pattern. From two subsequent measurement positions, the angle of aim of the antenna and the corresponding antenna gain were calculated and applied to each individual measurement sample.

### 3.1.4 Antenna Factor calculation

Measuring field strength requires a calibrated measurement antenna. The antenna functions as a transducer, capturing part of the power density of the electromagnetic wave arriving at the antenna and producing a voltage across its terminals.

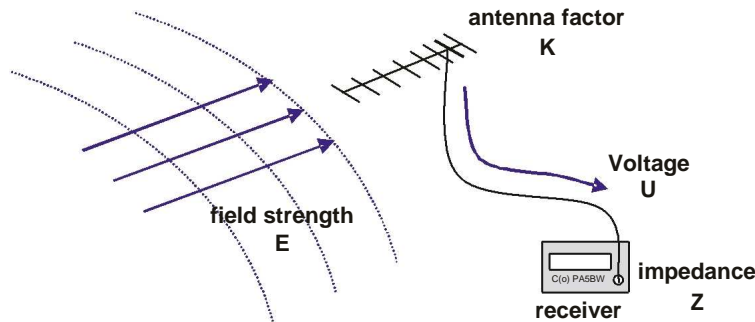


Figure 3-1: Field strength measurement

That voltage can be measured with a measurement receiver connected to the antenna. When the ‘antenna factor’ is known, and a certain antenna voltage is measured, we can calculate the corresponding field strength as:

$$E = K * U$$

Where:

- E = Electric field strength [V/m]
- K = Antenna factor [1/m]
- U = Antenna voltage [V]

When the free space antenna gain is known, we can calculate the antenna factor using the formula below. The antenna gain used in this formula is linear and isotropic. If the reference antenna is a half wave dipole, remember to correct for this.

(0 dBd = 2.15 dBi).

$$K = \sqrt{4\pi * \frac{G}{\lambda^2} * \frac{Z_0}{Z_{FS}}}$$

Where:

- K = Antenna factor [1/m]
- G = Antenna gain [linear]
- $\lambda$  = Wavelength [m]
- $Z_0$  = Characteristic impedance of antenna [ $\Omega$ ]
- $Z_{FS}$  = Characteristic impedance of free space [ $\Omega$ ]

Be sure to use free space antenna gain values here. Antenna factors specified for EMC calibration purposes cannot be used here. They are used in set-ups where the maximum of combination of the direct wave and the reflected wave is measured, above a metallic plate of specified dimensions, and at 1 and 3 metres distance. These gain values differ substantially from free space gain.

### 3.1.5 Cable loss

Cable losses for Harwich were measured on site and part of the antenna calibration. The cable losses in Hoek van Holland and Stena were measured as separate items.

The cable at Baldock was installed in a tower with no possibility to operate a test transmitter or test receiver at the top of it. The cable loss was therefore determined with a TDR to measure the cables length and the cable manufacturer’s data.

### 3.1.6 Combiner network

A combiner was only present in the set-up at Hoek van Holland where three antennas were connected to a single measurement receiver. During the measurement campaign, it was found that improvements were needed to assure interference-free reception under all circumstances. The correction factors for the combiner were measured, for the situation before modification as well as for the situation after modification. The right correction factor was applied to the measurement values.

### 3.1.7 Narrow filter impulse response

For analogue television, output power and measured field strength are defined as the peak value occurring during the vertical synchronization pulse. The slow impulse response of the 30 Hz receiver filter does not allow a correct measurement of the peak envelope power at the moment of the synchronization pulse of the television signal. The measured field strength is therefore slightly lower than the real value, and must be corrected.

The difference between the measured value and the peak-sync value has a fixed value. It is therefore possible to measure this difference close to the transmitter and add a calibration factor in the data processing to compensate for it. A correction was made on the measured values based on measurements performed with different filters on the Lopik transmitters.

### 3.1.8 Total calibration factor per site

The total calibration factor  $C_{tot}$  for each site is a combination of the parameters described in the previous chapters, it is the factor between the field strength  $E_{rx}$  and the voltage at the receiver's input terminal  $U_{rx}$ .

$$C_{tot} \text{ [dB/m]} = E_{rx} \text{ [dB}\mu\text{V/m]} / U_{rx} \text{ [dB}\mu\text{V]}$$

$$E_{rx} \text{ [dB}\mu\text{V/m]} = U_{rx} \text{ [dB}\mu\text{V]} + C_{pk} \text{ [dB]} + K_{ant} \text{ [dB/m]} + d(\text{align}) \text{ [dB]} + d(\text{cable}) \text{ [dB]} + d(\text{comb}) \text{ [dB]} \\ + \text{add } d(\text{comb}) \text{ [dB]}$$

$$K_{ant} \text{ [dB/m]} = -29.78 + 20 \cdot 10 \log(f \text{ [MHz]}) - G_{ant} \text{ [dBi]}$$

$$G_{ant} \text{ [dBi]} = G_{ant} \text{ [dBd]} + 2.15 \text{ [dBi]}$$

Where:

$K_{ant}$	=	antenna factor
$G_{ant}$	=	antenna gain (in resp. dBi or dBd)
$C_{pk}$	=	narrow filter correction
$d(\text{align})$	=	antenna alignment correction
$d(\text{cable})$	=	cable losses
$d(\text{comb})$	=	combiner losses
add $d(\text{comb})$	=	additional combiner losses



## 3.2 Validation

### 3.2.1 Overview of the collected measurements

The first measurements started in Hoek van Holland in March 2005. The measurement sites in Harwich and Baldock became operational in the month that followed. The measurement campaign lasted 500 days and ended August 2006.

In addition to the fixed site measurements, 18 maritime mobile measurements were conducted on board of the Stena HSS ferry between Hoek van Holland and Harwich. Those measurements were spread evenly over the total measurement period, and dates were randomly chosen.

A total of 23,500,000 measurement values were collected for 22 path/frequency combinations. A graphical representation of the collected data over time is shown in figure 3-2.

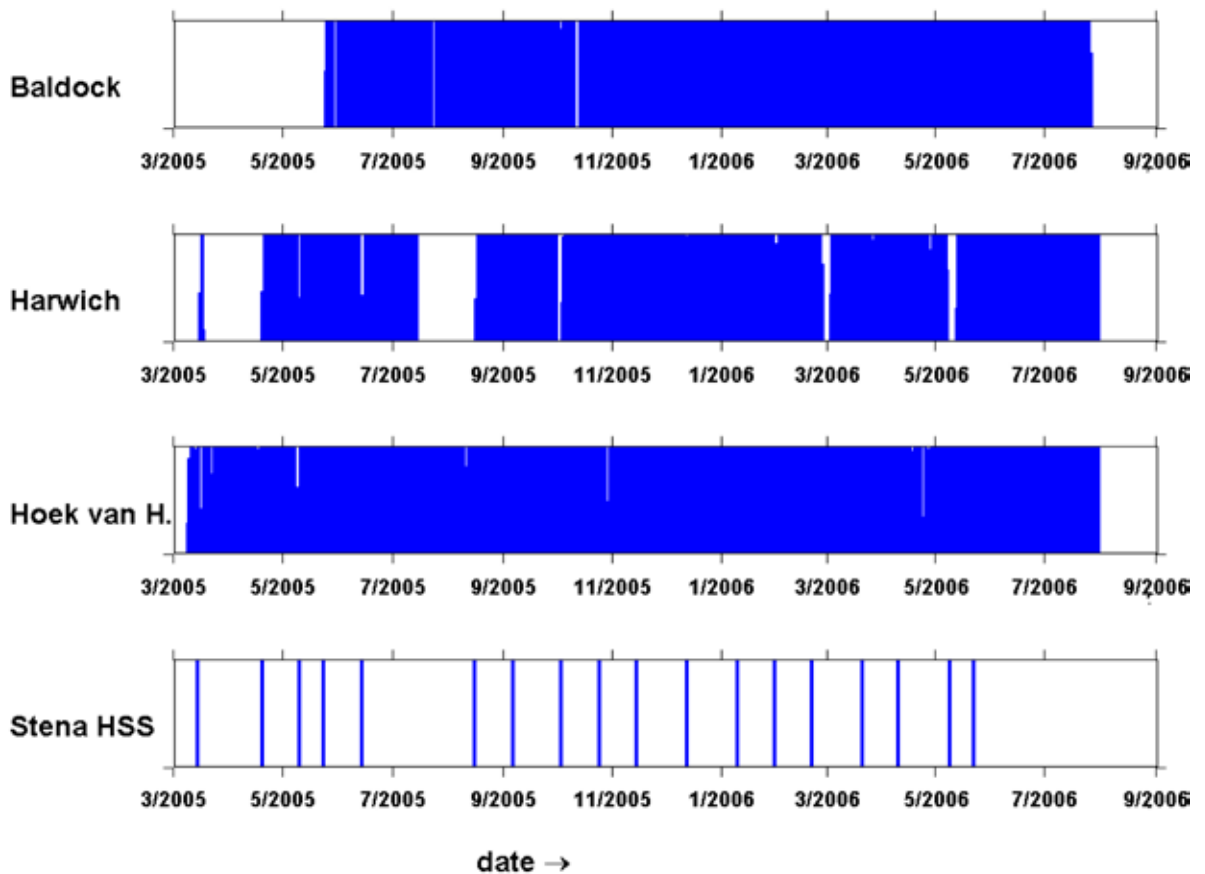


Figure 3-2: Collected measurement data on all measurement sites

### 3.2.2 Verification process

Taking an important number of calibrated field strength readings alone is not enough. The intrinsic value of the measurement campaign would change from mediocre to excellent if a validation method could be found to prove that the signals measured over such very long paths are not polluted with interferers or other flaws.

This quality assurance was difficult and required considerable human effort and skills. Using transmitter outages and transmitter frequency jumps as natural signal markers, and by comparing the measured absolute carrier frequency, we had enough information to validate all measurements. Also the signal-to-noise ratio and the number of measurements available for determining the low probability values needed to be taken into account.

The following paragraphs describe all steps that were taken to validate the collected measurement data.

### 3.2.3 Transmitter outages

Short transmitter outages were very suitable as markers with which to recognize the wanted signal. Identification of the wanted transmitter was easy at the Hoek van Holland site, where its signal was very strong. Short transmitter failures could be identified as short outages in the spectrogram. An example can be seen below:

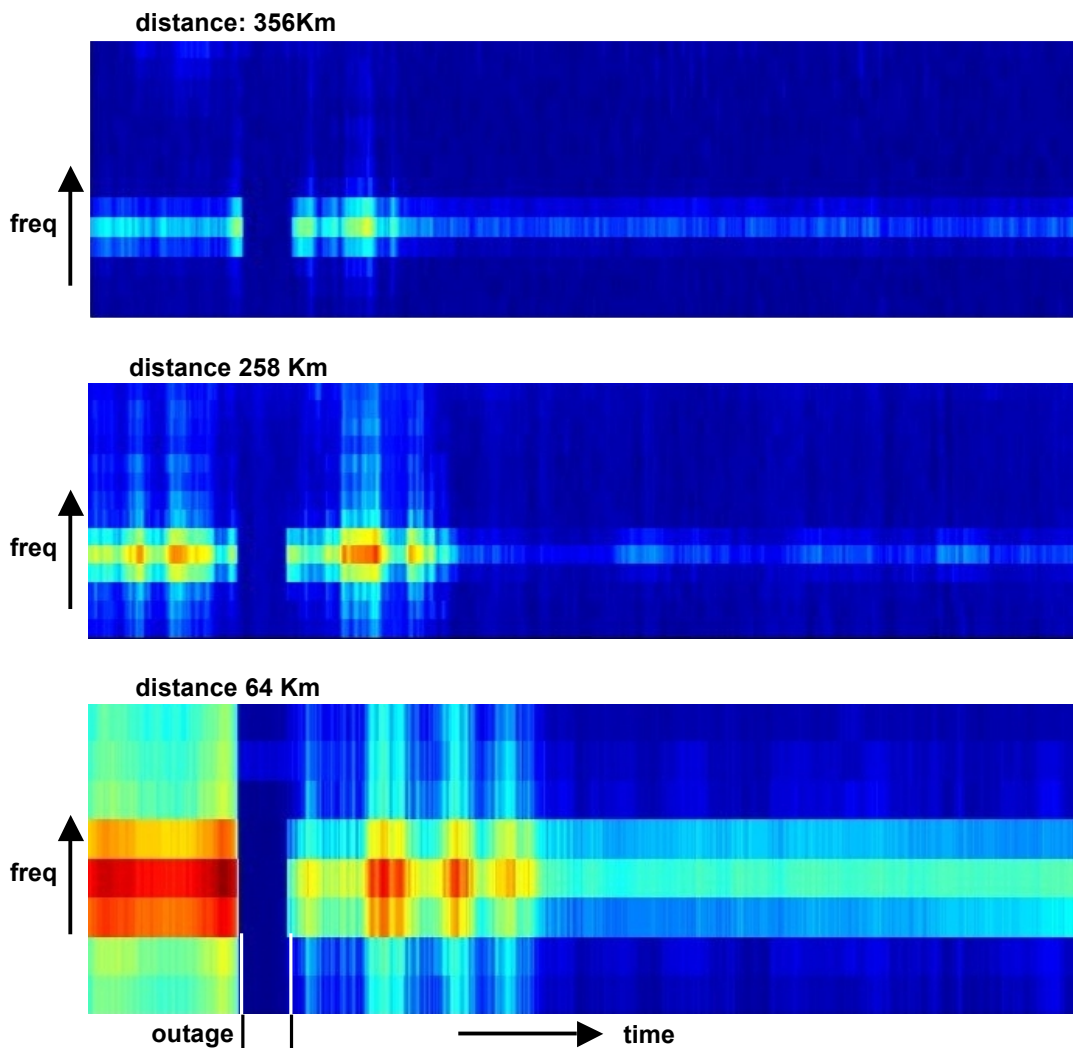


Figure 3-3: Transmitter outage used as a signal marker

By looking for outages in the spectrograms with the same starting time and duration and on the same frequency, the wanted signal could be identified with 100% certainty at the Harwich and Baldock receive sites. This was done throughout the whole propagation measurement period and for all 8 transmitters.

### 3.2.4 Frequency jumps

All TV transmitters observed had a backup transmitter. Primary and secondary transmitters were changed from time to time to assure equal wear and to allow for preventive maintenance. As each transmitter had its own frequency standard, this created sudden – if small – frequency jumps. These could be used as signal markers in the same way as the transmitter outages.

Figure 3-4 shows an example of such a frequency jump of the transmitter. In this example, a weak interferer is present on the remote receive sites, but the wanted signal can easily be identified by the carrier frequency jump. In this case, by dropping the highest three frequency bins at the 258 km site, we would get rid of the interferer and adaptive filtering would do the rest. At 356 km, dropping the highest six frequency bins would do the job.

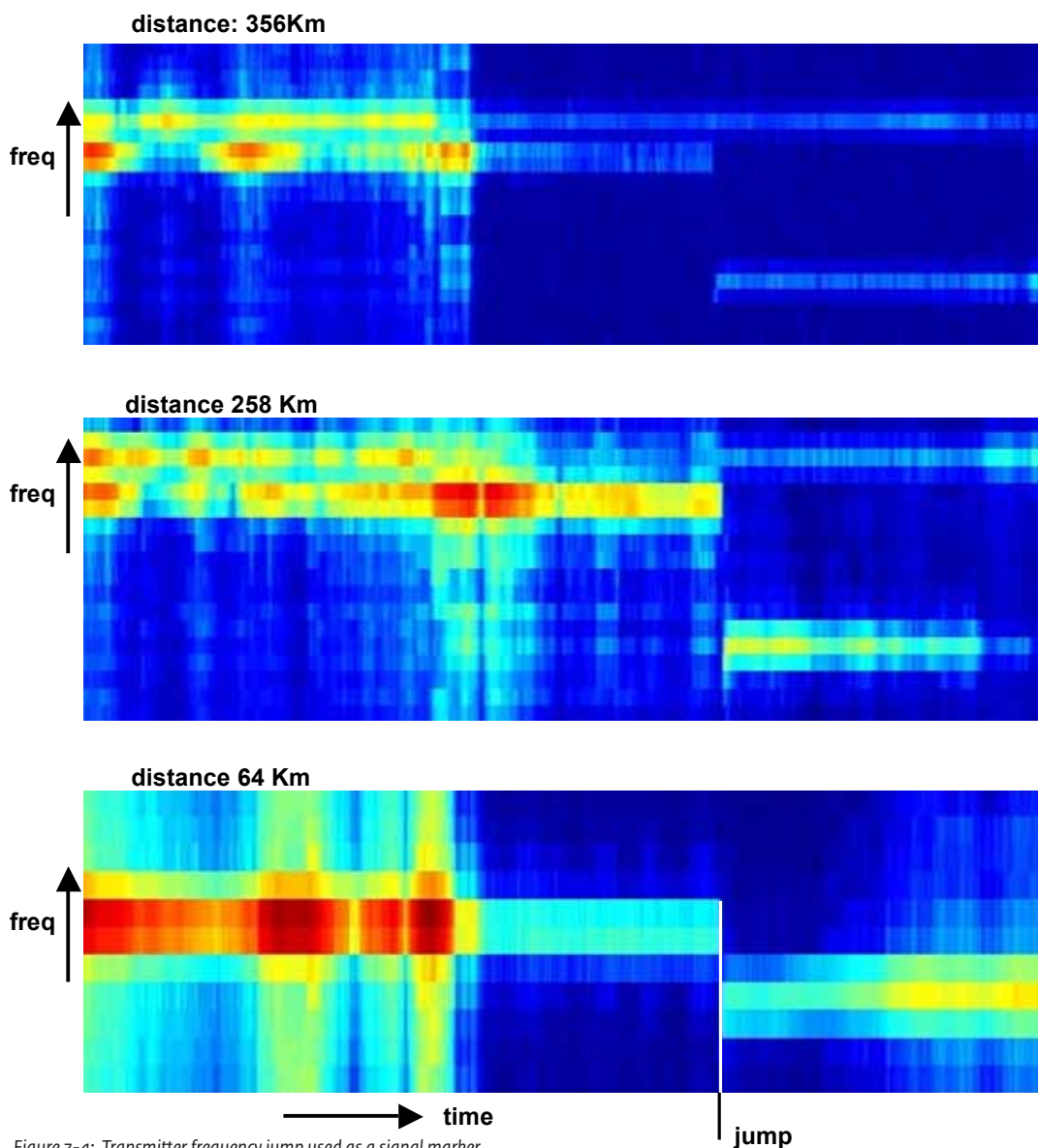


Figure 3-4: Transmitter frequency jump used as a signal marker

Not only the transmitter outages and frequency jumps of the wanted signal helped to distinguish between the wanted signal and possible interferers. Also an outage present in an interferer that was not observed in the signal of the wanted signal at 64 km distance gave clear information on what is what.

### 3.2.5 Field strength changes (not suitable)

In some early publications, sudden and very similarly shaped field strength variations on different points along the same propagation path have been submitted as “proof” of those measurements being on the same signal. However, our measurements proved this method was not valid.

We concluded this after comparing a substantial number of such occasions on the path from Lopik via Hoek van Holland and Harwich to Baldock. In many such instances of significant propagation enhancements, the propagation on totally unrelated paths could peak also at the same time and show very similar amplitude-over-time curves.

Yet, when looking at signal markers present, the amplitude-over-time curves of the wanted signal at the three different distances along the same path were often not correlated. Often the propagation enhancements had substantial time differences in their occurrence.

Worse still, interfering signals would pop out of the background noise almost simultaneously and could cause wrong readings if not filtered properly. Any measurement set-up using a bandwidth wider than ours would have measured a random mix of the wanted and the unwanted signal, resulting in a polluted data set.

We concluded that enhanced propagation on more than one geographical location was an extra reason to carefully validate the measurements in that interval, rather than a reason to assume correlation.

### 3.2.6 Pre-filtering

Using all techniques described above, the complete set of measurements from all sites was checked thoroughly. This was done by scrutinizing the spectrograms of the raw data and comparing the measurements performed on the same transmitter but at different receive sites.

In case the measurements of a specific day were not trusted, that data was discarded and not used for further analysis. In case the spectrogram showed signs of a weak interferer, pre-filtering parameters were added to a table, to help the adaptive filter to discard the frequency bins that only contained interference signals prior to the automated carrier detection and measurement.

The reception of Wieringen TV2 and TV3 in Baldock was impossible due to local signals on the same channel. Therefore those particular measurements were discarded.

### 3.2.7 Signal to noise ratio

Using this cleansed data set, analysis software was run to determine the >50%-of-time, >10%-of-time and >1%-of-time field strength thresholds. On those values, two additional questions were posed:

- Is the signal to noise ratio sufficient to give a meaningful value?
- Is the number of measurements for that percentage sufficient?

Table 3-5 shows the signal-to-noise ratio for each path and for each frequency on that path, calculated for the level of the 50%, 10% and 10%-time field strength value.

	HvH			Harw			Bald		
	50%	10%	1%	50%	10%	1%	50%	10%	1%
Gs1	64	70	78	39	72	87	10	22	48
Gs2	64	71	76	38	73	87	8	17	45
Gs3	64	72	78	35	70	86	-2	9	38
Lpk2	80	82	85	31	58	80	12	21	45
Lpk3	79	82	84	31	58	80	18	30	53
Wgm1	38	61	76	13	40	65	10	22	47
Wgm2	33	60	75	14	46	68	local interference		
Wgm3	33	59	74	13	40	65	local interference		

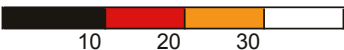


Table 3-5: Signal-to-noise ratio (dB)

The values in black boxes indicate an insufficient signal to noise ratio for further use. The values in red and orange should be considered with some healthy suspicion. The number of measurements for each 1% value was still between 4400 and 7500 measurements, so the second question posed no problem.

### 3.2.8 Correlation between fixed and maritime measurements

The maritime path profile measurements were performed on 18 randomly picked days spread evenly over the whole measurement period. To confirm that the propagation on these 18 days correctly represented the propagation over the full 500 day period, we compared the fixed site measurements for these 18 days on both ends of the maritime path with the measurements over the full 500 days period. The results are shown in figures 3-6 and 3-7.

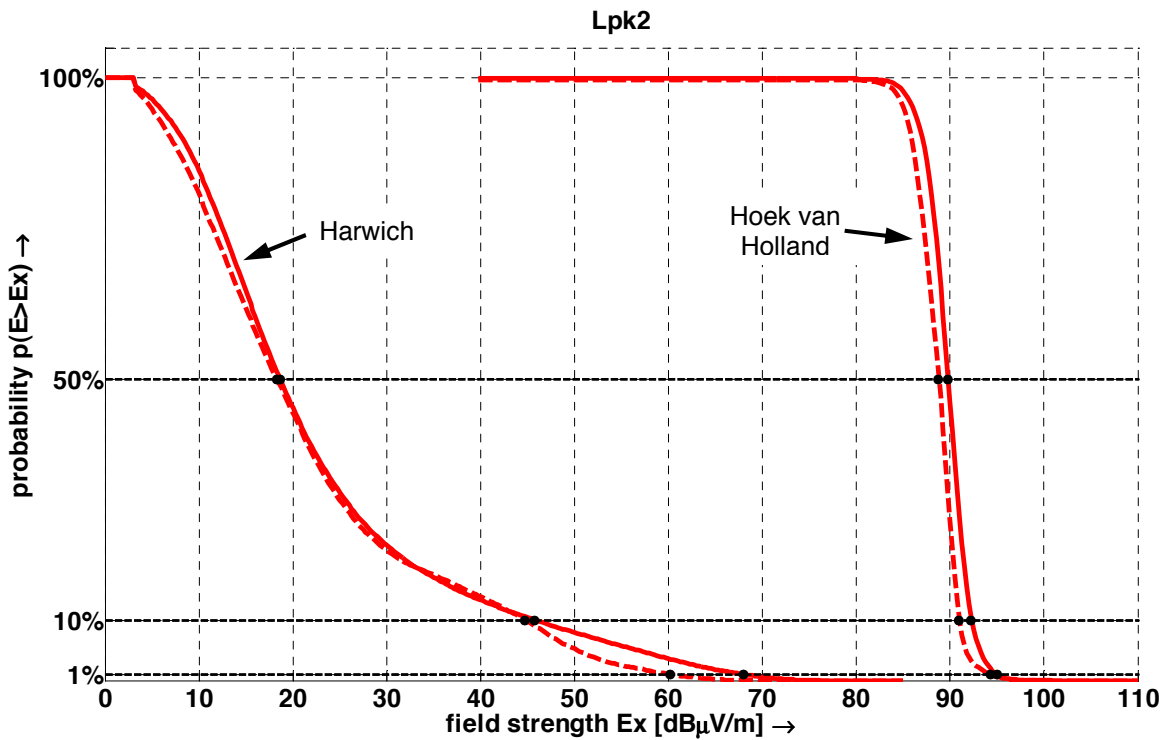


Figure 3-6 Comparison between 18 random days (dashed line) and 500 days continuous measurement (solid line) for Lopik TV2

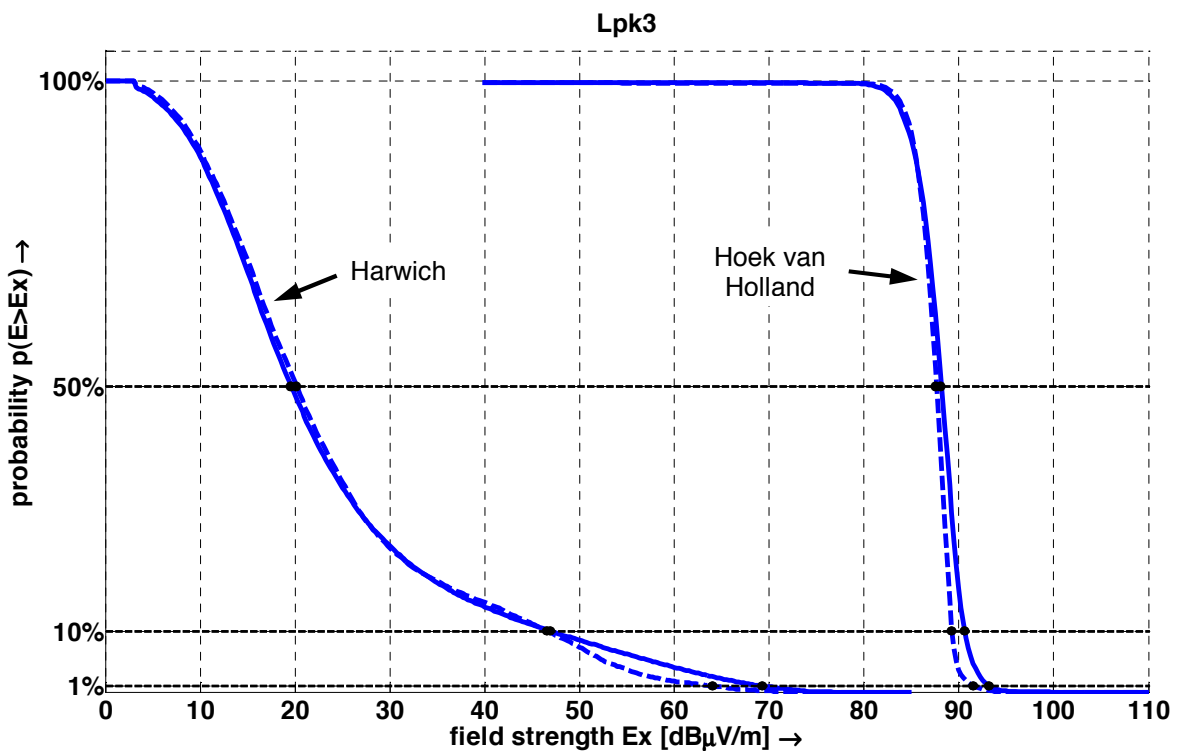


Figure 3-7: Comparison between 18 random days (dashed line) and 500 days continuous measurement (solid line) for Lopik TV3

As we can see, the measurements over 18 days (dashed line) exhibit a probability distribution very similar to that over 500 days (solid line). The differences at probability levels below 10% at low probability values are logical effects of the small sample size. So the 18 day sample is judged to be a good representation of the propagation over the total 500 day period.

### 3.2.9 Number of measurements left after validation

The validation effort results in a data set for the fixed measurement sites that is about 11% smaller than the original unchecked data. The remaining data set is still quite large and now has a very high reliability.

Path	Raw data		After validation		Loss
1: Lpk - HvH - HSS - Harw - Bald	507 days	3.000.430 meas.	500 days	2.970.524 meas.	
	18 days	46.316 meas.	18 days	46.316 meas.	
	428 days	1.391.758 meas.	403 days	1.293.797 meas.	
	425 days	1.481.980 meas.	425 days	1.480.073 meas.	
	total	5.920.484 meas.	total	5.790.710 meas.	
				-2%	
Path	Raw data		After validation		Loss
2: Goes - HvH	507 days	4.500.645 meas.	500 days	4.422.089 meas.	-2%
3: Goes - Harw	428 days	2.087.637 meas.	428 days	1.936.533 meas.	-7%
4: Goes - Bald	425 days	2.222.970 meas.	425 days	2.179.092 meas.	-2%
5: Wgm - HvH	507 days	4.500.645 meas.	507 days	4.496.443 meas.	0%
6: Wgm - Harw	428 days	2.087.637 meas.	413 days	1.604.123 meas.	-23%
7: Wgm - Bald	425 days	2.222.970 meas.	246 days	445.712 meas.	-80%
	grand total	23.542.988 meas.	grand total	20.874.702 meas.	-11%

Table 3-8: Data volume after validation

# 4 The measurement results

The results of the propagation measurement campaign are documented here, and some remarkable observations are highlighted.

## 4.1 The measurement results: general observations

This chapter contains general observations made during the measurements and during the analysis of the measurements. They are not path specific and do not yield results that can be quantified very specifically. Yet they give insight in the radio propagation processes involved.

### 4.1.1 Frequency dependency of the propagation

The three graphs show the signal from Goes transmit site over the full 500-day period of the path Goes-Hoek van Holland. The shown probability density functions (PDF) are plots directly from the (calibrated) measurement data, and the x-axis resolution is 0.25 dB. One graph is made for each of the transmit frequencies of the Goes TV tower.

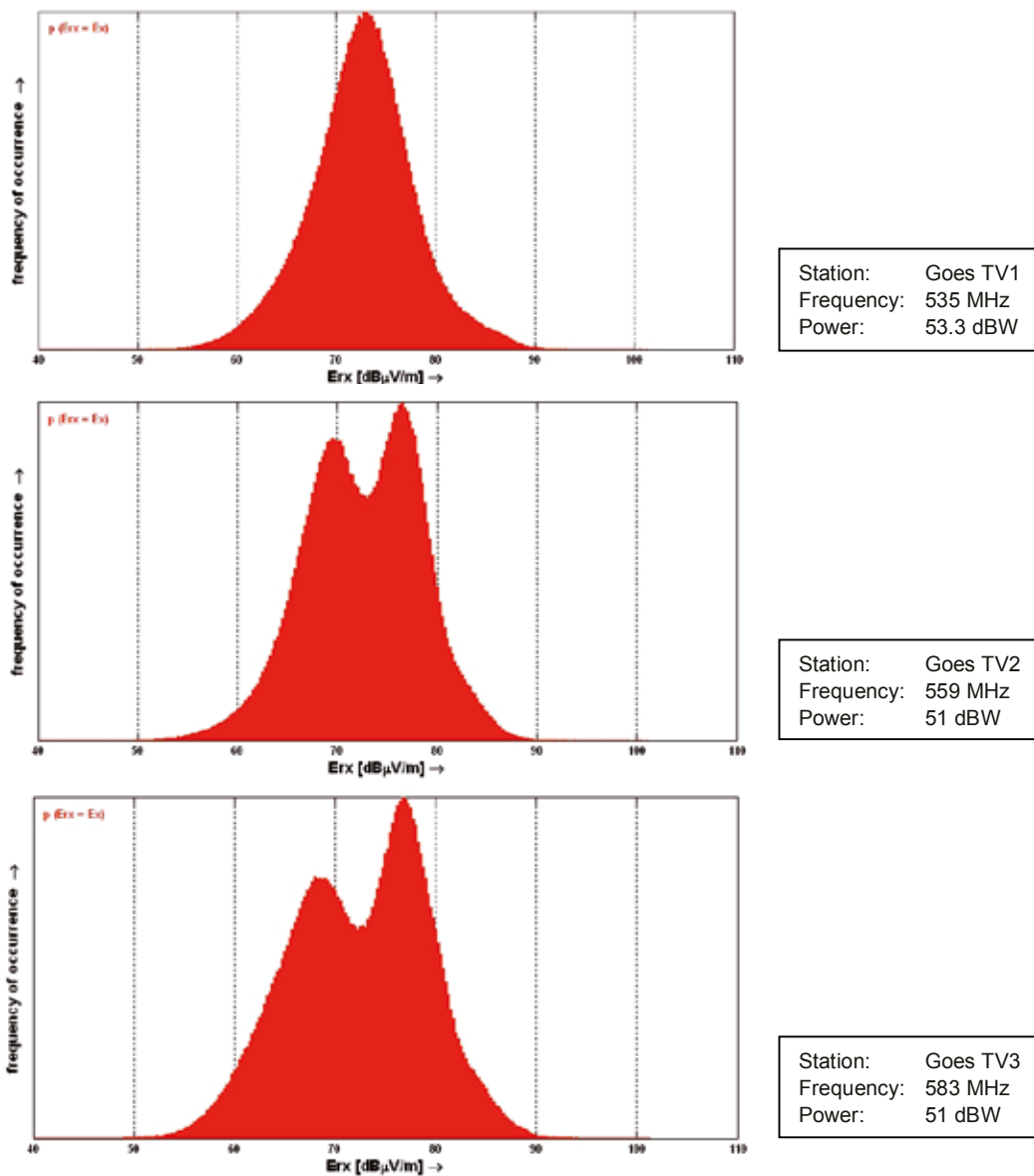


Figure 4-1: Frequency dependent probability distribution

The three measured stations have a fairly small difference in frequency: just 4.5% and 9%. Yet the shape of each PDF is completely different. There is no interference from other signals here; a very thorough check has been performed to assure only unpolluted data is used. See chapter 3.2.



On the lowest frequency we see a bell-shaped PDF. As the frequency increases, however, the PDF shows two peaks, indicating two field strength values occurring nearly as often. When the frequency increases further, the higher peak becomes even more pronounced. It seems that this path has two propagation modes that both occur with nearly the same probability, with a difference in the mean value of about 8 dB. The propagation of these modes seems to be strongly frequency dependent.

The mean value of the measurements is identical for all three frequencies; see the cumulative distribution functions for path 2 in figure 4-15.

The path from Goes to Hoek van Holland is a short one, only 55 km. The other paths also show a clear frequency dependent behaviour, but the changes to the PDF may be more complex, as indicated in figure 4-2:

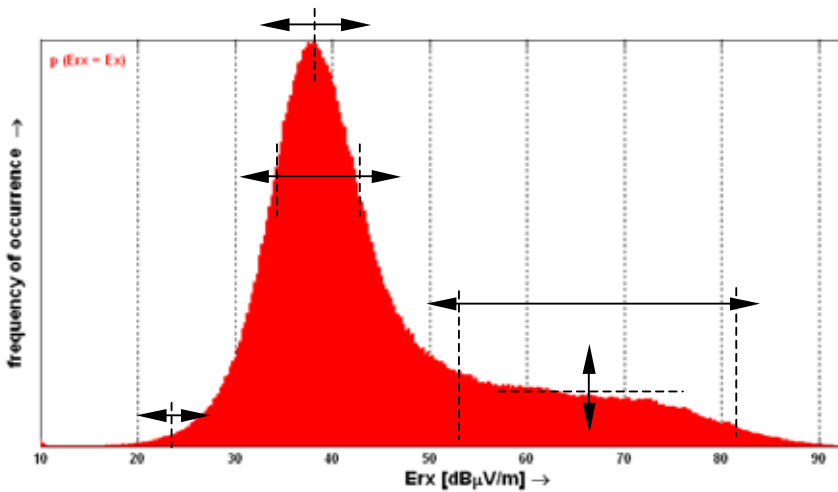


Figure 4-2: Longer paths: changes to the probability distribution depending on the frequency

#### 4.1.2 Probability density function is not Gaussian

Close to the transmitter, where line of sight propagation is dominant, the field strength distribution resembles a Gaussian (log-normal) field strength distribution. At greater distances, other propagation effects distort this shape.

Figure 4-3 shows the probability density function of the measured field strength over a 121 km path as an example. A Gaussian (log-normal) distribution is superimposed over the measured probability density for comparison. This PDF is typical for most paths in this measurement campaign.

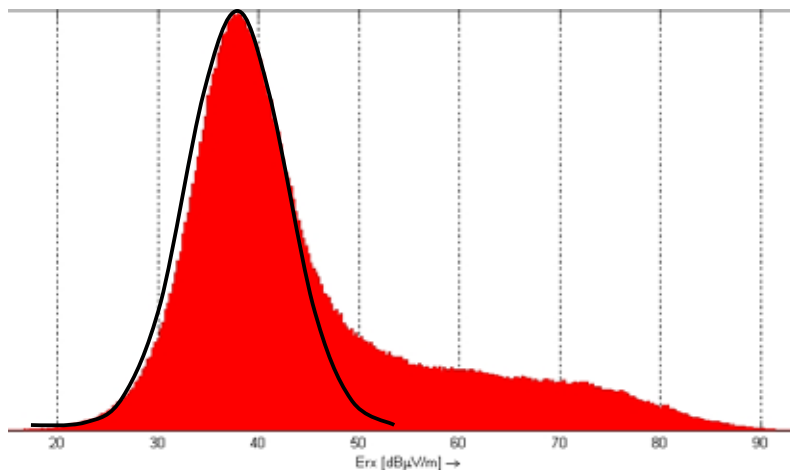


Figure 4-3: Example of a 500-day PDF over 121 km, 45% sea (Wgm3 to HvH)

Our measurements show that already at 70 or 80% of the distance of radio horizon, the probability density function becomes asymmetrical, with substantial deviations to higher field strength values. On longer paths, these effects becomes very prominent. Conclusion: a Gaussian (log-normal) distribution is not adequate to describe the probability distribution of the received field strength or the path loss.

The propagation measurements we performed concentrated on combined land-sea propagation paths. We therefore can only submit proof for the above conclusion for such paths, and not for long distance land mass only propagation paths. However, experience with many individual events of enhanced UHF propagation over land masses, makes us believe this same conclusion may be valid for land mass only UHF propagation as well.

#### 4.1.3 Composition of the probability density function

To find out how this probability density function receives its shape, we have to split the total measurement campaign period in smaller time intervals. When the intervals are chosen to show more or less stable propagation (whether that propagation is enhanced or not), they show a near-Gaussian probability distribution. The median value and standard deviation per interval differs. As a result of that, and of their individual probability of occurrence, the individual Gaussian distributions add up to the total PDF and the shape we have seen takes form.

The next step is to try to compose the measured PDF from a minimum number of self defined Gaussian PDF's. If this is successful, the identified components distributions could help to understand the underlying propagation modes. We start out by fitting the dominant peak of the PDF with a single Gaussian distribution. This first distribution represents the propagation modus that occurs most of the time.

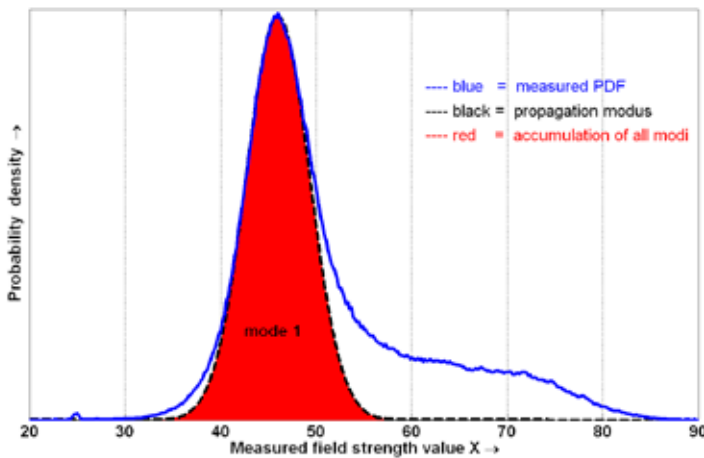


Figure 4-4

Next we add another Gaussian distribution, with such parameters that it follows the upper slope of the PDF. This distribution represents the propagation mode that yields the greatest signal enhancement.

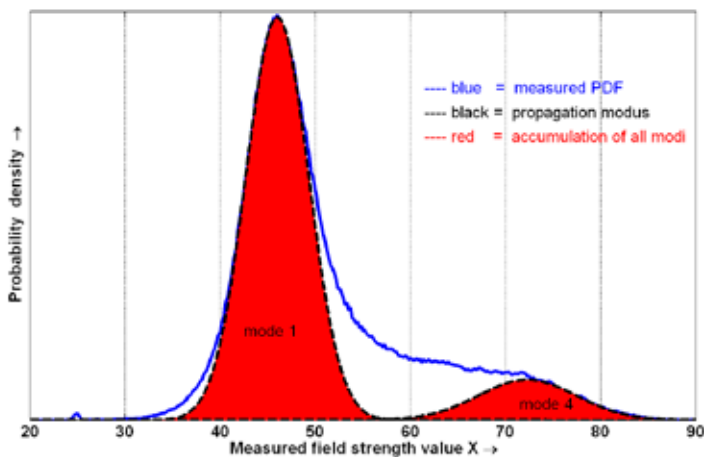


Figure 4-5

Two more Gaussian distributions are needed to fill up the space in between these two.

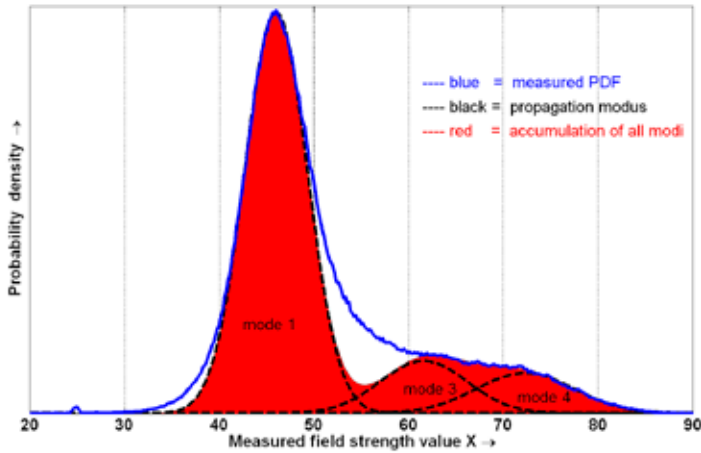


Figure 4-6

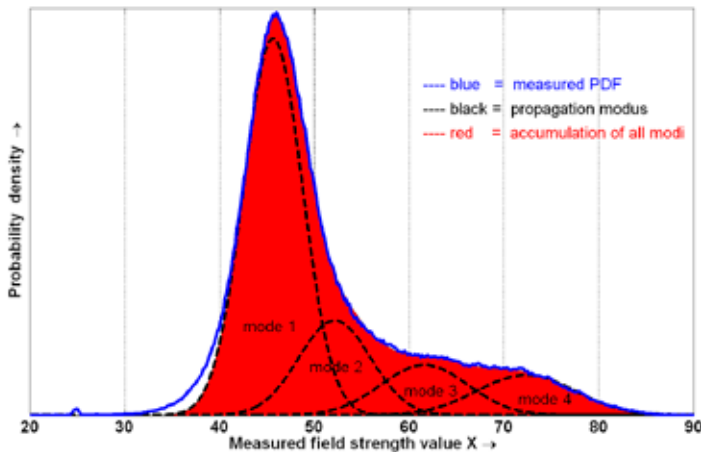


Figure 4-7

Up to this point, the match is already very good. Only the left side of the graph leaves a difference with the measured PDF. To fill in the difference between the dominant Gaussian distribution and the measured PDF on the left side, we have to add a distribution left (!) of the dominant peak.

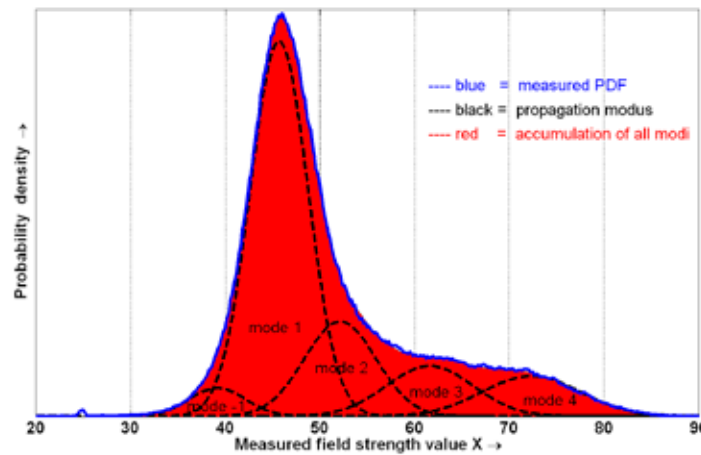


Figure 4-8

The result is a near perfect replication of the measured PDF.

The parameters used for generating the previous graph are as follows:

Propagation mode	Mean field strength	Standard deviation	Occurance
-1	39 dB $\mu$ V/m	3.0 dB	4%
1	46 dB $\mu$ V/m	3.1 dB	57%
2	52 dB $\mu$ V/m	3.8 dB	18%
3	62 dB $\mu$ V/m	4.6 dB	11%
4	72 dB $\mu$ V/m	5.2 dB	10%

Table 4-9: Individual propagation modes and occurrence

So apparently the measured probability density function can be seen as a composition of 5 propagation modes, each having a Gaussian distribution. These values are only valid in this example. Each path yields its own specific values.

When we try to relate these composing distributions with propagation modes that exist, mode 1 would represent the dominant propagation mode for this particular path, while modes 2 through 4 represent the different tropospheric ducting scenario's. Mode -1 represents measurements during periods of time where there is refraction away from the horizon, causing signal loss compared to the dominant mode.

Of course this exercise to compose the measured PDF with the smallest number of virtual propagation modes is only a theoretical one. In reality many more propagation modes may temporarily occur. There is no need to assume there are only 5 modes. Yet these plots give some insight in the phenomenon creating this non-Gaussian distribution.

#### 4.1.4 Seasonal influences

VHF and UHF radio propagation over long distances is marked by events of tropospheric ducting, caused by temperature inversion layers in the troposphere. These inversions "bend" the radio path over the horizon, causing a dramatically enhanced signal strength. An excellent description of this ducting phenomenon can be found in 'VHF and Microwave Propagation Characteristics of Ducts' by Andrew Martin [8].

VHF transmission beyond line-of-sight was already discovered by Marconi in 1933 [9]. The first one to associate this phenomenon with meteorological conditions in 1934 was Ross Hull, a radio amateur [10].

Enhanced propagation due to tropospheric ducting may last a fraction of an hour, but stable long distance tropospheric radio paths sometimes remain in place for several days. These special conditions may occur at any time of the year, but autumn is known for its high probability of exceptional tropospheric radio propagation.

We analyzed our measurement data to see if we could see any seasonal influences on the median, 10% time and 1% time values as function of the month. During our measurement campaign, the enhanced propagation occurred from April through October and in January and February. The signal enhancement was significant: up to 40 dB enhancements of the 1% time value.

The aforementioned preference for autumn was not confirmed by our measurements. Maybe the 500-day duration of this measurement campaign was not long enough to show this yearly periodicity.

## 4.2 The measurement results for each path

### 4.2.1 Path 1: fixed locations

The radio path from Lopik to Baldock is the best documented path of this measurement campaign. The transmitter is located near Utrecht in the Netherlands, the receivers are located:

- in Hoek van Holland, in the dunes close to the sea front;
- on the Stena HSS ferry between Hoek van Holland and Harwich;
- in Harwich, in a lighthouse overlooking the sea;
- in Baldock, on a hill looking in the direction of the Netherlands.

See the map below:

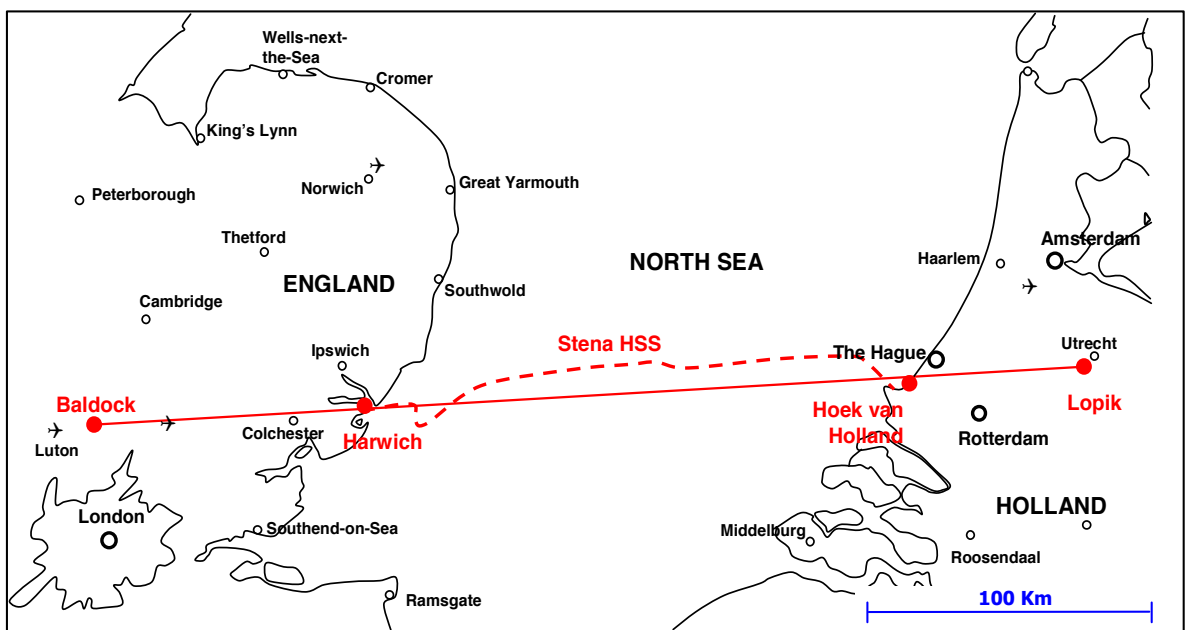


Figure 4-10: Map showing path 1 and its receive locations

All technical path information can be found in annex A. A summary of the path distances:

- The distance from Lopik to Hoek van Holland is 64 km and the signal travels over land only;
- The distance from Lopik to Harwich is 258 km and 75% of the path consists of sea;
- The distance from Lopik to Baldock is 356 km and 53% of the path consists of sea.

The measurements were performed on two frequencies: 519 MHz and 543 MHz. The transmit power was 59 dBW on both frequencies. The transmit antenna height was 363 metres.

A total of 5,800,000 measurements values were collected on this path. A cumulative distribution figure of the measured field strength is plotted for the receive locations in Baldock, Harwich and Hoek van Holland. See figure 4-11.

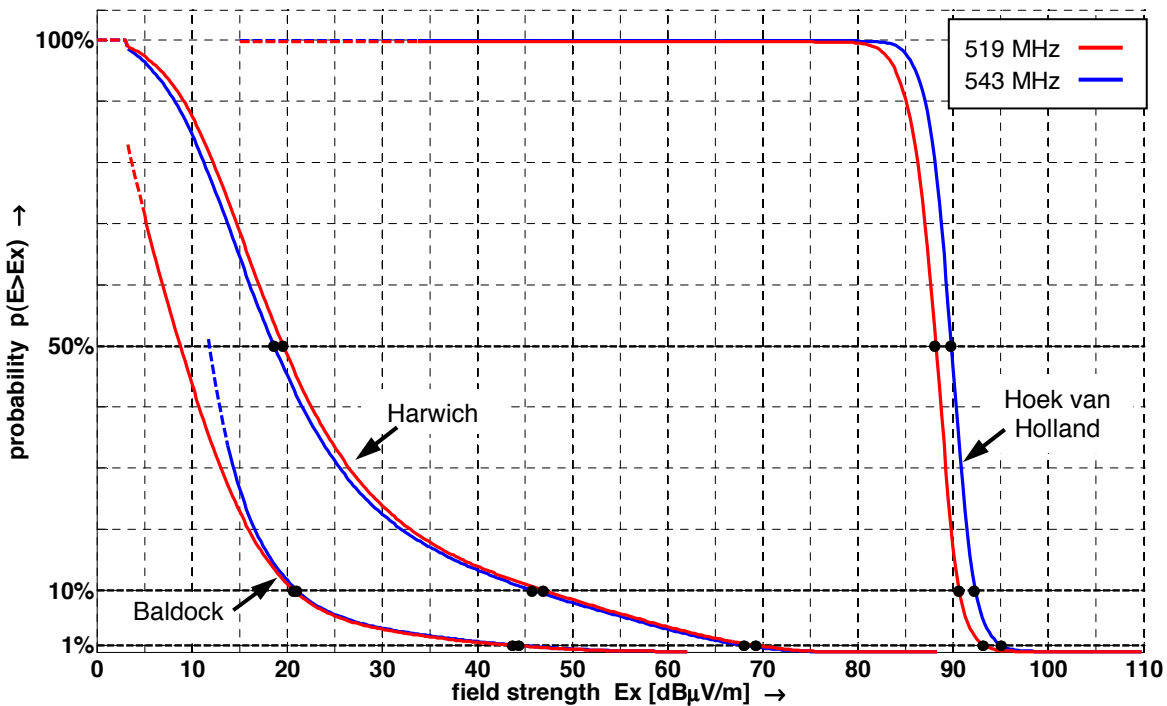


Figure 4-11: Cumulative distribution function for three receive locations on path 1

An example taken from this graph: in Harwich, the signal strength of the Lopik transmitter can be received 10% of the year with a signal strength of 46 dBμV/m.

The values taken from the cumulative distribution graph are useful for frequency planning and interference management purposes. They show the probability that the signal strength of a distant transmitter will exceed a certain threshold value, and will cause interference in the coverage area of another.

For frequency planning and interference management, the field strength values above which the signal has occurred 1% of the time, 10% of the time and 50% of the time (the median value) are often used. They are shown in the graph as black bullet points. The exact values have been determined by the analysis software that also created the graph. They are:

Field strength (dBμV/m)		Hoek van Holland			Harwich			Baldock		
Transmitter	Ch	50% time	10% time	1% time	50% time	10% time	1% time	50% time	10% time	1% time
Lopik TV2	27	89,8	92,3	95,0	18,8	45,8	68,0	-	21,0	44,5
Lopik TV3	30	88,3	90,8	93,3	19,5	47,0	69,3	-	20,8	43,8

Table 4-12: Field strength values above which the signal has occurred n% of the time

The 50% values for Baldock are not given, as the signal quality at the receive location was too low. The field strength of both frequencies differs slightly, but the general trend is very similar.

#### 4.2.2 Path 1: maritime mobile measurements

The measurements on board the Stena HSS 'Discovery' yielded a path profile between Hoek van Holland and Harwich. Measurements were performed on 18 days spread evenly over the 1.5 year period that the measurement campaign lasted. Measurements were always taken sailing from Hoek van Holland to Harwich.

A total of 46,000 measurements values were collected. From these values, the 50%, 10% and 1% time values were determined as a function of the distance to the transmitter. See figure 4-13. The light blue dots show the individual measurement values.

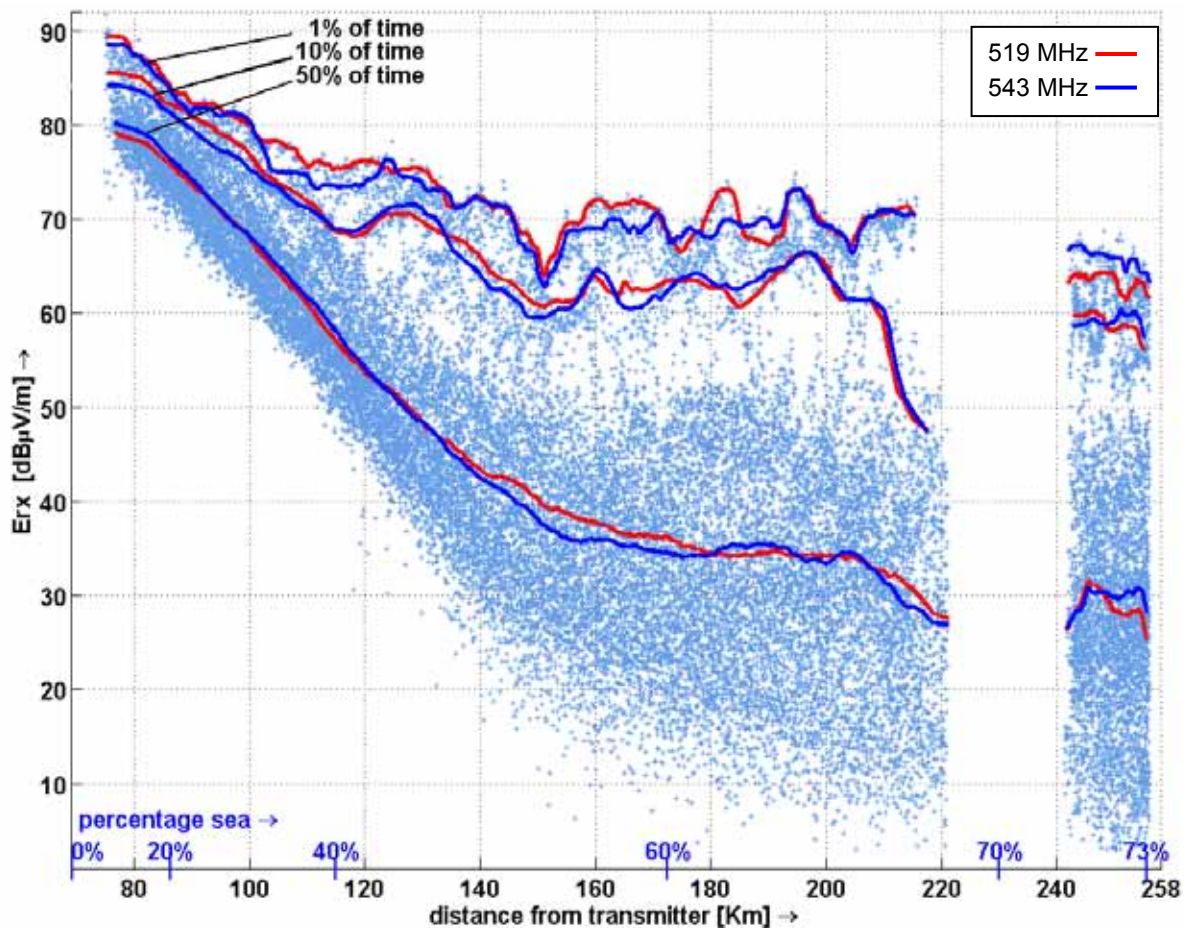


Figure 4-13: Path profile measured on board the Stena HSS 'Discovery'

The maritime path of the Stena HSS 'Discovery' high speed ferry starts in Hoek van Holland at 69 km from Lopik and ends in the harbour of Harwich at 258 km distance. The percentage of sea versus the total distance is shown on a secondary axis for reference. Measurements were performed over the major part of this path, but some gaps can be seen:

- The first 10 km, the ship is manoeuvring out of the Hoek van Holland harbour, and is partly shielded from the transmitter by the high dunes. So the measurements start at approximately 75 to 80 km from the transmitter.
- During the normal crossover from Holland to England, the fast catamaran ferry has to manoeuvre in order to avoid other ship traffic. The antenna misalignment caused by these movements is always less than 20°. The momentary direction of the vessel is calculated from the GPS position measurements, and the antenna gain loss is compensation for using the known horizontal antenna diagram.
- From 220 km to 240 km, the ship makes a wide zigzag movement to access the Harwich harbour. During these movements, the beam direction of the measurement antenna deviates too much from the direction towards the transmitter, so these measurements are not used. The measurements close to Harwich harbour are included again, although they may suffer from shielding by high objects between the harbour and Lopik.

#### 4.2.3 Paths 2, 3 and 4

Using the transmitter in Goes, three other radio paths were measured in this measurement campaign. They are depicted as path numbers 2, 3 and 4 and shown on figure 4-14.



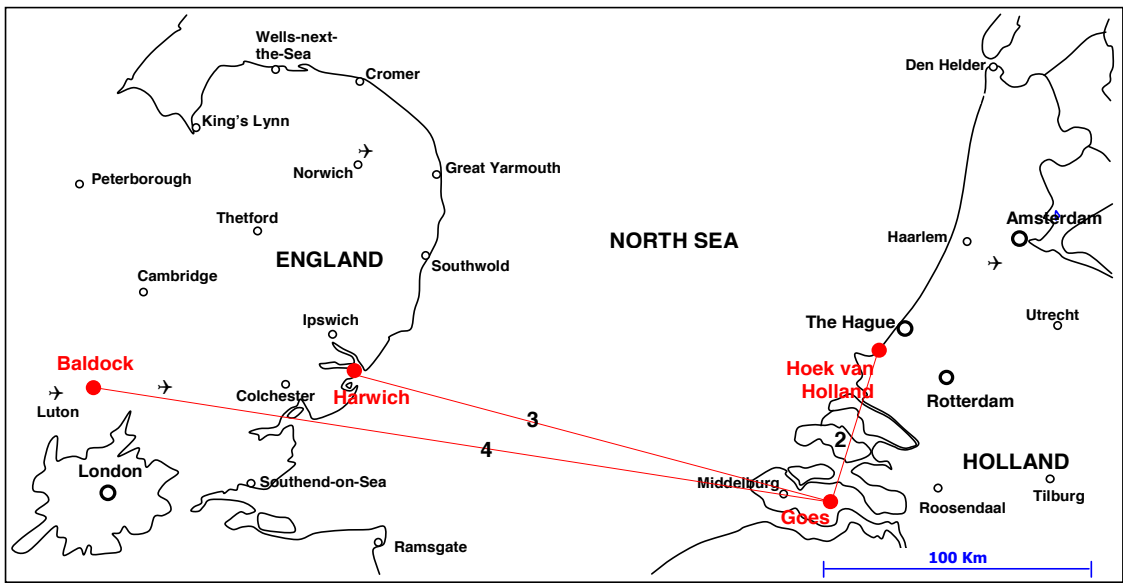


Figure 4-14: Map showing path 2, 3 and 4 and its receive locations

A summary of the path distances:

- The distance from Goes to Hoek van Holland is 55 km, and 17% of the path consists of sea;
- The distance from Goes to Harwich is 186 km, and 85% of the path consists of sea;
- The distance from Goes to Baldock is 282 km, and 56% of the path consists of sea.

The measurements were performed on three frequencies: 535 MHz, 559 MHz and 583 MHz. Transmit power is 53 dBW on the first frequency, and 51 dBW on the other two. Transmit antenna height is 137 metres. An overview of all technical information can be found in annex A.

A total of 8,500,000 measurements values was collected on these three paths. A cumulative distribution figure of the measured field strength is plotted for the receive locations in Baldock, Harwich and Hoek van Holland. See figure 4-15.

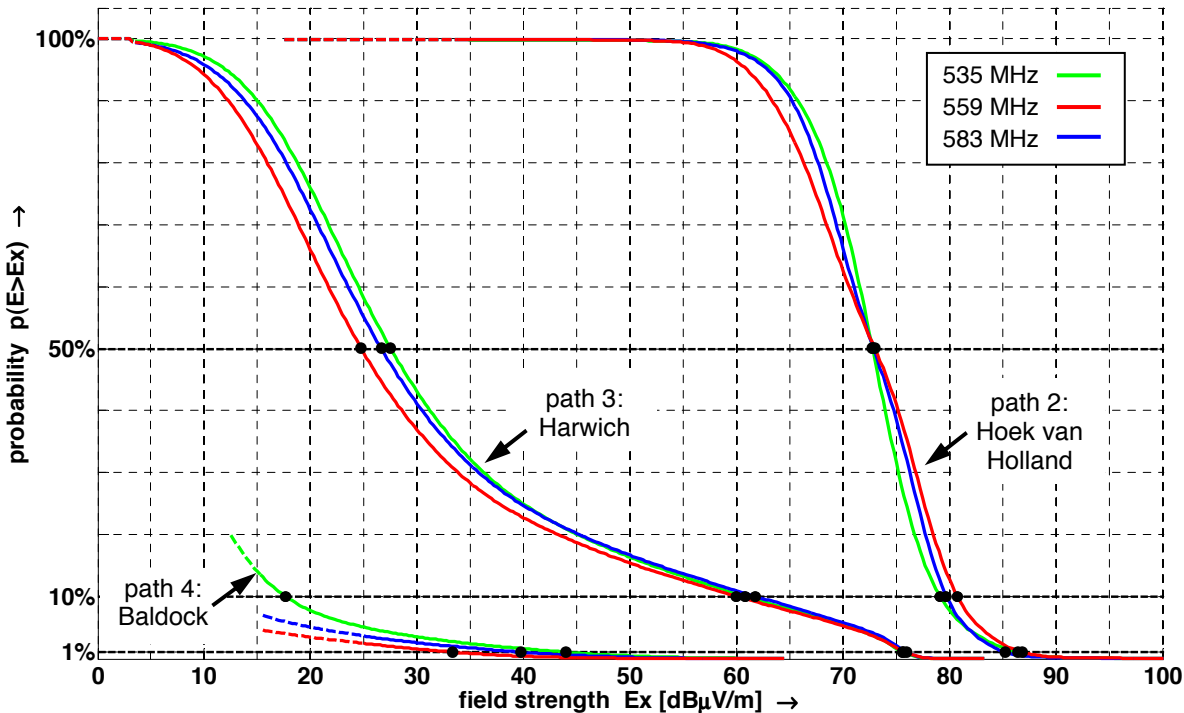


Figure 4-15: Cumulative distribution function for three receive locations on paths 2, 3 and 4



The field strength values above which the signal occurred 1% of the time, 10% of the time and 50% of the time (the median value) are shown in the table below:

Field strength (dB $\mu$ V/m)		Hoek van Holland			Harwich			Baldock		
Transmitter	Ch	50% time	10% time	1% time	50% time	10% time	1% time	50% time	10% time	1% time
Goes TV1	29	72,8	79,3	86,5	27,5	60,8	75,8	-	17,8	44,0
Goes TV2	32	73,0	79,8	85,3	26,8	61,8	76,0	-	-	39,8
Goes TV3	35	73,0	80,8	86,8	24,8	60,0	75,8	-	-	33,5

Table 4-16: Field strength values above which the signal has occurred n% of the time

#### 4.2.4 Paths 5, 6 and 7

Using the transmitter in Wieringen, another three radio paths were measured in this measurement campaign. They are depicted as path numbers 5, 6 and 7 and shown on the map below:

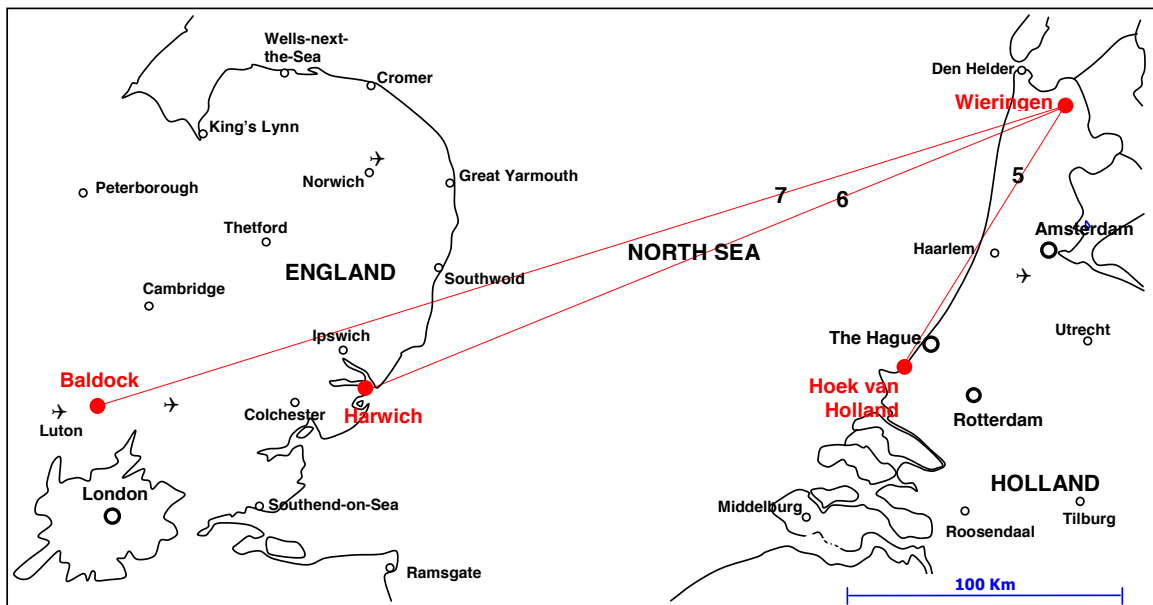


Figure 4-17: Map showing path 5, 6 and 7 and its receive locations

A summary of the path distances:

- The distance from Wieringen to Hoek van Holland is 121 km. 45% of the path consists of sea;
- The distance from Wieringen to Harwich is 277 km, and 88% of the path consists of sea;
- The distance from Wieringen to Baldock is 367 km, and 58% of the path consists of sea.

The measurements were performed on three frequencies: 615 MHz, 639 MHz and 663 MHz. Transmit power is 55 dBW on all three frequencies. Transmit antenna height is 196 metres. An overview of all technical information can be found in annex A.

A total of 6,500,000 measurements values was collected on these three paths. A cumulative distribution figure of the measured field strength is plot for the receive locations in Baldock, Harwich and Hoek van Holland. See figure 4-18.

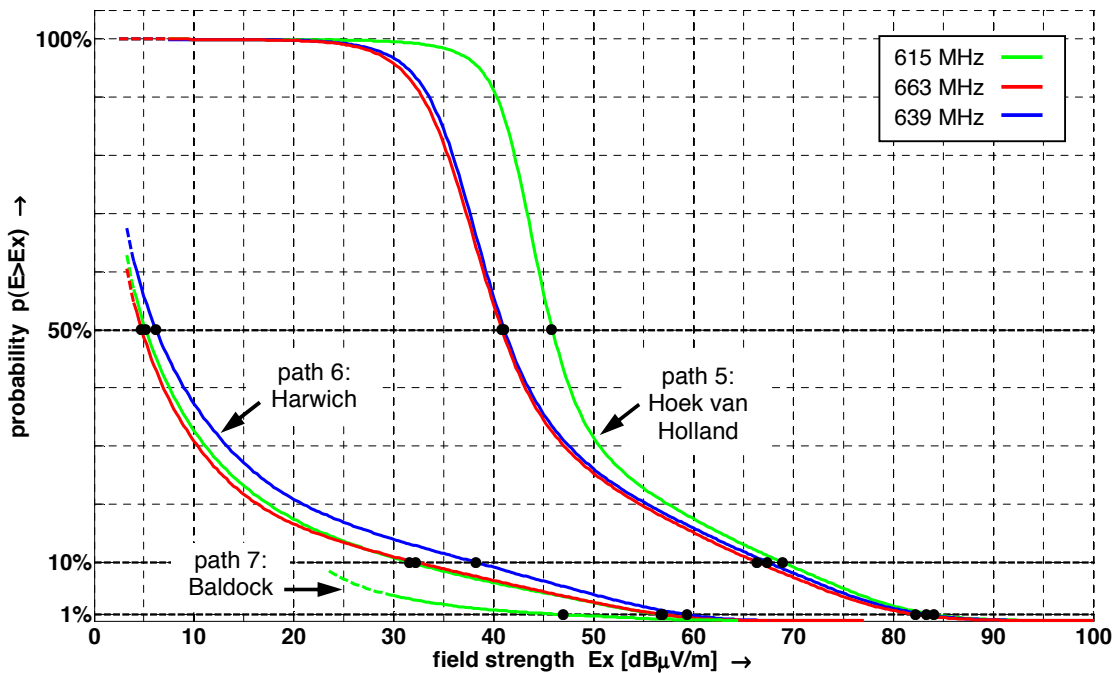


Figure 4-18: Cumulative distribution function for the receive locations on path 5, 6 and 7

The field strength values above which the signal occurred 1% of the time, 10% of the time and 50% of the time (the median value) are shown in the table below:

Field strength (dBμV/m)		Hoek van Holland			Harwich			Baldock		
Transmitter	Ch	50% time	10% time	1% time	50% time	10% time	1% time	50% time	10% time	1% time
Wieringen TV1	39	45,8	69,0	84,0	-	31,5	56,8	-	22,3	47,0
Wieringen TV2	45	41,0	67,5	83,3	-	38,3	59,5	-	-	-
Wieringen TV3	42	40,8	66,5	82,3	-	32,3	57,0	-	-	-

Table 4-19: Field strength values above which the signal occurred n% of the time

#### 4.2.5 An overview of all paths (measured)

An overview of the field strength values of all paths, above which the signal occurred 1% of the time, 10% of the time and 50% of the time (the median value) is shown below:

Field strength (dBμV/m)		Hoek van Holland			Harwich			Baldock		
Transmitter	Ch	50% time	10% time	1% time	50% time	10% time	1% time	50% time	10% time	1% time
Goes TV1	29	72,8	79,3	86,5	27,5	60,8	75,8	-	17,8	44,0
Goes TV2	32	73,0	79,8	85,3	26,8	61,8	76,0	-	-	39,8
Goes TV3	35	73,0	80,8	86,8	24,8	60,0	75,8	-	-	33,5
Lopik TV2	27	89,8	92,3	95,0	18,8	45,8	68,0	-	21,0	44,5
Lopik TV3	30	88,3	90,8	93,3	19,5	47,0	69,3	-	20,8	43,8
Wieringen TV1	39	45,8	69,0	84,0	-	31,5	56,8	-	22,3	47,0
Wieringen TV2	45	41,0	67,5	83,3	-	38,3	59,5	-	-	-
Wieringen TV3	42	40,8	66,5	82,3	-	32,3	57,0	-	-	-

Table 4-20: Field strength values above which the signal occurred n% of the time

### 4.3 Measurement uncertainty

All previous measurement values have been expressed in absolute field strength values. That means that all values can be traced to international standards through the calibration of measurement equipment and calibrated measurements of auxiliary equipment (antennas, cables etcetera).

The term 'absolute' in 'absolute field strength' could be misinterpreted though. Although the absolute level of the field strength is measured, as opposed to a relative level, the value is not exact. Each measurement value shown has a small but real error margin. That error margin is statistically defined and known as 'measurement uncertainty'. Measurement value and measurement uncertainty describe the interval in which the real absolute field strength lies with 95% certainty.

The parameters that contribute significantly to the overall measurement uncertainty are used in a measurement uncertainty calculation. Their probability distribution and standard deviation are known from calibrations or are estimated, and the total measurement uncertainty is calculated.

The methodology and definitions used were taken from "Expression of the Uncertainty of Measurement in Calibration", EA-4/02, of the "European co-operation for Accreditation". The detailed analysis can be found in annex D.

The combined expanded measurement uncertainty (95% confidence), calculated for one individual measurement value is:

Location	Expanded measurement uncertainty ( $2\sigma$ )
Hoek van Holland	2,4 dB
Harwich	2,6 dB
Baldock	2,6 dB
Stena HSS	3,3 dB

Table 4-21: Expanded measurement uncertainty ( $2\sigma$ ) for an individual measurement value

The field strength values for 50%, 10% or 1% of the time were calculated from more than 250,000, 50,000 and 5000 measurements respectively. This reduces the random error sources of the measurement uncertainty to nil, leaving only the systematic error sources. So the expanded measurement uncertainty for these values is slightly lower than the values of table 4-21.



# 5 Predictions using ITU-R P.1546

Using all known transmitter and path parameters, the expected radio propagation was calculated using the ITU propagation model.

## 5.1 Model used and input parameters

In the previous chapters we have described the measurement campaign and the calibration and validation of the measurement data and the analyzed results per propagation path. As we want to compare these measurement results with the predictions of the propagation model described in Recommendation ITU-R P.1546, we calculate the received field strength at the fixed receive locations. The predicted path profile for the maritime mobile measurement between Hoek van Holland and Harwich is also calculated.

For these calculations we use the actual transmitter and receiver site parameters, determined as accurately as possible. The choice of the P.1546 version and the input parameters are described in this chapter. The calculations themselves are found in chapter 5.2, and the prediction uncertainty is treated in chapter 5.3. The comparison with the measurement results is described in chapter 6.

### 5.1.1 Version of the model

Since its introduction in 2001, the ITU-R has revised Recommendation P.1546 on a number of occasions. So when we compare our propagation measurements with P.1546, we have to be specific in the version of the model used. Every revision is indicated by an extra suffix on the recommendation number, the first revision being P.1546-1. The latest version is P.1546-4 and dates from 2009 [1].

In the final acts of the RRC 2006 (see paragraph 1.4), a special version of P.1546-2 was coded for coordination-purposes. This version is widely used at the moment for international coordination of digital television. However, the difference between this version and P.1546-4 are negligible for the Dutch situation. The main difference between version 2 and 4 is the ability to cope with more types of propagation media. The relevant media for the Dutch situation are the same in both models.

We therefore chose P.1546-4 as our reference model in this study. Occasionally we side-step to older model versions (including ITU-R P.370-7) to highlight differences with past versions. The computer programs used to do the calculations were first verified with manual calculations to see if they did really give the same results as the model described in the ITU-R recommendation.

### 5.1.2 Propagation prediction software verification

We had the possibility to use a commercial propagation prediction software package with an integrated terrain database. To avoid wrong conclusions because of errors in the commercial software, we thoroughly checked the implementation of P.1546-4 in this software. To do so, we did our calculations manually and straight from the procedure described in the recommendation P.1546-4 for some simple paths and for some of the paths we study here. We compared the results of our manual calculations with those from the commercial implementation.

We found differences with the official ITU-R model, and differences that were too large to ignore. As a result of that, we could not use the commercial software for our path calculations, and were obliged to do all calculations by hand. To speed up those manual calculations, we implemented them in MatLab. Of course, we had to check the predictions of the MatLab scripts as well.

### 5.1.3 Model input parameters

Before calculations could be done, the right input parameters of the model had to be determined. The following input parameters were required:

- transmitter: transmit frequency, transmitter location, ERP, antenna diagram and effective transmit antenna height;
- receiver: receiver location, receiver antenna height, clutter height and Terrain Clearance Angle;
- path: distance and percentage sea.

The input parameters are described in the following paragraphs.

### 5.1.4 Transmitter input parameters

The transmitter parameters that are relevant for the P.1546-4 calculations are: transmit frequency, transmitter location, ERP, antenna diagram and effective transmit antenna height. Table 5-1 gives the location and the frequency of the transmitter parameters used in the calculations.

Transmitter	Channel	Vision carrier	Coordinates
Goes	TV1	29	535,24 MHz
	TV2	32	559,26 MHz
	TV3	35	583,25 MHz
Lopik	TV2	27	519,24 MHz
	TV3	30	543,26 MHz
Wieringen	TV1	39	615,25 MHz
	TV2	42	639,25 MHz
	TV3	45	663,20 MHz

Table 5-1: Transmitter frequency and transmitter location

The maximum ERP of the transmitter and antenna gain reductions can be found in table 5-2. These reductions are caused by the shape of the antenna diagram. The reductions are specific for the specific path directions, and are frequency dependent.

Transmitter	Maximum		Reductions			
	ERP		Hoek van Holland	Harwich	Baldock	
Goes	TV1	250 kW	54,0 dBW	0,7 dB	1,6 dB	1,3 dB
	TV2			3,0 dB	2,4 dB	2,7 dB
	TV3			3,0 dB	2,2 dB	1,6 dB
Lopik	TV2	1000 kW	60,0 dBW	1,0 dB	1,0 dB	0,8 dB
	TV3			1,0 dB	1,0 dB	0,8 dB
Wieringen	TV1	300 kW	54,8 dBW	0,2 dB	3,0 dB	3,6 dB
	TV2			0,0 dB	0,0 dB	0,6 dB
	TV3			0,2 dB	1,0 dB	1,6 dB

Table 5-2: ERP and reductions per frequency and per path

The effective height of the transmitter is determined by averaging the height profile provided by the commercial planning software CHIRplus between 3 and 15 kilometres along the path. See table 5-3.

Transmitter	Receiver	Antenna above gnd	Gnd level	Avg height 3-5 km	Effective height
Goes	Hoek van Holland	137 m	0 m	0	137 m
Goes	Harwich	137 m	0 m	0	137 m
Goes	Baldock	137 m	0 m	0	137 m
Lopik	Hoek van Holland	363 m	2 m	-2	367 m
Lopik	Harwich	363 m	2 m	-2	367 m
Lopik	Baldock	363 m	2 m	-2	367 m
Wieringen	Hoek van Holland	196 m	-3 m	-4	197 m
Wieringen	Harwich	196 m	-3 m	-2	195 m
Wieringen	Baldock	196 m	-3 m	-1	194 m

Table 5-3: Effective height calculations

### 5.1.5 Receiver input parameters

The receiver parameters that are relevant for the P.1546-4 calculations are: receiver location, receiver antenna height, clutter height and Terrain Clearance Angle (TCA). The values used are shown in table 5-4. The value for “h2” is the receiver antenna height used in the calculations.

Receiver site	Coordinates	Antenna height	Ground level	h2	Terrain	Clutter height	TCA Rx
Hoek van Holland	51° 59' 03" N 04° 06' 58" E	5 m	18 m	23 m	Rural	10 m	<0.55°
Harwich	51° 56' 40" N 01° 17' 19" E	18 m	2 m	20 m	Sea / Suburban*	10 m	<0.55°
Baldock	52° 00' 00" N 00° 07' 45" W	29 m	107 m	29 m	Rural	10 m	<0.55° *
Stena HSS	52° 03' 00" N 03° 54' 00" E to 51° 54' 00" N 01° 54' 00" E	15 m	0 m	15 m	Sea	10 m	<0.55°

Table 5-4: Receiver parameters used as input for the calculations

\* = see text

A further explanation of the chosen parameters per receiver site is given below.

#### Hoek van Holland

This receiver site was located on a dune near the Dutch coast. It is the highest point of the surroundings. The signals from the three transmitters arrive from three different directions and hence cover three different paths. In the direction of Lopik, the terrain falls flat at sea level almost immediately behind the dune. Although P.1546 requires the height above ground for calculations, we took the height above the landscape in this case (23 metres). In the direction of Goes, the path almost immediately crosses a waterway and some industrial area, all at sea level. In this case, we also took a receiver height of 23 metres.

In the direction of Wieringen the path follows the dunes for a few kilometres. Noting that the dune with the receive site on it is the highest point in the surroundings, we chose the receiver height at 23 metres and a clutter height of 10 metres.

#### Stena HSS

All eighteen Stena Line HSS “Discovery” crossings follow a slightly different trajectory. Calculations were performed along a path that is a good approximation of those eighteen trajectories. That path is very close to the line Lopik via Hoek van Holland to Harwich, but not exactly. Therefore a number of test points were defined along the path, and for each of them, the percentage of sea was determined prior to calculation.

#### Harwich

This receiver site was located in an old lighthouse near the coast. The signals do not arrive from exactly the same direction, but the three paths are similar. The lighthouse is the highest point in the surroundings and is located 150 metres from the coastline. What makes this site a bit complicated is the peninsula almost 2 km from the lighthouse in the direction of the transmitters. The peninsula is between 500 m and 2 km wide, depending on the path. The container terminal “Felixtowe South” is located on the side of the peninsula that faces the lighthouse. For all three paths, the height of the tower above sea will be used (20 m).

#### Baldock

This receiver site was located on top of a hill, but more inland. The height of the antenna above ground (29 metres) was used for the calculations.

It was more difficult to judge whether or not this location has an unobstructed path towards the Dutch transmitters. Therefore we studied the terrain profile of the three paths to Baldock in detail and calculated the clearance angle. The terrain profile is generated by our planning software CHIRplus from LS telcom, which uses the height map “DTM 50m-NL + Western Europe”.



The height profile of the last 20 km of the path from Goes to Baldock is provided below:

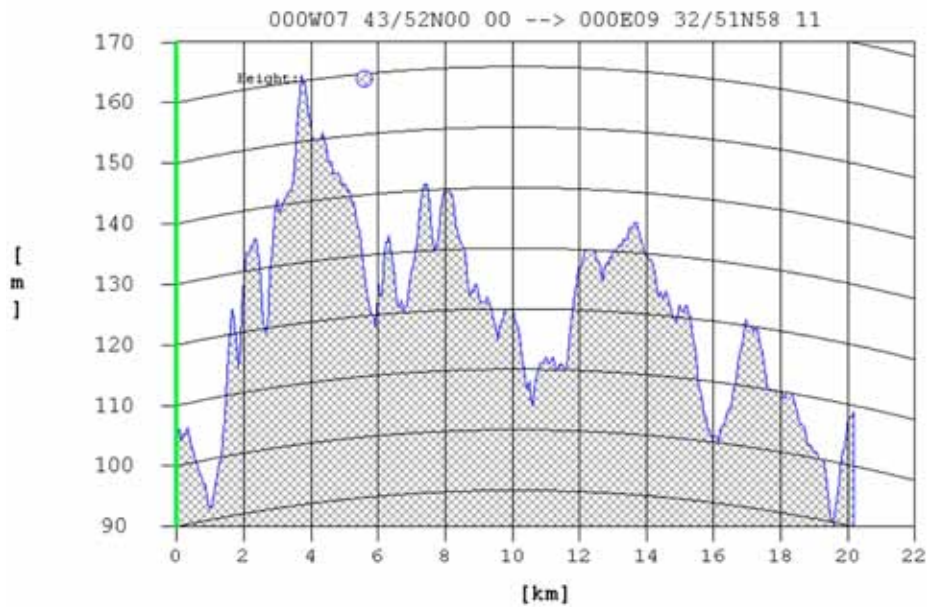


Figure 5-5: Terrain profile for the last 20 km of the path Goes – Baldock

Using this profile (but ignoring the curvature of the earth) and the height of the site and the antenna, we calculated a terrain clearance angle of 0.43 degrees. This is below the minimum level of 0.55 degrees which is stated in P.1546. We conclude that according to P.1546, the hills can be ignored.

The height profile of the last 20 km of the path from Lopik to Baldock is provided below:

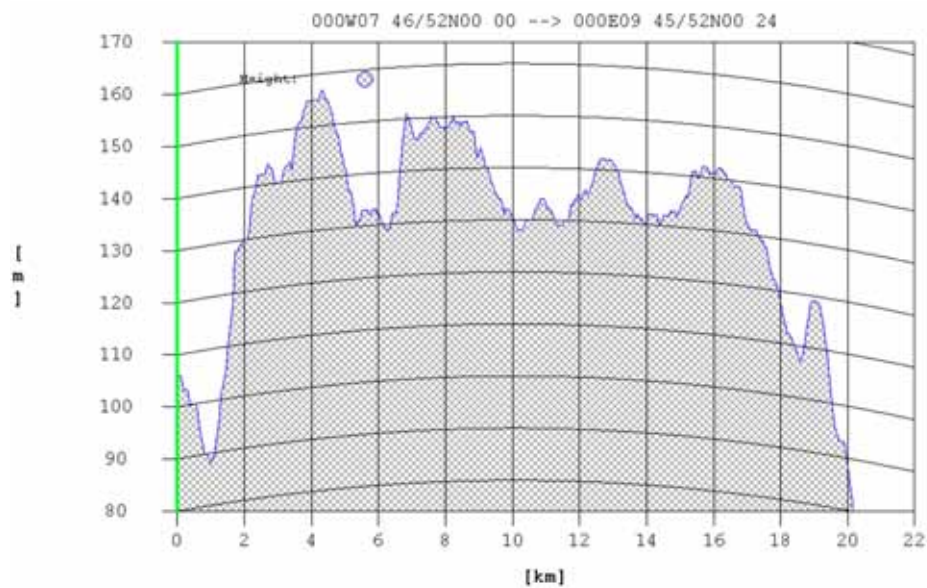


Figure 5-6: Terrain profile for the last 20 km of the path Lopik – Baldock

Also in this case, the terrain clearance angle is 0.33 degrees. This is below the minimum level of 0.55 degrees which is stated in P.1546. We conclude that according to P.1546, the hills can be ignored.

The height profile of the last 20 km of the path from Wieringen to Baldock is provided below:

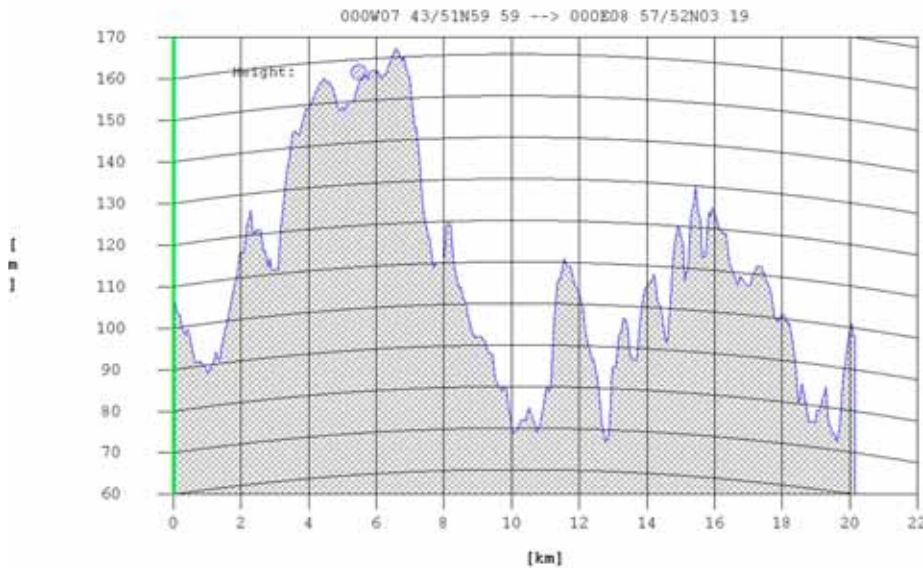


Figure 5-7: Terrain profile for the last 20 km of the path Wieringen – Baldock

Also in this case, the terrain clearance angle is 0.33 degrees. This is below the minimum level of 0.55 degrees which is stated in P.1546. We conclude that according to P.1546, the hills can be ignored.

### 5.1.6 Path specific input parameters

The path parameters that are relevant for the P.1546-4 calculations are: distance and percentage sea. The distances are calculated from the transmitter and receiver locations. The percentage of sea and land along the propagation path is one of the most crucial path parameters in P.1546. For every fixed path, the percentage of sea was determined in two ways:

- with the help of the IDWM database incorporated in the LS telcom CHIRplus software;
- with the help of the online geographical tool Google Earth.

Both methods produced comparable results with the exception of the path between Goes and Hoek van Holland. Distances and azimuths were calculated with the Coordinate Calculator software, version 4.1, of the Rijkswaterstaat Geo-Information and ICT Department [5]. See table 5-8.

Transmitter	Receiver	Distance	%sea
Goes	Hoek van Holland	55 km	17 – 40
Goes	Harwich	186 km	85
Goes	Baldock	282 km	56
Lopik	Hoek van Holland	64 km	0
Lopik	Harwich	258 km	75
Lopik	Baldock	356 km	53
Wieringen	Hoek van Holland	121 km	45
Wieringen	Harwich	277 km	88
Wieringen	Baldock	367 km	58

Table 5-8: Path distance and percentage sea used as input for the calculations

## 5.2 Field strength predictions using ITU-R P.1546

Using the input parameters described in the previous chapter and for each propagation path, the expected field strength value that will be exceeded 1% of the total observation time, 10% of the time and 50% of the time was calculated.

### 5.2.1 Path 1: fixed locations

The radio path from Lopik to Baldock is observed in four locations:

- Hoek van Holland;
- Maritime mobile between Hoek van Holland and Harwich;
- Harwich;
- Baldock.

The model predicts the following field strengths for the fixed receive sites:

Transmitter	Receiver	Ch	FS 50% (dB $\mu$ V/m)	FS 10% (dB $\mu$ V/m)	FS 1% (dB $\mu$ V/m)
Lopik TV2	Hoek van Holland	27	77,1	78,6	84,1
Lopik TV3	Hoek van Holland	30	77,0	78,5	84,1
Lopik TV2	Harwich	27	30,3	45,9	60,6
Lopik TV3	Harwich	30	30,2	45,9	60,6
Lopik TV2	Baldock	27	21,8	33,9	45,7
Lopik TV3	Baldock	30	21,6	33,8	45,5

Table 5-9: Predictions for path 1

### 5.2.2 Path 1: maritime mobile measurements

The trajectory of the Stena Line HSS “Discovery” can be approximated by a straight line, provided we discard the parts near the coast on both ends of the crossing. To calculate the field strength profile from Hoek van Holland to Harwich, we defined 10 test points on that line, see table 5-10.

Test point	Coordinates		Heading (°)	heff (m)	Distance (km)	Sea (%)
Stena 1	52N03 54	03E54 00	275	367	79,4	25,3
Stena 2	52N03 32	03E40 40	274	367	94,6	30,4
Stena 3	52N03 10	03E27 20	273	367	109,8	35,5
Stena 4	52N02 48	03E14 00	273	367	125,0	40,6
Stena 5	52N02 26	03E00 40	272	367	140,2	45,7
Stena 6	52N02 04	02E47 20	272	367	155,5	50,8
Stena 7	52N01 42	02E34 00	272	367	170,7	55,9
Stena 8	52N01 20	02E20 40	271	367	186,0	61,0
Stena 9	52N00 58	02E07 20	271	367	201,3	66,1
Stena 10	52N00 36	01E54 00	271	367	216,5	71,2

Table 5-10: Test points along the trajectory of the Stena HSS Discovery

The trajectory of the Stena HSS comes close to the radio path from Lopik to Harwich, but it is not completely aligned with it. As a result of that, the land portion of the radio path is not constant, but changes slowly from test point to test point. The calculation of the percentage sea takes this effect into account. For the given test points, the model predicts the following field strengths:

Test point	Lopik TV2			Lopik TV3		
	Fs 50% (dBµV/m)	Fs 10% (dBµV/m)	Fs 1% (dBµV/m)	Fs 50% (dBµV/m)	Fs 10% (dBµV/m)	Fs 1% (dBµV/m)
Stena 1	67.7	70.4	77.2	67.6	70.3	77.1
Stena 2	61.7	65.9	73.2	61.6	65.7	73.1
Stena 3	56.6	62.3	69.9	56.5	62.1	69.8
Stena 4	52.1	59.5	67.3	52.0	59.3	67.2
Stena 5	47.9	57.0	65.2	47.8	56.9	65.1
Stena 6	44.2	55.0	63.7	44.1	54.9	63.5
Stena 7	41.0	53.2	62.6	40.9	53.1	62.4
Stena 8	38.2	51.5	61.7	38.1	51.4	61.6
Stena 9	35.8	50.0	61.4	35.6	49.9	61.3
Stena 10	33.6	48.7	61.5	33.4	48.6	61.4

Table 5-11: Predictions on the Stena HSS test points

The preceding predictions were made to create a predicted path profile from Hoek van Holland to Harwich, for later comparison with the measured path profile.

### 5.2.3 Paths 2, 3 and 4

Using the transmitter in Goes, three other radio paths were measured:

- Path 2 from Goes to Hoek van Holland;
- Path 3 from Goes to Harwich;
- Path 4 from Goes to Baldock.

Path 2 runs from the TV transmitter of Goes to the receive site in Hoek van Holland. The percentage sea path between Goes and Hoek van Holland was especially difficult to determine. The radio path crosses wide waterways, some inland salt water lakes, and skims several small islands. We calculated two extreme values in this case. Depending on assumptions, the percentage sea can be anywhere between 17% and 40% for this path. Therefore calculations were performed for the minimum and maximum values.

The model predicts the following field strength for path 2:

Field strength (dBµV/m)			assuming 17% sea			assuming 40% sea		
Transmitter	Receiver	Ch	50% time	10% time	1% time	50% time	10% time	1% time
Goes TV1	Hoek van Holland	29	66,0	67,9	73,4	68,1	70,3	76,0
Goes TV2	Hoek van Holland	32	63,6	65,5	71,0	65,8	67,9	73,7
Goes TV3	Hoek van Holland	35	63,5	65,5	71,0	65,7	67,9	73,7

Table 5-12: Predictions for path 2

For paths 3 and 4:

Transmitter	Receiver	Ch	FS 50% (dBµV/m)	FS 10% (dBµV/m)	FS 1% (dBµV/m)
Goes TV1	Harwich	29	30,1	48,1	64,7
Goes TV2	Harwich	32	29,2	47,4	63,9
Goes TV3	Harwich	35	29,3	47,6	64,2
Goes TV1	Baldock	29	20,2	32,6	44,2
Goes TV2	Baldock	32	18,6	31,1	42,6
Goes TV3	Baldock	35	19,6	32,1	43,6

Table 5-13: Predictions for paths 3 and 4

### 5.2.4 Paths 5, 6 and 7

Using the transmitter in Wieringen, three other radio paths were measured:

- Path 5 from Wieringen to Hoek van Holland;
- Path 6 from Wieringen to Harwich;
- Path 7 from Wieringen to Baldock.

The model predicts the following values:

Transmitter	Receiver	Ch	FS 50% (dBµV/m)	FS 10% (dBµV/m)	FS 1% (dBµV/m)
Wieringen TV1	Hoek van Holland	39	47,0	55,6	63,2
Wieringen TV2	Hoek van Holland	45	46,9	55,7	63,2
Wieringen TV3	Hoek van Holland	42	46,9	55,5	63,1
Wieringen TV1	Harwich	39	17,9	36,8	57,6
Wieringen TV2	Harwich	45	20,7	40,3	60,8
Wieringen TV3	Harwich	42	19,8	39,1	59,7
Wieringen TV1	Baldock	39	9,8	22,8	35,6
Wieringen TV2	Baldock	45	12,6	26,0	38,4
Wieringen TV3	Baldock	42	11,7	24,9	37,5

Table 5-14: Predictions for paths 5, 6 and 7

### 5.2.5 Overview of all paths (predictions)

An overview of the predicted field strength values that is superseded 1% of the time, 10% of the time and 50% of the time (the median value) for all paths are shown below. For the path originating in Goes, values are given assuming 17% sea and 40% sea.

Field strength (dBµV/m)		Hoek van Holland			Harwich			Baldock		
Transmitter	Ch	50% time	10% time	1% time	50% time	10% time	1% time	50% time	10% time	1% time
Goes TV1 (40%)	29	68,1	70,3	76,0	30,1	48,1	64,7	20,2	32,6	44,2
Goes TV2 (40%)	32	65,8	67,9	73,7	29,2	47,4	63,9	18,6	31,1	42,6
Goes TV3 (40%)	35	65,7	67,9	73,7	29,3	47,6	64,2	19,6	32,1	43,6
Goes TV1 (17%)	29	66,0	67,9	73,4	(same as above)			(same as above)		
Goes TV2 (17%)	32	63,6	65,5	71,0	(same as above)			(same as above)		
Goes TV3 (17%)	35	63,5	65,5	71,0	(same as above)			(same as above)		
Lopik TV2	27	77,1	78,6	84,1	30,3	45,9	60,6	21,8	33,9	45,7
Lopik TV3	30	77,0	78,5	84,1	30,2	45,9	60,6	21,6	33,8	45,5
Wieringen TV1	39	47,0	55,6	63,2	17,9	36,8	57,6	9,8	22,8	35,6
Wieringen TV2	45	46,9	55,7	63,2	20,7	40,3	60,8	12,6	26,0	38,4
Wieringen TV3	42	46,9	55,5	63,1	19,8	39,1	59,7	11,7	24,9	37,5

Table 5-15: Predictions for all paths

### 5.3 Prediction uncertainty

Similar to the measurement uncertainty, we can describe and analyze the uncertainty contained in the predicted values. The P.1546 model itself is described in an exact way, yet the input parameters contain uncertainties. Those uncertainties propagate in the model and influence the predicted value. As a result, the prediction itself based on those input parameters is no longer an exact value, but has become an estimate with a known uncertainty.

This uncertainty can be determined using the same methodology that is used for the measurement uncertainty. The analysis yielding the expanded prediction uncertainty is given in annex E. The results are summarized in the table below:

Path	Expanded prediction uncertainty ( $2\sigma$ )
Lopik - Hoek van Holland	1,6 dB
All other paths	3,8 dB

Table 5-16: Expanded prediction uncertainty ( $2\sigma$ )

If we want to do a meaningful and founded comparison between the measured values and the predicted values, we have to consider the uncertainties involved. Even if both measurement and prediction yield different values, they could still describe the same event, depending on the overlap of their individual probability distributions. If we know both nominal values and both uncertainties, expressed as standard deviation, we can calculate the probability that measurement value and prediction value describe the same event.

# 6

## Comparison of measurements and predictions

Differences between the measurements and predictions are analyzed here.

Some suggestions are made to improve the model.

## 6.1 Comparison: a non-Gaussian distribution?

All measurement results over paths longer than 55 km showed field strength probability distributions far from Gaussian (log-normal) distributions. An example is given in figure 6-1. This raised the question what kind of distribution is assumed in the Recommendation.

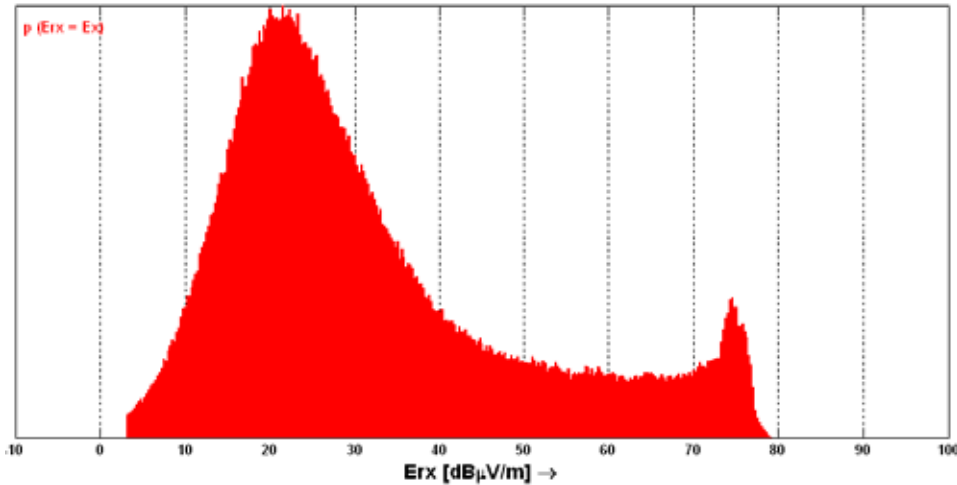


Figure 6-1: Probability distribution of the field strength from Goes TV2 in Harwich

At first observation, P.1546 seems to assume a log-normal probability distribution of the predicted field strength as a function of time. The interpolation to obtain predictions for different percentages of time than the 1%, 10% and 50% curves is based on this assumption. See section 7 of annex 5 of the Recommendation, entitled “Interpolation of field strength as a function of percentage time”. Yet we suspected that this was not the whole story.

To investigate this issue, we analyzed the propagation curves for propagation over land and cold sea at 600 MHz, assuming an antenna height of 300 metres. If those curves would represent a log normal field strength distribution, we could calculate the standard deviations from any two of the 50%, 10% and 1% curves, and the results would be the same. We therefore calculated the standard deviation from the 50% and 10% values, from the 10% and 1% values and from the 1% and 50% values. The results can be found in figures 6-2 (land) and 6-3 (cold sea).

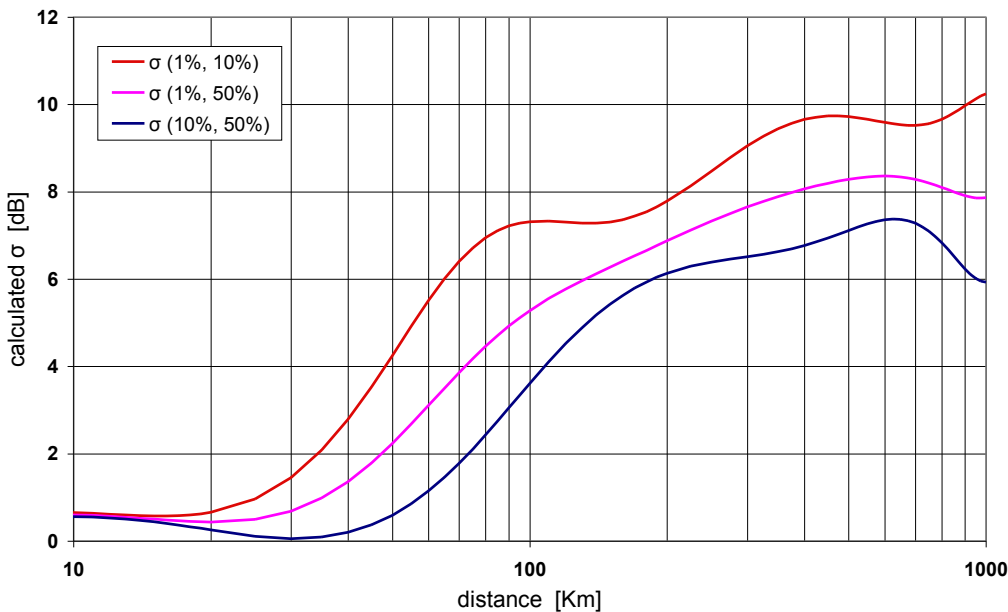


Figure 6-2: Standard deviation derived from the P.1546-4 curves, for propagation over land.



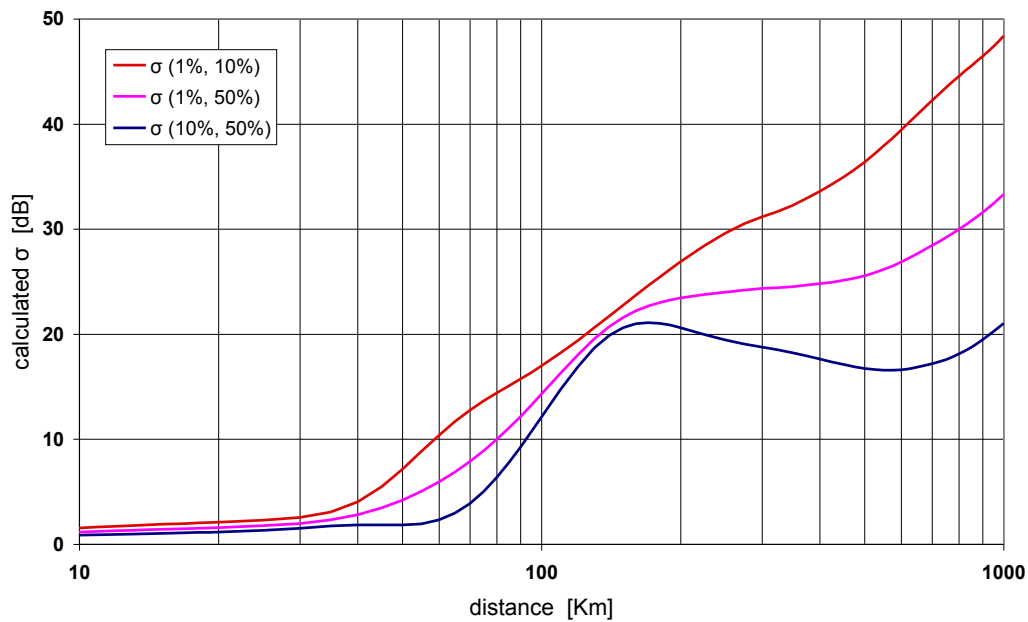


Figure 6-3: Standard deviation derived from the P.1546-4 curves, for propagation over cold sea.

These figures show that the calculated standard deviations differ substantially from each other. So our conclusion was that the P.1546-4 curves do describe a time-probability distribution that differs substantially from a log-normal distribution. Especially the cold sea case shows remarkable deviations from a normal distribution. From the graphs it can also be seen that the distribution has longer tails than a normal distribution. As these curves originally were based on measurements in the (remote) past, this is not really surprising, but deserves to be explicitly stated.

## 6.2 Comparison of the measurements with the P.1546 predictions

In this chapter we will compare the measured results with predictions using the propagation model described in Recommendation ITU-R P.1546. Unless otherwise noted, P.1546-4 was the version of the model used.

We look into the differences between the measured and predicted values for 50%, 10% and 1% of the time. Finally we compare the differences observed when using P.1546-4 with those observed when P.370-7 is used.

The measurement results were given in chapter 4.2. The P.1546-4 predictions were given in chapter 5.2. They are combined below:

Field strength (dB $\mu$ V/m)		Hoek van Holland			Harwich			Baldock		
		50%	10%	1%	50%	10%	1%	50%	10%	1%
Goes TV1	Measured	73	79	87	28	61	76		18	44
	P1546-4	68	70	76	30	48	65	20	33	44
Goes TV2	Measured	73	80	85	27	62	76			40
	P1546-4	66	68	74	29	47	64	19	31	43
Goes TV3	Measured	73	81	87	25	60	76			34
	P1546-4	66	68	74	29	48	64	20	32	44
Lopik TV2	Measured	90	92	95	19	46	68		21	45
	P1546-4	77	79	84	30	46	61	22	34	46
Lopik TV3	Measured	88	91	93	20	47	69		21	44
	P1546-4	77	79	84	30	46	61	22	34	46
Wieringen TV1	Measured	46	69	84		32	57		22	47
	P1546-4	47	56	63	18	37	58	10	23	36
Wieringen TV2	Measured	41	68	83		38	60			
	P1546-4	47	56	63	21	40	61	13	26	38
Wieringen TV3	Measured	41	67	82		32	57			
	P1546-4	47	56	63	20	39	60	12	25	38

Table 6-4: Measured and predicted values.

Although all shown figures are rounded to 1 dB, the calculations are done with the original unrounded values. The grey sections of the table indicate paths and percentages of time for which no reliable measurements are available.

For the paths originating in Goes, we had the choice between the 17% sea and 40% sea values. As the 17% sea value results in an extreme difference with measurements on the short Goes – Hoek van Holland path, we chose the 40% sea value for further analysis.

The differences between the measured values and the predicted values are shown in table 6-5. When the measured value is greater than the predicted value, the shown difference is positive.

Difference (dB)	Hoek van Holland			Harwich			Baldock		
	50%	10%	1%	50%	10%	1%	50%	10%	1%
Goes TV1	5	9	11	-3	13	11		-15	0
Goes TV2	7	12	12	-2	14	12			-3
Goes TV3	7	13	13	-5	12	12			-10
Lopik TV2	13	14	11	-12	0	7		-13	-1
Lopik TV3	11	12	9	-11	1	9		-13	-2
Wieringen TV1	-1	13	21		-5	-1		-1	11
Wieringen TV2	-6	12	20		-2	-1			
Wieringen TV3	-6	11	19		-7	-3			

Table 6-5: Difference between measured and predicted values.

A positive value indicates that the measured value is higher than the value predicted using P.1546-4.

As we see, only a few entries show a close match between prediction and measurements. We also see very big differences, up to 20 dB, in some entries.

### 6.2.1 Wasserstein Metric

If we want to do a meaningful and founded comparison between the measured values and the predicted values, we have to consider the uncertainties involved. Both the measured and the predicted value are not exact, they consist of a nominal value and an uncertainty range around that value. The true value can be found within that range with a specified probability.

If both measurement and prediction yield different values, they may still describe the same event, depending on the overlap of their individual probability distributions. If we know both nominal values and both uncertainties, expressed as standard deviation, we can calculate the probability that measurement value and prediction value describe the same event.

A common method to express the mismatch between two distributions is the Wasserstein Metric [11], also popularly known as “the earth mover’s distance”. In our case we are more interested in a figure for the match between two distributions, so we use the inverse method:

$$W = \int_{-\infty}^{\infty} \min \left[ \frac{1}{\sigma_1 \sqrt{2\pi}} e^{-0.5(x-\mu_1)^2}, \frac{1}{\sigma_2 \sqrt{2\pi}} e^{-0.5(x-\mu_2)^2} \right] dx$$

where  $\mu_1$  and  $\sigma_1$  are the mean value and standard deviation of the measurement and  $\mu_2$  and  $\sigma_2$  the same for the P.1546 prediction. Often used threshold values for W are >50% for a clear match and <1% for a clear mismatch. Values in between are left undecided.

The formula has been depicted in figure 6-6. The metric calculates the overlapping surface of both probability density functions, shown as a green coloured surface in the graph. In this example, the measured and predicted value for the path Goes TV3 to Harwich are shown.

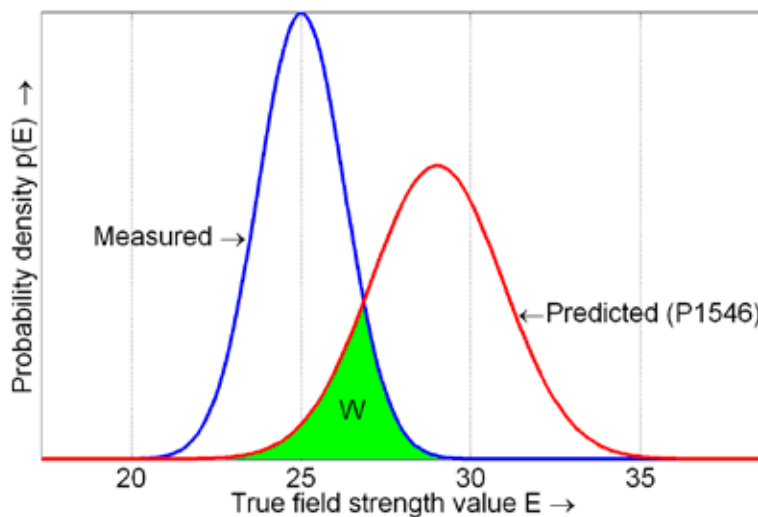


Figure 6-6: Overlap of the PDF of the measured value and the predicted values.

### 6.2.2 Match between measurement and prediction

The expanded uncertainty of the measurements is 2.4 to 2.6 dB for the fixed measurement sites, and 3.3 dB for the maritime mobile site. See chapter 4.3 and annex D. The expanded uncertainty of the predictions ranges is 1.6 dB for the path from Lopik to Hoek van Holland and 3.8 dB for the other paths. See chapter 5.3 and annex E. All uncertainty values have a normal probability distribution and are specified for a 95% confidence level ( $2\sigma$ ).

Using the Wasserstein metric we calculate the probability that the measured value matches the predicted value. The results are shown in table 6-7.

	Hoek van Holland			Harwich			Baldock		
	50%	10%	1%	50%	10%	1%	50%	10%	1%
Goes TV1	10%	0,4%	<0.1%	<b>51%</b>	<0.1%	<0.1%		<0.1%	<b>82%</b>
Goes TV2	2%	<0.1%	<0.1%	<b>51%</b>	<0.1%	<0.1%			34%
Goes TV3	2%	<0.1%	<0.1%	21%	<0.1%	<0.1%			0,2%
Lopik TV2	<0.1%	<0.1%	<0.1%	<0.1%	<b>82%</b>	3%		<0.1%	<b>71%</b>
Lopik TV3	<0.1%	<0.1%	<0.1%	0,2%	<b>71%</b>	1%		<0.1%	<b>51%</b>
Wieringen TV1	<b>69%</b>	<0.1%	<0.1%		12%	<b>71%</b>		<b>82%</b>	<0.1%
Wieringen TV2	5%	<0.1%	<0.1%		<b>51%</b>	<b>71%</b>			
Wieringen TV3	5%	<0.1%	<0.1%		3%	34%			

Table 6-7: Probability of a match between measurement value and predicted value.

If the values shown in the table are >50% (bold type black figures), P.1546-4 and the measurements concur. If the value is <1% (red figures), there is a clear mismatch between the predicted value and the measured value. Values in between are indecisive.

### 6.2.3 Fixed paths: a poor match

From the table, we see that the P.1546-4 predictions do not match the measurements in 31 out of 55 cases. Only in 12 out of 55 cases do they positively match. This clearly indicates that the mixed path predictions of P.1546-4 need to be improved, in order to give meaningful results in situations similar to the ones observed in this extensive measurement campaign.

The most surprising differences between prediction and measurement are found at the site Hoek van Holland. Although the paths to Hoek van Holland are mainly land-based and only cover small distances, the difference between measurement and prediction are quite large.

The distance from Lopik to Hoek van Holland is only 64 km and the terrain between transmitter and receiver is very flat and near sea level. The transmit antenna height is very high: 367 metres. The receive site is 23 metres, well above its surroundings; in short: line of sight conditions. Yet the predicted field strength is 10-15 dB lower than the value measured over 500 days.

#### 6.2.4 Maritime measurements: a poor match

This is further illustrated by the graph below, in which we combine the maritime field strength profile measurements and the P.1546 field strength profile predictions between Hoek van Holland and Harwich.

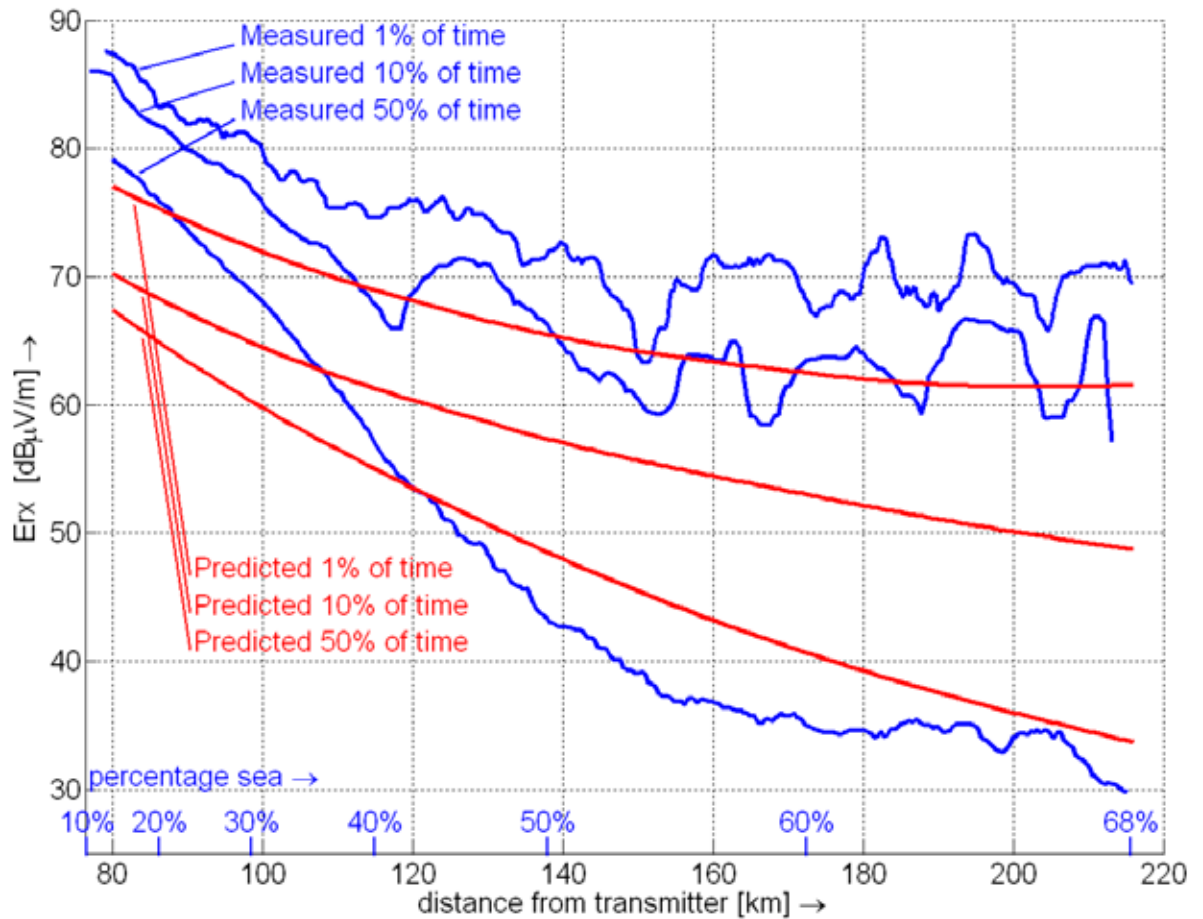


Figure 6-8: Measured and predicted path profile from Hoek van Holland to Harwich (Lopik TV2 & TV3)

The measured path profile combines all measurement points of the measurements on board the Stena HSS 'Discovery'. The results of both frequencies from the Lopik transmitter were combined to yield a higher number of measurements, and in that way a more stable 1% curve. The channels differ only 24 MHz in frequency, hence the difference in propagation loss is small.

The field strength profile graphs show a significant difference between predictions and measurements. At the locations closest to the Lopik transmitter, the calculated values are far below the measured values. The predictions seem to improve when we get closer to the UK coast. This graph is consistent with the measurements and predictions at the fixed station Hoek van Holland.

### 6.2.5 Comparison with P370-7

The propagation model described in Recommendation ITU-R P.1546 has a long history and is partly based on the old Recommendation ITU-R P.370-7. We have the impression that the older versions were better suited for the Dutch situation.

Due to time constraints, we decided not to implement P.370-7 in MatLab, but used our planning software tool CHIRplus from LStelcom. After some experimentation, we decided to use the  $\Delta h$  correction in the calculations, as this provided the best match with the measurements. The predicted field strength values can be compared in table 6-9.

Field strength (dB $\mu$ V/m)		Hoek van Holland			Harwich			Baldock		
		50%	10%	1%	50%	10%	1%	50%	10%	1%
Goes TV1	Measurement	73	79	87	28	61	76		18	44
	P1546-4	68	70	76	30	48	65	20	33	44
	P370-7	73	77	83	29	50	73	19	36	54
Lopik TV2	Measurement	90	92	95	19	46	68		21	45
	P1546-4	77	79	84	30	46	61	22	34	46
	P370-7	85	86	91	29	49	69	20	37	53
Wieringen TV1	Measurement	46	69	84		32	57		22	47
	P1546-4	47	56	63	18	37	58	10	23	36
	P370-7	51	59	69	17	38	64	9	25	44

Table 6-9: A comparison between P370-7 and P1546-4

The same information is shown in table 6-10, but now as a difference between the prediction and the measurements.

Difference (dB)		Hoek van Holland			Harwich			Baldock		
		50%	10%	1%	50%	10%	1%	50%	10%	1%
Goes TV1	P1546-4	5	9	11	-2	13	11		-15	0
	P370-7	0	2	4	-1	11	3		-18	-10
Lopik TV2	P1546-4	13	13	11	-11	0	7		-13	-1
	P370-7	5	6	4	-10	-3	-1		-16	-8
Wieringen TV1	P1546-4	-1	13	21		-5	-1		-1	11
	P370-7	-5	10	15		-6	-7		-3	3

Table 6-10: Difference of both predictions with the measured value.

A positive value indicates that the measured value is higher than the predicted value. The best result is of course a value around zero. Absolute values greater than 7 dB have been marked in red. This threshold is arbitrary.

It can be seen that P.370-7 is better in predicting the land based field strength values. This is mainly the effect of the  $\Delta h$  correction factor. This correction factor in P.370-7 compensates for the relative flatness of the Netherlands.

The land curves of P.370-7 are valid for a  $\Delta h$  of 50 metres, whereas the true  $\Delta h$  for the paths in the Netherlands we observed is in the order of a few metres. Using the lowest  $\Delta h$  available in the Recommendation (10 metres), we get a substantial correction: the predicted field strength increases 10 dB for distances between 50 and 100 kilometres. One could argue that a correction even higher than 10 dB would be realistic, noting that the real  $\Delta h$  is below 10 metres on the paths concerned.

## 6.3 Suggestion for improvement of P.1546

In the previous chapter we studied the differences between our measurements and the predictions of P.1546. In this chapter we check some modifications to P.1546 which could improve the predictions for the Dutch situation and for mixed land/sea paths.

We noted that the predecessor of P.1546, recommendation P.370, included some provisions for corrections which can compensate for the relative flatness of the Dutch landscape. We study two possible modifications, the first taking account of the terrain heights within 50 km from the transmitter and the second taking into account the terrain near the receiver. So we modify P.1546-4 by:

1. the  $\Delta h$  correction as described in P.370-7;
2. removing the minimum of  $+ 0.55^\circ$  for the receiver terrain clearance angle (TCA) and allowing for positive correction values for the terrain clearance angle, as in P.370-7.

and observe the effects of these modifications. We see that both methods improve the predictions on the land based paths in Holland, but have different implications for the longer mixed paths to the United Kingdom.

### 6.3.1 $\Delta h$ correction

We assume that the basic curves of P.1546 are based on the same measurements as P.370. So the land path curves refer to a value of  $\Delta h = 50$  m, which applies to rolling terrain commonly found in Europe and North America.

The  $\Delta h$  correction is implemented according to figure 8 of Recommendation ITU-R P.370-7. For  $\Delta h$  values not found in this figure, we use linear interpolation between the  $\Delta h$  lines nearest to the required value. Before the calculations can be performed, we need to determine the  $\Delta h$  for the different paths of our measurement campaign. For this we use our topological database and let CHIRplus determine the  $\Delta h$  for the different propagation paths. See the table below:

$\Delta h$	Goes	Lopik	Wieringen
Hoek van Holland	14.4 m	8.8 m	8.8 m
Harwich	12.0 m	13.6 m	12.8 m
Baldock	9.6 m	10.4 m	12.0 m

Table 6-11:  $\Delta h$  values for the three transmitter sites

### 6.3.2 TCA correction at the receive side

When detailed information about the topology in the vicinity of the receiver site is available, the Terrain Clearance Angle (TCA) correction can be used to improve the accuracy of the predictions of both P.370-7 and P.1546. Since version P.1546-2 of 2005 however, positive TCA correction values were no longer allowed. In those cases where a positive TCA correction was used, the difference with the previous version of the model could be up to 16 dB at 600 MHz.

Past experience with predictions for the Netherlands had given some trust in replacing the  $\Delta h$  correction by the more detailed TCA correction. We therefore reintroduced this method in the existing P.1546-4 to see whether this would improve the predictions. The calculated Terrain Clearance Angles for the different propagation paths are given in the table below. The corrections are calculated according to the description given in ITU-R Rec. P.1546-1, annex 5, section 11.

TCA	Goes	Lopik	Wieringen
Hoek van Holland	- 0.07°	- 0.07°	-0.01°
Harwich	- 0.07°	- 0.07°	+ 0.04°
Baldock	+ 0.38°	+ 0.28°	+ 0.26°

Table 6-12: TCA values for the three receiver sites

### 6.3.3 Effect of the modifications

In the two tables below, the results of these two modifications are shown. The first table lists the measured value and the predicted value in four different cases:

1. P.1546-4 as is;
2. P.370-7 with  $\Delta h$  correction;
3. P.1546-4 modified with  $\Delta h$  correction;
4. P.1546-4 modified with TCA correction;

For each of the paths, only one frequency has been presented, to keep the table simple.

See table 6-13.

Field strength (dB $\mu$ V/m)		Hoek van Holland			Harwich			Baldock		
		50%	10%	1%	50%	10%	1%	50%	10%	1%
Goes TV1	Measurement	73	79	87	28	61	76		18	44
	P1546-4	68	70	76	30	48	65		33	44
	P370-7 with $\Delta h$	73	77	83	29	50	73		36	54
	P1546-4 with $\Delta h$	76	79	84	38	56	72		38	49
	P1546-4 with TCA	76	78	84	35	53	70		34	46
Lopik TV2	Measurement	90	92	95	19	46	68		21	45
	P1546-4	77	79	84	30	46	61		34	46
	P370-7 with $\Delta h$	85	86	91	29	49	69		37	53
	P1546-4 with $\Delta h$	88	89	95	34	50	65		39	51
	P1546-4 with TCA	85	86	92	38	53	68		37	49
Wieringen TV1	Measurement	46	69	84		32	57		22	47
	P1546-4	47	56	63		37	58		23	36
	P370-7 with $\Delta h$	51	59	69		38	64		25	44
	P1546-4 with $\Delta h$	56	65	73		41	62		27	40
	P1546-4 with TCA	54	63	70		43	64		26	39

Table 6-13: Measured value and predicted value using 4 different models

The same information is shown in table 6-14, but now as a difference between the prediction and the measurements. A positive value indicates that the measured value is higher than the predicted value. The best result is of course a value around zero.

Difference (dB)		Hoek van Holland			Harwich			Baldock		
		50%	10%	1%	50%	10%	1%	50%	10%	1%
Goes TV1	P1546-4	5	9	11	-2	13	11		-15	0
	P370-7 with $\Delta h$	0	2	4	-1	11	3		-18	-10
	P1546-4 with $\Delta h$	-3	0	3	-10	5	4		-20	-5
	P1546-4 with TCA	-3	1	3	-7	8	6		-16	-2
Lopik TV2	P1546-4	13	13	11	-11	0	7		-13	-1
	P370-7 with $\Delta h$	5	6	4	-10	-3	-1		-16	-8
	P1546-4 with $\Delta h$	2	3	0	-15	-4	3		-18	-6
	P1546-4 with TCA	5	6	3	-19	-7	0		-16	-4
Wieringen TV1	P1546-4	-1	13	21		-5	-1		-1	11
	P370-7 with $\Delta h$	-5	10	15		-6	-7		-3	3
	P1546-4 with $\Delta h$	-10	4	11		-9	-5		-5	7
	P1546-4 with TCA	-8	6	14		-11	-7		-4	8

Table 6-14: Difference between measured value and predicted value using 4 different models

As can be seen, the proposed corrections significantly improve the predictions for paths over land, for example Lopik to Hoek van Holland. Also the relative short mixed paths within the Netherlands show improvements. However the longer mixed path predictions show no consistent improvements.



While digging into the Recommendation in the hope to find clear causes for this, at least one question arose on the origin of the 100% sea curves. As we already saw in chapter 6.1, the cold sea curves show an unexpected change in probability distribution localized around 120 kilometres.

When we compared versions of Recommendations P.370 and P.1546, we noticed that the 100% sea curves have changed going from P.370 to P.1546. See figure 6-15

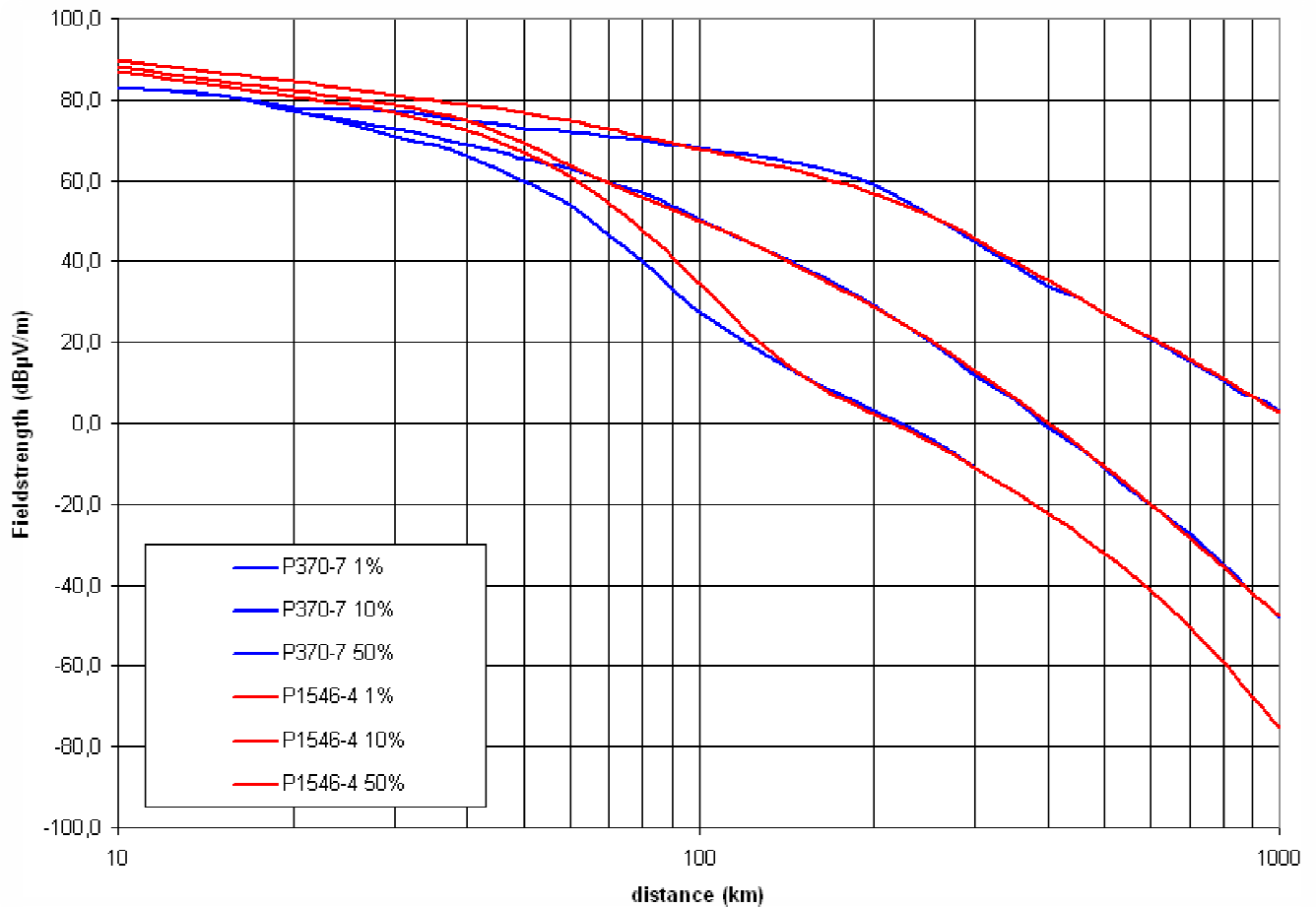


Figure 6-15: The 100% cold sea curves for the P.370 and P.1546 models (300 m, 600 MHz)

If errors were introduced when these changes were made, this could account for some of the differences observed. It is known that the changes were made in order to improve the dependency on the transmitter height for shorter distances, but they should not have effected the longer distances. Unfortunately we did not measure any 100% sea path during our campaign, so we lack information to pinpoint specific imperfections in the 100% sea curves.

Further analysis of the differences in mixed path predictions becomes rather complicated. The mixed path predictions are based on the 100% land curves, the 100% sea curves and an interpolation factor. With probably more than one imperfec-tion, it is very difficult to do suggestions for further improvements. Accurate measurements for 100% sea paths could help to straighten out some questions, so such measurements are strongly advised.

The available time did not allow for further investigation in mixed path calculation methods and possible improvements. We trust that the above information provides a good starting point for a critical evaluation of the model. The measurement data obtained during our 500 day measurement campaign will provide solid reference material enabling the validation of solutions sought.

## 6.4 Conclusions

An extensive propagation measurement campaign, lasting 500 days, has been performed along paths between the Netherlands and the United Kingdom. The campaign was aimed at UHF propagation on mixed land/sea paths. A lot of emphasis has been laid on calibration accuracy and validation of the measurement data. This resulted in a highly accurate and very extensive set of measurement data, that can be used for validation of existing propagation models and models being (re)developed.

The measurement results are compared with the predictions of the version 'in force' of the ITU propagation model described in Recommendation ITU-R P.1546-4. This comparison shows that this ITU-R propagation model requires improvement for mixed paths, but also for paths over very flat terrain.

While double-checking the results, some flaws in commercially available propagation prediction (planning) software have been found. The development of a quality assurance procedure for implementations of propagation models seems advisable. Specific test cases with known results would be helpful for verification, and peer review of software tools used by negotiating administrations should be promoted.

Some initial analysis has been performed to track any obvious errors in the P.1546 model. Although some indications for possible improvements could be given, no all inclusive solution has been found. This may indicate that the model has more than one flaw, making error tracking difficult.

A correction on the implementation of TCA at the receive side is solicited. A modified version of P.1546-4 with added improved TCA correction shows promising results, at least for very flat terrain (typical of The Netherlands) and distances up to 100 kilometres.

As doubts have risen on the correctness of the 100% cold sea curves, further efforts should focus on those issues. Detailed measurements to confirm the 100% sea (and 100% land) curves are needed. The interpolation method for mixed path should be verified.

The measurement data obtained during our 500 day measurement campaign will provide solid reference material enabling the validation of new modelling proposals. They can complement measurement data previously collected by others. Similar extensive measurement campaigns over other terrain are strongly encouraged.

# References

- <sup>[1]</sup> Recommendation ITU-R P.1546-4, Radio Wave Propagation, Method for point-to-area predictions for terrestrial services in the frequency range 30 MHz to 3 000 MHz, International Telecommunication Union, 2009;
- <sup>[2]</sup> Recommendation ITU-R P.370-7, VHF and UHF propagation curves for the frequency range from 30 MHz to 1000 MHz, International Telecommunication Union, 1995;
- <sup>[3]</sup> News Release: "EGEE helps achieve international digital broadcasting agreement", EGEE, Geneva July 11th, 2006;
- <sup>[4]</sup> UHF long distance propagation over land and sea paths from 1999 to 2001, Joe Middleton, BBC Research & Development, Technical Note R&D 1881, 2002;
- <sup>[5]</sup> CoordinateCalculator version 4.1, Geo-information and ICT department, Dutch Ministry of Transport and Public Works, ([http://www.rdnap.nl/download/setup\\_cc41.exe](http://www.rdnap.nl/download/setup_cc41.exe));
- <sup>[6]</sup> FSP-SCAN, by Erik van Maanen, Radio Communications Agency Netherlands;
- <sup>[7]</sup> Antennas, John D. Kraus, 2nd edition, ISBN 0-07-035422-7, page 828;
- <sup>[8]</sup> VHF and Microwave Propagation Characteristics of Ducts, Andrew L. Martin, Wireless Institute of Australia, January 17, 2007;
- <sup>[9]</sup> Guglielmo Marconi and communication beyond the horizon: a short historical note, G.,A. Isted, IEE Symposium on Long-Distance Propagation above 30 Mc/s, 28 Jan 1958, pp. 79-83;
- <sup>[10]</sup> R. A. Hull, "Air-Mass Conditions and the Bending of Ultra High Frequency Waves", QST, June 1935;
- <sup>[11]</sup> On Choosing and Bounding Probability Metrics, Alison L. Gibbs and Francis Edward Su, International Statistical Review, 2002.

# Annexes

Annex A and B summarize path details, measured and predicted values, enabling fast information access for the informed reader.

Annex C contains all calibration figures for completeness.

Annex D and E contain the uncertainty calculations for the measurements and the predictions.



## Annex B Measurement results and predictions

### B 1 Measured values

Field strength (dB $\mu$ V/m)		Hoek van Holland			Harwich			Baldock		
Transmitter	Ch	50% time	10% time	1% time	50% time	10% time	1% time	50% time	10% time	1% time
Goes TV1	29	72,8	79,3	86,5	27,5	60,8	75,8	-	17,8	44,0
Goes TV2	32	73,0	79,8	85,3	26,8	61,8	76,0	-	-	39,8
Goes TV3	35	73,0	80,8	86,8	24,8	60,0	75,8	-	-	33,5
Lopik TV2	27	89,8	92,3	95,0	18,8	45,8	68,0	-	21,0	44,5
Lopik TV3	30	88,3	90,8	93,3	19,5	47,0	69,3	-	20,8	43,8
Wieringen TV1	39	45,8	69,0	84,0	-	31,5	56,8	-	22,3	47,0
Wieringen TV2	45	41,0	67,5	83,3	-	38,3	59,5	-	-	-
Wieringen TV3	42	40,8	66,5	82,3	-	32,3	57,0	-	-	-

Table B-1: Measured values of the individual propagation paths

### B 2 Predicted values (P1546-4)

Field strength (dB $\mu$ V/m)		Hoek van Holland			Harwich			Baldock		
Transmitter	Ch	50% time	10% time	1% time	50% time	10% time	1% time	50% time	10% time	1% time
Goes TV1 (40%)	29	68,1	70,3	76,0	30,1	48,1	64,7	20,2	32,6	44,2
Goes TV2 (40%)	32	65,8	67,9	73,7	29,2	47,4	63,9	18,6	31,1	42,6
Goes TV3 (40%)	35	65,7	67,9	73,7	29,3	47,6	64,2	19,6	32,1	43,6
Goes TV1 (17%)	29	66,0	67,9	73,4	(same as above)			(same as above)		
Goes TV2 (17%)	32	63,6	65,5	71,0	(same as above)			(same as above)		
Goes TV3 (17%)	35	63,5	65,5	71,0	(same as above)			(same as above)		
Lopik TV2	27	77,1	78,6	84,1	30,3	45,9	60,6	21,8	33,9	45,7
Lopik TV3	30	77,0	78,5	84,1	30,2	45,9	60,6	21,6	33,8	45,5
Wieringen TV1	39	47,0	55,6	63,2	17,9	36,8	57,6	9,8	22,8	35,6
Wieringen TV2	45	46,9	55,7	63,2	20,7	40,3	60,8	12,6	26,0	38,4
Wieringen TV3	42	46,9	55,5	63,1	19,8	39,1	59,7	11,7	24,9	37,5

Table B-2: Predicted values of the individual propagation paths

## Annex C Calibration figures

This annex contains the calibration factors and their associated values as described in chapter 3.1.

### C 1 Antenna gain

The gain figures for all antennas and all measured TV stations are given in the following table:

TV transmitter	Antenna gain [dBd]			
	Hoek van Holland	Stena HSS	Harwich	Baldock
Goes TV1	8		11,5	14,6
Goes TV2	8,4		11,7	16,5
Goes TV3	8,4		11,8	17,2
Lopik TV2	6,7	9,7	11,9	14,6
Lopik TV3	8	10,4	11,8	15,4
Wieringen TV1	8,5		11,5	17,3
Wieringen TV2	8,7		10,8	16,4
Wieringen TV3	8,5		11,4	14,1

Table C-1: Antenna gain figures

### C 2 Antenna misalignment corrections

The antenna at Baldock was aimed at the transmitter Lopik; this results in a misalignment error of  $-17^\circ$  for Wieringen and is  $+12^\circ$  for Goes. The manufacturer's antenna pattern specifications were used to determine the antenna gain loss because of the misalignment. For Goes this factor is  $-3.4$  dB, for Wieringen it is  $-6.8$  dB.

### C 3 Cable losses

Cable losses for Harwich were part of the antenna calibration and therefore need not be corrected for. The cable at Baldock was installed in a tower with no possibility to operate a test transmitter or test receiver at the top of it. The cable loss was therefore determined with a TDR to measure the cables length and the cable manufacturer's data. Cable loss for Hoek van Holland and Stena were measured as separate items. The following table gives an overview of the cable losses.

TV transmitter	Cable losses [dB]			
	Hoek van Holland	Stena HSS	Harwich	Baldock
Goes TV1	2,1		0	4,4
Goes TV2	2,2		0	4,5
Goes TV3	2,2		0	4,6
Lopik TV2	2,1	2,1	0	4,3
Lopik TV3	2,1	2,1	0	4,4
Wieringen TV1	2,3		0	4,7
Wieringen TV2	2,4		0	4,9
Wieringen TV3	2,4		0	4,8

Table C-2: Cable losses

### C 4 Combiner network losses

In the first months of measurement campaign, it was found that in Hoek van Holland improvements were needed more isolation between signals coming in on the different antennas connected to the receiver. This was achieved in two steps. A temporary solution was found by interchanging the antennas on two combiner ports. The final solution was achieved by adding additional filtering.



The following table gives the losses for the full measurement campaign and for the intermediate solution (23 March 2005 to 20 April 2005) :

TV transmitter	Hoek van Holland [dB]	
	Combiner losses	Additional loss (interim period)
Goes TV1	6,5	0
Goes TV2	6,6	0
Goes TV3	6,4	0
Lopik TV2	6,3	-3,1
Lopik TV3	6,5	-3,3
Wieringen TV1	3,3	3,2
Wieringen TV2	3,4	3,2
Wieringen TV3	3,2	3,3

Table C-3: Combiner network losses in Hoek van Holland

### C 5 Narrow filter correction

The correction factor needed to translate from the narrowband RMS measurements to the correct field strength value as measured in a wideband receiver (> 5 MHz) with a peak detector. To obtain this value, measurements were taken a short distance from the TV tower, in clear surroundings and over a time interval. The measurement time of the second measurement is chosen in such a way that the horizontal synchronization pulse always occurs within a measurement interval. The measured values for the different filter values are shown in a histogram in figure C-4. This figure shows an example of several measurements that were performed.

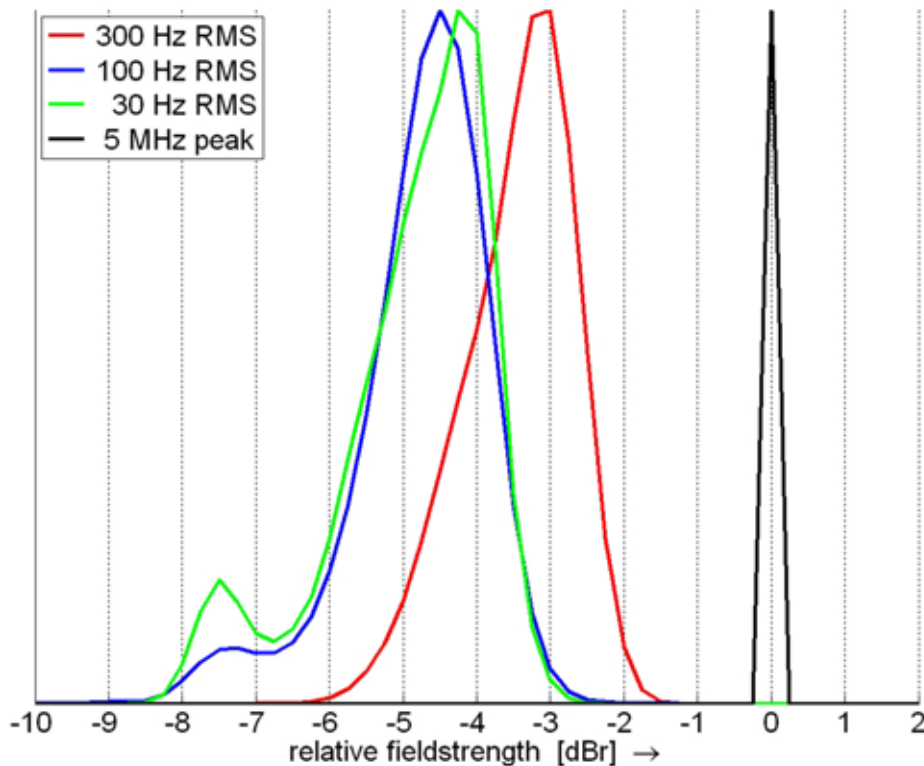


Figure C-4: Comparison of narrow filter values with wideband peak values (Lopik TV2)

The measurements with 5 MHz bandwidth capture the energy of the carrier including the energy of the synchronization pulse. The measurements with the narrow bandwidth miss some of the energy contained in the synchronization pulse, so they are somewhat lower. The 100 Hz bandwidth used in Hoek van Holland captures slightly more power than the 30 Hz filters. For the sake of simplicity, a correction factor of 4 dB is chosen for all locations and both bandwidths.

## C 6 Overview of all calibration factors per site

Rx location	TV transmitter	Pk-RMS corr. (dB)	Antenna gain (dBd)	Misalign. Loss (dB)	Cable att.(dB)	Comb. att.(dB)
Hoek van Holland	Goes TV1	4	8		2,1	6,5
	Goes TV2	4	8,4		2,2	6,6
	Goes TV3	4	8,4		2,2	6,4
	Lopik TV2	4	6,7		2,1	6,3
	Lopik TV3	4	8		2,1	6,5
	Wieringen TV1	4	8,5		2,3	3,3
	Wieringen TV2	4	8,7		2,4	3,4
	Wieringen TV3	4	8,5		2,4	3,2
Stena HSS	Lopik TV2	4	9,7	dynamic	2,1	
	Lopik TV3	4	10,4	dynamic	2,1	
Harwich	Goes TV1	4	11,5		0	
	Goes TV2	4	11,7		0	
	Goes TV3	4	11,8		0	
	Lopik TV2	4	11,9		0	
	Lopik TV3	4	11,8		0	
	Wieringen TV1	4	11,5		0	
	Wieringen TV2	4	10,8		0	
	Wieringen TV3	4	11,4		0	
Baldock	Goes TV1	4	14,6	3,4	4,4	0
	Goes TV2	4	16,5	3,4	4,5	0
	Goes TV3	4	17,2	3,4	4,6	0
	Lopik TV2	4	14,6	0	4,3	0
	Lopik TV 3	4	15,4	0	4,4	0
	Wieringen TV1	4	17,3	6,8	4,7	0
	Wieringen TV2	4	16,4	6,8	4,9	0
	Wieringen TV3	4	14,1	6,8	4,8	0

Table C-5: All correction factors and their total

## Annex D Measurement uncertainty calculation

### D 1 Description of measurement

The field strength measurements are performed with very similar setups on all four measurement locations. The antenna configurations differ from location to location. Hoek van Holland uses multiple antennas and a combining filter unit, in Baldock we have to correct for the antenna misalignment error. On the Stena HSS we perform dynamic antenna misalignment corrections by calculating the real-time antenna direction using the DGPS position data.

### D 2 Mathematical model

The field strength values shown in the graphs throughout the report are absolute field strength values. They are calculated from the measured receiver input voltage by correcting for the attenuation of the cables and filters between antenna and receiver, and by adding the antenna transfer factor calculated from the antenna gain. At each connector interface a mismatch loss can occur. In formula:

$$E = U_{RX} \cdot \frac{K_{ANT}}{d_{ALIGN} \cdot d_{CABLE} \cdot d_{FILT} \cdot d_{MIS}} \cdot d_{PK-RMS}$$

where:

E	=	Field strength	[V/m]
$U_{RX}$	=	Receiver input voltage	[V]
$K_{ANT}$	=	Antenna factor	[1/m]
$d_{ALIGN}$	=	Antenna misalignment	[1]
$d_{CABLE}$	=	Cable attenuation	[1]
$d_{FILT}$	=	Filter/combiner attenuation	[1]
$d_{MIS}$	=	Mismatch losses	[1]
$d_{PK-RMS}$	=	Peak RMS conversion	[1]

These factors are shown in the following figure:

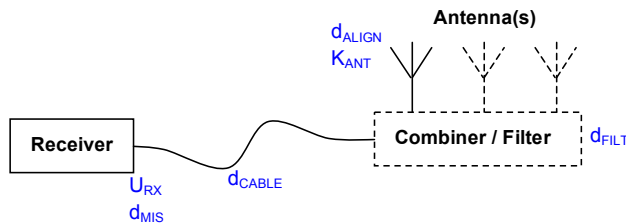


Figure D-1 Schematic diagram of a measurement station

### D 3 Description of individual elements influencing the combined uncertainty

#### $U_{RX}$

Measurements were performed with a Rohde & Schwarz FSP3 with a measurement accuracy of 0.5 dB normally distributed, 95% confidence ( $2\sigma$ ).

#### $K_{ANT}$

The antenna factor of the measurement antenna is used as a “translation” between the input voltage of the receiver at a certain receiver input impedance to the actual field strength. The antenna factor is derived from the antenna gain. The antenna gain of all the antennas for Hoek van Holland, Baldock and the maritime mobile measurements are determined using the three antenna method and distance scanning. The two reference antennas are calibrated at the NPL and have an uncertainty of 0.7 dB, normally distributed, 95% confidence. The derived measurement uncertainty is estimated as 1.2 dB for the antennas at Hoek van Holland, 1.5 dB for the antenna at Baldock and 2.5 dB for the antenna of the Stena HSS. All values are normally distributed, 95% confidence.

The actual gain of the antenna used in Harwich in the direction of the wanted transmitters has been measured on-site by statistically comparing the received field strength with the same reference antennas calibrated at the NPL. Estimated resulting uncertainty is 1.5 dB, normally distributed, 95% confidence.

#### **d<sub>ALIGN</sub>**

##### *Hoek van Holland*

One antenna per received TV transmitter is used, so each antenna could be aligned optimally by measurement and calculation. This alignment has been verified manually and found correct. The resulting misalignment loss uncertainty is less than 0.2 dB and is uniformly distributed.

##### *Harwich*

The gain of this antenna in the direction of the wanted transmitters has been measured in situ. Therefore there is no misalignment loss in this measurement site.

##### *Baldock*

Only one single long-Yagi is used at Baldock. The distance to the TV transmitters is such that their angular difference is small. The antenna has been aligned optimally for Lopik. The antennas diagrams are measured individually by the manufacturer. The misalignment loss for the other two transmitters has been compensated for, using these measurements. Resulting uncertainty is less than 0.2 dB, uniformly distributed.

##### *Maritime mobile measurements*

The HSS 'Discovery' does not follow a straight line while crossing the Channel, but manoeuvres to avoid other ships. This results in momentary misalignment of the measurement antenna of up to 30°. The antenna selected for these measurements has a wide horizontal opening angle with gain decaying smoothly with increasing misalignment angle. The actual direction of the ship can be derived by differentiating its position information during the crossing. Using this information and the horizontal antenna diagram, the misalignment gain loss is compensated for dynamically.

The horizontal diagram of the antenna is derived by simulation. Simulated and measured gain are in close correspondence, so the error in these figures is estimated to amount to less than 0.4 dB. This error has a uniform distribution.

The misalignment angle is calculated using several subsequent positions of the vessel. These positions are determined with a DGPS with an accuracy of 2 metre, uniform distributed. The distance between the individual measurements is not constant but can be assumed 200 m. The maximum error caused by this position error is 1.2°, resulting in an additional gain error of < 0.1 dB uniform distributed.

#### **d<sub>CABLE</sub>**

The uncertainty for the cable attenuation of the Harwich, Hoek van Holland and the mobile setup equals the accuracy of the network analyzer used. The cable used in Baldock was a high diameter low loss cable preinstalled in the antenna tower and was measured with a professional TDR as well as calculated. The uncertainty of the measured loss is less than 0.2 dB in both cases.

#### **d<sub>FILT</sub>**

At Hoek van Holland, a cross-over filter is used between the antennas and the receiver. The attenuation of the filter is determined using a Rohde & Schwarz ZVX network analyzer with a measurement accuracy of < 0.2 dB.

#### **d<sub>MIS</sub>**

The impedances of the antenna and filters are determined using a Rohde & Schwarz ZVX network analyzer with a measurement accuracy of < 0.2 dB. The measured return losses were all better than 20 dB. The setup of Hoek van Holland differs from the other ones, as it includes a filter/combiner for three antennas.

Hoek van Holland

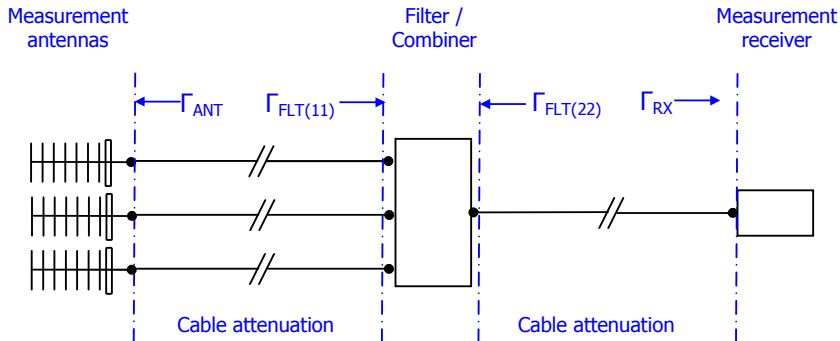


Figure D-2 Schematic diagram of attenuation and mismatch of the Hoek van Holland setup

Mismatch uncertainty between the measurement antenna and the filter is

$$M_U = \frac{1}{|1 - \Gamma_{ANT} \Gamma_{FLT}|}$$

and between the filter and the receiver

$$M_U = \frac{1}{|1 - \Gamma_{FLT} \Gamma_{RX}|}$$

This is in both cases 0.09 dB with a U-shaped distributed. The total uncertainty of these two uncertainties is 0.2 dB with a U-shaped distribution.

Harwich, Baldock and the Stena HSS setup

These setups are schematically identical with regard to the calculation of the mismatch uncertainty. Mismatch uncertainty between the measurement antenna and the filter is

$$M_U = \frac{1}{|1 - \Gamma_{ANT} \Gamma_{RX}|}$$

This is 0.09 dB with a U shaped distribution.

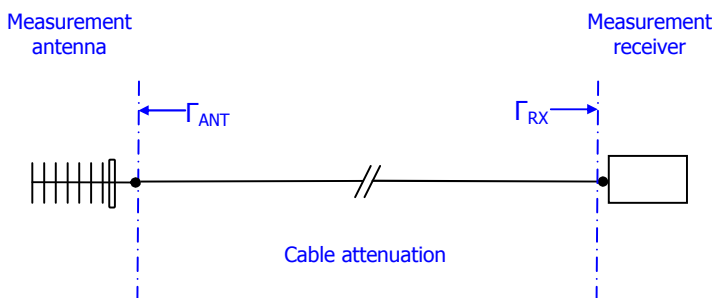


Figure D-3 Schematic diagram of attenuation and mismatch of the Harwich, Baldock and maritime mobile setup

**d<sub>PK-RMS</sub>**

Measurements are performed in a very narrow bandwidth relative to the actual bandwidth of the television signal. To convert between the actual peak ERP value of the transmitter and the measured RMS value, a conversion factor is used. This empirically is determined with a measurement; the uncertainty of this factor is 2 dB.

#### D 4 Combined measurement uncertainty

The overall measurement uncertainty calculation per site is found in the tables below. Although very similar, each site has a slightly different configuration. As we can conclude from the table, the receiver and antenna calibration are the main contributors to the measurement uncertainty.

Symbol	Source of uncertainty	Uncertainty dB	Distribution	Divisor	Sensitivity coefficient $c_i$	Standard source uncertainty $u_i(A_x)$ dB	degrees of freedom $v_i$ of $v_{eff}$
$U_{RX}$	Measurement receiver	0.5	normal	2	1	0.25	$\infty$
$K_{ANT}$	Antennagain	1.2	normal	2	1	0.6	$\infty$
$d_{ALIGN}$	Alignment error	0.2	uniform	1.7321	1	0.12	$\infty$
$d_{CABLE}$	Cable attenuation	0	normal	2	1	0	$\infty$
$d_{FILT}$	Filter attenuation	0.2	normal	2	1	0.1	$\infty$
$d_{MIS}$	Mismatch losses	0.1	U shaped	1.4142	1	0.07	$\infty$
$d_{PK-RMS}$	Peak RMS conversion	2	normal	2	1	1	$\infty$
E	Combined standard uncertainty		normal			1.2	$\infty$
E	Expanded standard uncertainty (95% conf.)		normal (k=2)			2.4	$\infty$

Table D-4: Measurement uncertainty budget of Hoek van Holland

Symbol	Source of uncertainty	Uncertainty dB	Distribution	Divisor	Sensitivity coefficient $c_i$	Standard source uncertainty $u_i(A_x)$ dB	degrees of freedom $v_i$ of $v_{eff}$
$U_{RX}$	Measurement receiver	0.5	normal	2	1	0.25	$\infty$
$K_{ANT}$	Antennagain	1.5	normal	2	1	0.75	$\infty$
$d_{ALIGN}$	Alignment error	0	uniform	1.7321	1	0	$\infty$
$d_{CABLE}$	Cable attenuation	0	normal	2	1	0	$\infty$
$d_{MIS}$	Mismatch losses	0.1	U shaped	1.4142	1	0.07	$\infty$
$d_{PK-RMS}$	Peak RMS conversion	2	normal	2	1	1	$\infty$
E	Combined standard uncertainty		normal			1.3	$\infty$
E	Expanded standard uncertainty (95% conf.)		normal (k=2)			2.6	$\infty$

Table D-5: Measurement uncertainty budget of Harwich

Symbol	Source of uncertainty	Uncertainty dB	Distribution	Divisor	Sensitivity coefficient $c_i$	Standard source uncertainty $u_i(A_x)$ dB	degrees of freedom $v_i$ of $v_{eff}$
$U_{RX}$	Measurement receiver	0.5	normal	2	1	0.25	$\infty$
$K_{ANT}$	Antennagain	1.5	normal	2	1	0.75	$\infty$
$d_{ALIGN}$	Alignment error	0.2	uniform	1.7321	1	0.12	$\infty$
$d_{CABLE}$	Cable attenuation	0.2	normal	2	1	0.1	$\infty$
$d_{MIS}$	Mismatch losses	0.1	U shaped	1.4142	1	0.07	$\infty$
$d_{PK-RMS}$	Peak RMS conversion	2	normal	2	1	1	$\infty$
E	Combined standard uncertainty		normal			1.3	$\infty$
E	Expanded standard uncertainty (95% conf.)		normal (k=2)			2.6	$\infty$

Table D-6: Measurement uncertainty budget of Baldock

Symbol	Source of uncertainty	Uncertainty dB	Distribution	Divisor	Sensitivity coefficient $c_i$	Standard source uncertainty $u_i(A_{x_i})$ dB	degrees of freedom $v_i$ of $v_{eff}$
$U_{RX}$	Measurement receiver	0.5	normal	2	1	0.25	$\infty$
$K_{ANT}$	Antennagain	2.5	normal	2	1	1.25	$\infty$
$d_{ALIGN}$	Alignment error (antenna simulation)	0.4	uniform	1.7321	1	0.23	$\infty$
$d_{ALIGN}$	Alignment error (due to DGPS errors)	0.1	uniform	1.7321	1	0.06	$\infty$
$d_{CABLE}$	Cable attenuation	0	normal	2	1	0	$\infty$
$d_{MIS}$	Mismatch losses	0.1	U shaped	1.4142	1	0.07	$\infty$
$d_{PK-RMS}$	Peak RMS conversion	2	normal	2	1	1	$\infty$
E	Combined standard uncertainty		normal			1.6	$\infty$
E	Expanded standard uncertainty (95% conf.)		normal (k=2)			3.3	$\infty$

Table D-7: Measurement uncertainty budget of the maritime mobile setup

### D 5 Overview of all measurement uncertainty values

The next table summarizes the calculated combined measurement uncertainty values for each individual measurement. The calculated 50%, 10% and 1% medians have the same combined uncertainty.

Location	Expanded measurement uncertainty ( $2\sigma$ )
Hoek van Holland	2,4 dB
Harwich	2,6 dB
Baldock	2,6 dB
Stena HSS	3,3 dB

Table D-8: Combined measurement uncertainty

Note: The spread of the measurement values due to propagation effects is much larger than the calculated measurement uncertainties. This spread should not be mistaken with measurement uncertainty. We can measure each momentary value with the specified uncertainty which is quite accurate. The phenomenon itself remains delusive and can only be described in the form of median values over a period of time.

## Annex E Prediction uncertainty calculation

### E 1 Description of prediction

In this chapter we list the different parameters and discuss their relevance in predicting field strength using Recommendation ITU-R P.1546. We also discuss the uncertainty with which they are determined.

We first estimate the uncertainty of each of the input parameters themselves. After that, we determine their influence on the prediction results, and estimate the uncertainty in the predictions that is caused by the uncertainty of the input parameter.

### E 2 Mathematical model

The mathematical model can be found in annex 6 of Recommendation P.1546 and is fairly complex. The following input parameters are used in our specific calculations:

ERP, frequency, path length, effective transmitter height, receiver height, percentage land/sea, receiver 'adjacent to sea', clutter height, terrain clearance transmitter, terrain clearance receiver.

In the following chapter we describe each of the parameters, and analyze their influence on the predicted value.

### E 3 Description of input parameters

#### P (ERP and reductions)

The power and antenna pattern are values provided by the operator. The antenna pattern is provided only on radials which are a multiple of 10 degrees and for other angles the reduction is estimated by a linear interpolation between the closest values. The uncertainty introduced by this interpolation method is 0.5 dB. The uncertainty of the peak ERP is estimated in the order of 0.7 to 1.0 dB. These values would result in a combined uncertainty of the ERP of 0.9 to 1.1 dB.

No independent measurements of the power of the transmitters were performed during the measurement period. For that reason, the estimated uncertainty is set at 1.5 dB (95% confidence), which is a safe assumption.

#### f (Frequency)

The frequency used in the calculations is the frequency of the vision carrier. This is the strongest component present in the composite signal. The frequency of all transmitters was monitored during the campaign with an absolute accuracy better than 1 Hz. The variation of the transmitter frequency was dependent on the transmitter. The transmitter of Wieringen had the largest frequency error, at times about 430 Hz. Still this frequency error less than  $7 \cdot 10^{-7}$ , and its effect on the calculations is negligible.

#### d (Path length)

Calculation distances are based on the positions measured by the site surveillance team using DGPS. For the fixed locations, the position uncertainty is less than 2 metres. For the maritime mobile measurements, it is around 5 metres. This results in a distance uncertainty of 5.5 metres (RSS summation), a value that has no significant impact on the calculations.

#### Effective transmitter height

The effective height of the transmitter is based on the measured antenna height, the height of the site above sea level, and the average height of the ground above sea level at a distance between 3 and 15 km in the direction of the receiver. The height profile is determined using a height map with a resolution of 50 by 50 metres. The maximum error on a single point is estimated at a few metres. The effective height is the average of a large number of points at distances between 3 and 15 kilometres from the transmitter. We expect that this averaging will partly cancel out the error made on a single point. We estimate the resulting uncertainty in the effective height at 2 metres. This in turn results in an uncertainty of the calculated field strength of about 0.5 dB.

#### Receiver height

The height of the receive antenna above the ground is also measured by the site surveillance team using a laser distance and height metre with an uncertainty of less than one metre. In the Hoek van Holland case, the height of the antenna relative to the height of the surrounding landscape is used. This adds another 2 metres to the uncertainty of the antenna height.



Antenna height variations have considerable influence when the antenna height is close to or less than the clutter height. This is not the case here: all receive locations have an antenna height that is considerably larger than the clutter height.

#### **Mixed path percentage land/sea**

Mixed propagation paths are paths that consist partly of land, and partly of sea stretches. In P.1546 these paths are described by the percentage of the path that consists of land or sea. Determining what percentage of the path consists of sea is sometimes difficult to determine, depending on the geographical situation (see paragraph 5.2).

The calculations can be done by using ITU / IDWM databases or by using a geographical tool like Google Earth. All methods have their own limitations. We expect an uncertainty of about 2% in the percentages sea for normal paths.

The path between Lopik and Hoek van Holland has no uncertainty on this aspect, as it is 100% land.

The influence of this parameter is relatively large when the path is predominantly sea ( $\approx 90\%$ ) which is the case for two of the paths terminating in Harwich. In that case, the resulting uncertainty in the calculated field strength is in the order of 3 dB. For simplicity, this worst case value is used for all paths.

#### **Receiver 'adjacent to sea'**

If the receiver is located adjacent to or on sea, P.1546 dictates some corrections for receiver height. Only for our site in Harwich there is some uncertainty about this parameter. The path as seen from the receiver site towards the transmitters crosses about 1 kilometre of water before it crosses a peninsula of about 2 kilometres wide. After this peninsula, the next 185 kilometres consists of sea only.

We consider this site 'adjacent to sea', although one could also consider it 'on land in urban area'. The resulting uncertainty applies only to the site Harwich and is, with the parameters used here, negligible.

#### **Clutter height**

Most sites are located on sea, adjacent to sea or in an open rural area. We chose a representative clutter height of 10 metres for all sites. Only around the Harwich site there is some uncertainty about this value. This site overlooks a peninsula at 1 kilometre distance where a container terminal is located. It is not certain how this terminal needs to be classified. The large metal cases of the containers are usually stacked to at least 3 layers, but probably more. We suspect a clutter height which varies between 10 and 20 metre for this location. This value is still below the receiver height so no correction is necessary.

#### **Terrain clearance receiver**

A detailed study was performed for the site Baldock. The value of the terrain clearance angle of Baldock was still below the minimum value defined in P.1546. Although there is some uncertainty in the terrain detail, the calculated angle is still below the minimum value of P.1546, so the effect can be ignored.

### **E 4 Combined prediction uncertainty calculation**

As shown in paragraph E 3, the only input parameters that have a significant effect on the predicted value are: ERP, heff and the percentage sea. The latter is not of concern to the path from Lopik to Hoek van Holland, as that path is completely over land.

The following tables show the calculation of the expanded combined prediction uncertainty, calculated following the methodology and definitions in "Expression of the Uncertainty of Measurement in Calibration", EA-4/02, from the "European co-operation for Accreditation".

Symbol	Source of uncertainty	Uncertainty dB	Distribution	Divisor	Sensitivity coefficient $c_i$	Standard source uncertainty $u_i(A_x)$ dB	degrees of freedom $\nu_i$ of $\nu_{eff}$
P	TX power	1,5	normal	2	1	0,75	$\infty$
$h_{eff}$	Effective transmit antenna height	0,5	uniform	1,7321	1	0,29	$\infty$
E	Combined standard uncertainty		normal			0,8	$\infty$
E	Expanded standard uncertainty (95% conf.)		normal (k=2)			1,6	$\infty$

Table E-1: Combined prediction uncertainty calculation for Lopik - Hoek van Holland

Symbol	Source of uncertainty	Uncertainty dB	Distribution	Divisor	Sensitivity coefficient $c_i$	Standard source uncertainty $u_i(A_x)$ dB	degrees of freedom $\nu_i$ of $\nu_{eff}$
P	Effective Radiated Power	1,5	normal	2	1	0,75	$\infty$
$h_{eff}$	Effective transmit antenna height	0,5	uniform	1,7321	1	0,29	$\infty$
%sea	Percentage of the path that consists of sea	3	uniform	1,7321	1	1,73	$\infty$
E	Combined standard uncertainty		normal			1,9	$\infty$
E	Expanded standard uncertainty (95% conf.)		normal (k=2)			3,8	$\infty$

Table E-2: Combined prediction uncertainty calculation for all other paths

### E 5 Overview of all prediction uncertainty values

The maximum uncertainty in the prediction caused by the uncertainty of the input parameters is estimated as 1.6 dB (95% confidence) for the path Lopik – Hoek van Holland and 3.8 dB (95% confidence) for all other paths.

Path	Expanded measurement uncertainty ( $2\sigma$ )
Lopik - Hoek van Holland	1,6 dB
All other paths	3,8 dB

Table E-3: Combined prediction uncertainty

# Revision History

20 September 2011	First published
7 October 2011	Typographical error corrected in the Formula for the antenna factor calculations in section 3.1.4
11 November 2011	Error in figure 6-15 on page 80 corrected





ISBN 978 90 815732 3 8